ABSTRACT

TURNER, KATHERINE ANNE. Localization of *Red Clover Necrotic Mosaic Virus* Polymerase Proteins at the Endoplasmic Reticulum of Living Plant Cells. Prepared under the supervision of Dr. Steven A. Lommel, Dr. Nina S. Allen and Dr. Steven Spiker.

The replication of positive strand RNA viruses requires association with host membranes and frequently results in membrane proliferation and rearrangement. The fact that widely divergent virus families share form and function of replication strategies is likely due to common evolutionary origin and suggests that elucidating the reproduction strategies of one virus provides insight to virus life cycles in general.

Red clover necrotic mosaic virus (RCNMV) is a positive-strand RNA virus in the *Dianthovirus* genus, *Tombusviridae* family. RCNMV encodes N-terminally overlapping proteins of 27 kDa and 88 kDa (p27 and p88). p88 contains motifs characteristic of RNA-dependent RNA polymerases, and while the function of p27 is unclear, it is very likely to be part of the RCNMV replication complex.

I have investigated the localization of the RCNMV replicase proteins in plants using green fluorescent protein (GFP) fusions observed in live cells using confocal microscopy.

The GFP:p27 and GFP:p88 fusions were expressed in *N. benthamiana* epidermal cells and protoplasts. GFP:p27 consistently localized to the endoplasmic reticulum (ER) and caused membrane restructuring and proliferation. Fractionation of virus-inoculated leaves demonstrated the association of p27 with isolated ER membranes. Additionally, GFP:p27 co-localized with ER-targeted YFP. GFP:p88 also localized to the ER and co-localized with GFP:p27. In addition, GFP:p27 and GFP:p88 were associated with invaginations of the nuclear membrane. These grooves and channels of ER crossed the nucleus, giving the appearance of fluorescence within the nucleus, while the signal from GFP:p27/p88 was actually associated with ER. GFP:p88 co-localized with GFP:p27 in two expression systems. This and the fact that GFP:p27 localized to the cortical ER, the nuclear envelope, and cytoplasmic ER domains in the presence of viral genomes as well as in the absence of any viral proteins suggests that the two proteins co-localize to the ER during infection. Microscopic observations suggest that the virus remodels ER structure to create membranous bodies containing active viral replication complexes. The fact that both proteins independently accumulated in the ER and perturbed the ER morphology suggests that the proteins function together, as part of a larger replication complex. This is the first report of a Tombusvirus replicating in association with the ER.

LOCALIZATION OF RED CLOVER NECROTIC MOSAIC VIRUS POLYMERASE PROTEINS AT THE ENDOPLASMIC RETICULUM OF LIVING PLANT CELLS

by

KATHERINE ANNE TURNER

A dissertation submitted to the Graduate Faculty of NC State University in partial fulfillment of the requirements for the degree of Doctor of Philosophy

DEPARTMENT OF GENETICS

Raleigh

2002

APPROVED BY:

Steven A. Lommel

_____
Co-Chair of Advisory Committee

Nina Strömgren Allen

_____
Co-Chair of Advisory Committee

Steven L. Spiker

_____
Co-Chair of Advisory Committee

Dominique Robertson

_____

Michael D. Purugganan

_____

DEDICATION

This thesis is dedicated to my mother, Maureen Anne Sparks, who sacrificed much of her youth to provide a good life for me.

Mom- you always wanted me to have the best of everything, and wanted me to go to college so I could be a success in life. In college, you thought, I would learn how to think, and how to persevere, how to be strong and believe in myself. You thought I would learn how to be the best person I could be. But you taught me all those things yourself, long before I ever came to North Carolina

IN MEMORIAM

This thesis is also dedicated to the memory of my father, Van Arden Sparks, who taught me that life is not about work at all; rather, it is about love, and fun, and peace.

BIOGRAPHY

Katherine Anne Turner was born in 1973 in Reno, Nevada. She attended Mohave High School in Bullhead City, Arizona. Kathy always studied too much and worked too hard until she got into grad school in North Carolina. There she discovered that the best things in life happen outside the classroom.

ACKNOWLEDGEMENTS

I must recognize the contributions of many people, foremost among them Tim Sit, for his friendship, advice, guidance, and sympathy. So many other people have made a difference to the project or to me personally: Donna Cookmeyer, Mara Massel, Kirsten Nielson, Karin Shank, Paula Knabb, Jason Lowry, Jami Clements, Jen Smith, Gretchen Feulner, Chris Halweg, Kirk Francis, the entire NSCORT softball team, particularly during the Spring 2000 season, Rob Mapel, David Collings, John Love, Tracey Horn, Sarah Wyatt, Eva Johannes, and probably several others that I am forgetting in my haste.

I would be remiss if I didn't acknowledge the help and attention of my committee: Jon Swaffield, Niki Robertson, Steve Spiker, Nina Allen, and Steve Lommel, along with our recent addition Michael Purugganan. I must especially thank Steve Lommel for allowing me to do things my own way, and for never micromanaging.

I wish to thank particularly my RoomDog, Monica Longsdorf, who listened when I needed it, told me off when I needed it and took a whirlwind 36-hour trip to Missouri. I would never, ever have been able to do it without you, Mo. I love you dearly.

I also wish to thank my family: Dee and Van Sparks, for their love and support. Their level heads kept me from running into the hills many times. Also my Uncle, Hal Turner, the only sane Turner I know.

Thanks, Bill. You rock. I am truly blessed to have found you.

TABLE OF CONTENTS

LIST OF TABLES

LIST OF FIGURES

LIST OF ABBREVIATIONS

(-) strand	minus strand, the antisense strand
(+) strand	positive strand, the coding strand
ACLV	*Apple chlorotic leafspot virus*
AMV	*Alfalfa mosaic virus*
BMV	*Brome mosaic virus*
BrUTP	bromouridinetriphosphate
BYDV	*Barley Yellow dwarf virus*
CaMV	*Cauliflower mosaic virus*
CarMV	*Carnation mottle virus*
CIRV	*Carnation Italian ringspot virus*
CMV	*Cucumber mosaic virus*
CP	coat protein
CPMV	*Cowpea mosaic virus*
CRSV	*Carnation ringspot virus*
CymRSV	*Cymbidium ringspot virus*
EF-Ts	elongation factor Ts
EF-Tu	elongation factor Tu
eIF	eukaryotic translation initiation factor
em	emission wavelength
ER	endoplasmic reticulum
ex	excitation wavelength
FNSV	*Furcrea necrotic streak virus*
GA	Golgi apparatus
HF-1	host factor 1
kb	kilobases
kDa	kilodalton
LMV-E	*Lettuce mosaic virus* strain E
MP	movement protein
MSV	*Maize streak geminivirus*
MVB	multivesicular body
NE	nuclear envelope
ORF	open reading frame
PCV	*Peanut clump virus*
Pd	plasmodesmata
PLRV	*Potato leaf roll virus*
PSLV	*Poa semilatent virus*
RCNMV	*Red clover necrotic mosaic virus*
SCNMV	*Sweet clover necrotic mosaic virus*
TBSV	*Tomato bushy stunt virus*
TCV	*Turnip crinkle virus*
TEV	*Tobacco etch virus*
TGB	triple gene block
TMV	*Tobacco mosaic virus*
TYMV	*Turnip yellow mosaic virus*
wt	wild-type

Chapter 1

Previous Localizations of Plant Viral Polymerases and the Use of Green Fluorescent Protein as a Reporter Gene

Previous Localizations of Plant Viral Polymerases and the Use of Green Fluorescent Protein as a Reporter Gene

Introduction

Viral replication is fundamental to the infection cycle. The replication of positive strand RNA viruses takes place in association with host membranes. This membrane localization has been shown to be required for replication (Rohozinski and Hancock, 1996; Carette et al., 2000; Miller et al., 2001; Lee et al., 2001). Membrane association appears to be universal across (+) RNA viruses, including species that infect plants, animals, insects, and yeast (Schwartz et al., 2002).

Viruses exhibit modular evolution, and genetically compromised viruses can often be complemented by functionally related proteins from another, distantly related virus (Matthews, 1991). Viruses are the ultimate scavengers, and have evolved or appropriated a wide variety of replication strategies, genome organizations, and functional groups. It is their diversity and ability to rapidly develop new characteristics that make them such robust pathogens. It is very unusual for so many viruses to share a characteristic such as this requirement for membrane association during replication. If the mechanism underlying the requirement were known, it would have application to nearly all (+) strand viruses, and could be the foundation of broadly effective antiviral therapies.

We selected *Red clover necrotic mosaic virus* (RCNMV) as a model system to study the subcellular localization of a viral replicase. Labeled p27 and p88 were produced by fusing the *Aequoria victoria* green fluorescent protein (GFP) to the RCNMV proteins. GFP was chosen as the intracellular reporter because it provides the opportunity to observe the polymerase in live cells, reducing preparation artifacts and allowing dynamic observations. Laser scanning confocal microscopy allows images of the cell interior to be recorded in real-time, without distortion from out-of-focus light. Here, a review of RCNMV biology, related viruses, RNA virus replication, GFP, and the endomembrane system of plants is presented.

RCNMV taxonomy

RCNMV was first reported in 1976 as *Clover primary leaf necrosis virus* (Ragetli and Elder, 1976). It is a species of the *Dianthovirus* genus, named after the host genus (*Dianthus*) of the type species, *Carnation ringspot virus* (CRSV). *Sweet clover necrotic mosaic virus* (SCNMV) and *Furcrea necrotic streak* (FNSV) are the only other known species comprising this genus (Matthews, 1991). The key taxonomic feature that distinguishes this virus genus from other plant virus genera is their bipartite single-stranded (SS) RNA genome. Dianthoviruses are members of the plant RNA virus family *Tombusviridae*, which also contains the genera *Carmovirus, Tombusvirus, Necrovirus,* and *Machlomovirus* (Hull, 2002) (Matthews, 1991; Murphy et al., 1995) and others. This family was established on the basis of remarkable genetic conservation among the polymerases.

Interestingly, the polymerases of the *Tombusviridae* also have high sequence conservation with the polymerases of the barley yellow dwarf virus (BYDV)-like *Luteoviruses* (Xiong and Lommel, 1989). All of these virus genera fall within the sindbis (alpha) virus supergroup (Buck, 1996; Matthews, 1991).

Biology and economic significance

RCNMV is restricted to dicotyledonous hosts and is found throughout the temperate regions of the world. It is readily transmissible by physical contact between plants or through soil and groundwater. The natural host range includes red and white clover as well as alfalfa. Experimental hosts include legumes, cucurbits and members of the Solanaceae (Hamilton and Tremaine, 1996). Symptoms in natural infections include mosaic, vein clearing, stunting, and leaf deformation. In the laboratory hosts *Nicotiana benthamiana* and *Nicotiana clevelandii*, more severe symptoms of mosaic, necrotic spots, rings, and epinasty are observed after manual inoculation. Symptoms of the virus are masked at temperatures over 25° Celsius, appearing most strongly when plants are maintained at 15 to 20° C. It has recently been shown that the Canadian strain of RCNMV cannot replicate at elevated temperatures, and that the determinant of the temperature sensitivity resides in the 3' untranslated region of RNA-1 (Mizumoto et al., 2002).

In general, RCNMV does not kill its hosts. CRSV caused severe problems for the carnation industry (Hamilton and Tremaine, 1996) until the advent of certified virus-free plant propagation material and strict sanitation procedures.

RCNMV infections of forage legumes are often so mild that little impact on yield is realized, though economic loss can be a risk if temperatures remain below 20° C for extended periods (Ragetli and Elder, 1976).

Genetics

The RCNMV genome is split between two (+) sense genomic RNAs, RNA-1 (3883 nucleotides) and RNA-2 (1407 nucleotides) (See Figure 1). RNA-1 has 3 open reading frames (ORFs) encoding 27 kDa, 88 kDa, and 37 kDa proteins (Xiong and Lommel, 1989). The ORF 1 is expressed as a 27 kDa protein and an inclusive 88 kDa protein. A -1 ribosomal frameshift at the stop codon of p27 allows expression of the 88 kDa protein at low levels (Kim and Lommel, 1994). The mechanism of frameshifting is similar to that of retroviruses, and involves a shifty heptanucleotide at the p27 termination codon (Xiong et al., 1993). ORF 2 is the post-frameshift region of the 88 kDa protein, which produces a 57 kDa protein in *in vitro* translation assays. This protein cannot be identified *in vivo* (Xiong and Lommel, 1989).

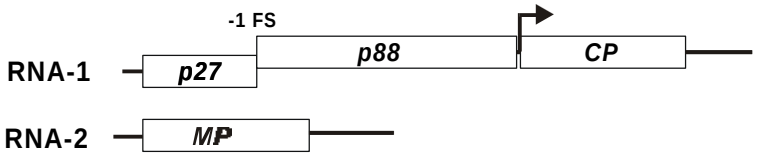

Figure 1. Schematic diagram of RCNMV RNA-1 and RNA-2. ORFs are indicated as open boxes, and the –1 frameshift site (FS) and subgenomic promoter site are indicated (arrow).

RNA-1 also produces a subgenomic RNA of 1524 nucleotides (Osman and Buck, 1990). The subgenomic promoter contains a 14 nucleotide positive strand promoter sequence homologous to the 5' terminus of RCNMV RNA-1. RNA structure mapping predicts a stable stem-loop structure at the 5' end of the sub-genomic RNA, including the (-) strand promoter, which could be important for transcription initiation from full-length negative sense RNA-1 (Zavriev et al., 1996). The coat protein (CP) is translated from this sub-genomic RNA because the CP ORF on RNA-1 is inaccessible to eukaryotic translation machinery. A conserved region of RNA-2, the trans-activator, is required for efficient transcription of sub-genomic RNA from RNA-1 (Vaewhongs and Lommel, 1995). The trans-activator is a 34 nucleotide stem loop on the genomic sense RNA 2 that base pairs to RNA-1 upstream from the start site of sub-genomic RNA synthesis (Turner and Buck, 1999; Sit et al., 1998). This region is within the subgenomic promoter of the CP. This mechanism for controlling the timing of coat protein expression may have evolved to ensure that sufficient quantities of RNA-1 and RNA-2 are present before viral assembly begins (Sit et al., 1998).

The p27 gene product and its p88 extension are the viral contribution to the replication complex. The p27 and p88 proteins have been shown by immunoprecipitation (Xiong et al., 1993; Bates, 1995) to be components of membrane-bound replicase isolated from infected tissue. *In vivo,* p27 is produced at 10- to 20 times the level of p88 due to the inefficiency of the ribosomal frame-shifting mechanism. This stoichiometery makes it unlikely that there is a 1:1 physical interaction between the proteins (Xiong et al., 1993; Xiong

and Lommel, 1991). However, p27 is essential for replication of the genome (Paje-Manalo and Lommel, 1989; Xiong and Lommel, 1991) and has sequence conservation with similarly located pre-readthrough portions of polymerases of the *Tombusviridae* (Koonin, 1991). p88 has high conservation with the polymerases of *Turnip crinkle virus* (TCV) and *Carnation mottle virus* (CarMV) (Xiong and Lommel, 1989) and contains the 'GDD' motif (Koonin, 1991), suggesting that it is the catalytic portion of the RCNMV replication complex. These data taken together strongly suggest that p27 and p88 are the viral contribution to the RCNMV replication complex and that they work in concert, if not by direct interaction, to replicate the genome and provide templates for translation.

The 3' ORF of RNA-1 produces the CP (Xiong and Lommel, 1989). 180 copies of the CP assemble to form a T=3 icosahedral virion. The CP is very basic (pI ~10) which suggests a mode of interaction with RNA (Xiong and Lommel, 1989). The CP has strong sequence conservation with *Turnip crinkle virus* (TCV) and *Carnation mottle virus* (CarMV)(Xiong and Lommel, 1989). The CP forms large cytoplasmic aggregates when expressed as a GFP fusion (S. Lommel, unpublished results). The CP is not necessary for replication or cell-to-cell movement and does not appear to interact with p27 or p88 *in vivo* (Paje-Manalo and Lommel, 1989; Buck, 1996).

RNA-2 is monocistronic, and encodes the 35 kDa movement protein (MP) (Lommel et al., 1988). The MP functions in cell-to-cell and long distance movement of the virus through plant cells (Lommel et al., 1988; Fujiwara et al.,

1993). The MP is functionally homologous to *Tobacco mosaic virus* (TMV) MP. Both MPs enlarge plasmodesmata size exclusion limits, transport RNA through plasmodesmata, and bind nucleic acids *in vitro* (Geisman-Cookmeyer et al., 1995). Although the two proteins have very low sequence identity, the two viruses appear to use a common mechanism for cell-to-cell movement (Geisman-Cookmeyer et al., 1995).

The MP itself is not required for replication (Paje-Manalo and Lommel, 1989) although the trans-activator, a RNA sequence motif present in the MP ORF, is necessary for transcription from the sub-genomic promoter of RNA-1 (Sit et al., 1998; Vaewhongs and Lommel, 1995) and translation of CP. Both the MP and trans-activator are necessary for systemic infection (Sit et al., 1998; Vaewhongs and Lommel, 1995; Wang et al., 1998). When fused to GFP, the MP appears at the cell wall of infected cells, in punctate spots assumed to be plasmodesmatal pit fields (Wang et al., 1998; S. A. Lommel, in preparation). Similar punctate spots have been shown to be associated with plasmodesmata in *Tobacco mosaic virus* infected leaves by immunogold cytochemical localization of virus proteins within the plasmodesmata (Tomenius et al., 1987).

Cytopathology of RCNMV

Very little is known about the intracellular localization of *Dianthoviruses*. CRSV causes large aggregates of virus and tubular inclusions in the nuclei of infected *Dianthus barbatus* (Sweet William) and *Vigna unguiculata* (cowpea) (Weintraub et al., 1975). Spherical inclusion bodies have also been seen in the

nuclei of Sweet William, but not of cowpea. Clusters of proliferated ER with dilated cisternae were common in CRSV-infected *Chenopodium quinoa* and *Nicotiana megalosiphon* (Koenig et al., 1988). Membranous vesicles and patches of densely stained amorphous material were present in the cytoplasm (Francki et al., 1985), and chloroplast vesiculation was observed in red clover infected with RCNMV-Can, a Canadian strain of RCNMV (Ragetli and Elder, 1976).

A review of the plant endomembrane system

The plant endomembrane system has many features in common with the more highly investigated animal endomembrane system, as well as several features found only in plants. Although not a membrane, the plant cell wall is of course a major addition that affects growth and expansion dramatically, as well as protein export from the cell, endocytosis, and cell division. Just inside the cell wall, the plasma membrane is the first of many bilayers that are important for the health and productivity of the cell. As one moves through the cell, the endoplasmic reticulum (ER), Golgi apparatus (GA), nucleus, vacuole, plastids and mitochondria are encountered, as well as many types of transfer vesicles. In past years, the cell was often considered a ‘bag of molecules’ and shown as a rectangular box (in the case of walled cells) with a few spheroid organelles seemingly hanging unsupported within. We now know that this image of the cells as relatively empty and unstructured is incorrect. The cytoskeleton (actin, microtubules, and their associated proteins) interacts with every organelle in the

cell (Buchanan, 2000), sometimes passing completely through them (Collings et al., 2000). The organelles also interact with each other, forming connections and subdomains that provide for communication and material transfer (Buchanan, 2000). We are now learning how dynamic and flexible the endomembrane system can be. It has been suggested that the organelles and their membranes are more like the appendages of one entity, rather than individuals acting autonomously (Check, 2002; Cole and Lippincott-Schwartz, 1995). It is certainly the case that the lipids cycle between organelles freely (Grabski et al., 1993; Staehelin, 1997), carrying membrane proteins and vesicle contents like cargo. For purposes of this discussion, we will focus on the ER and its downstream partner, the GA.

The plant ER has many different domains and shapes. It functions in almost all important cellular processes, including the synthesis, processing, and sorting of proteins, production of lipids and glycolipids, and regulation of cytosolic calcium. Morphological features or functional properties can be used to distinguish the 16 elucidated domains, some of which include rough ER, nuclear envelope, protein bodies, oil bodies, microtubule nucleation domains, lipid recycling domains, cortical, smooth (tubular), and transitional ER (See figure 2).

The ER extends throughout the cytoplasm, composed of both flat lamellae and tubular networks. The earliest observations of the ER suffered from the effects of fixatives used to prepare samples for the electron microscope. It wasn't until contrasting agents such as osmium ferricyanide were included post-fixation that the fine cortical tubules and the ER lumen were studied (Harris, 1979). The

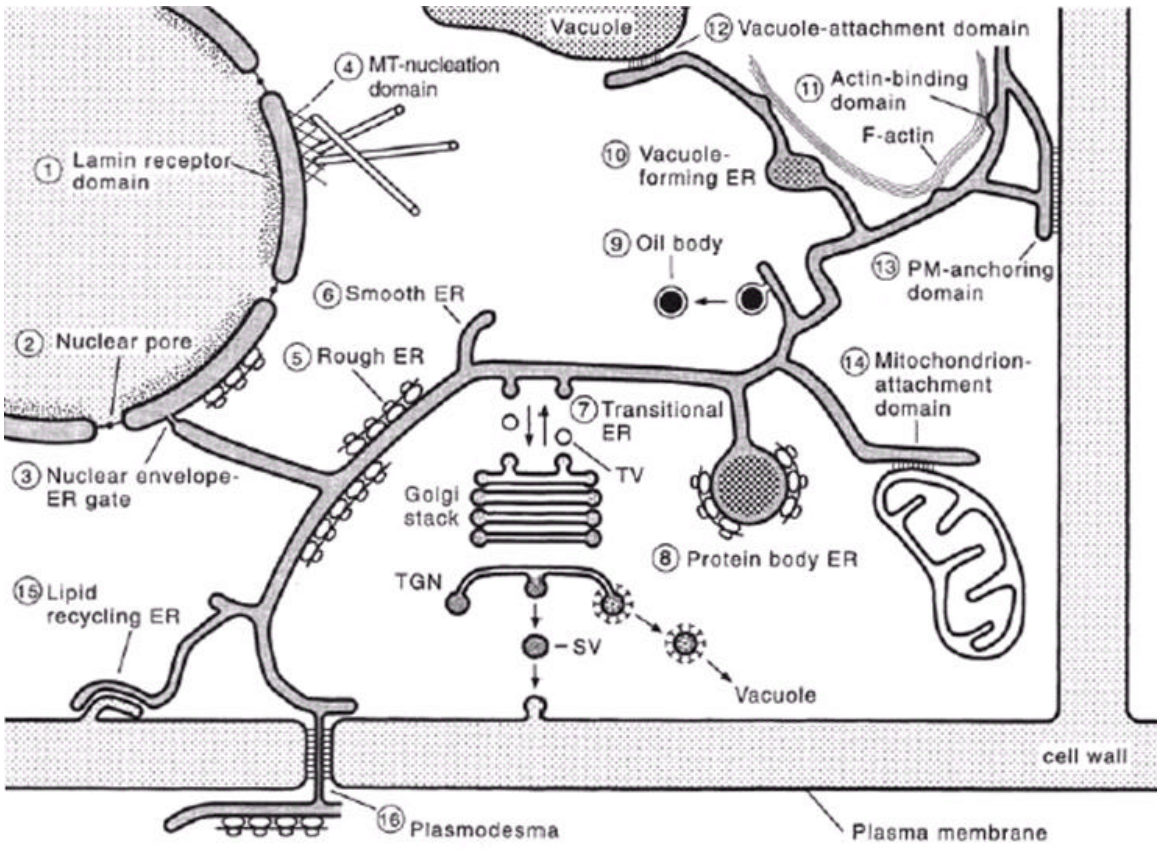

Figure 2. Schematic diagram depicting the 16 described types of ER in the plant cell. Reprinted with permission from Blackwell Publishing, Oxford, UK. Staehelin, 1997. The Plant Journal **6**;1151-65.

cortical ER is directly under the plasma membrane, and is distinguished from the ER tubules that cross the cytoplasm by its relatively static and two-dimensional structures (Figure 3) (Hepler, 1981; Hepler et al., 1990). The flat lamellae are the polysome-bearing rough ER domains, and the tubular cisternae are smooth (Staehelin, 1997). The tubular strands that cross the cell interior (Figure 3) are more mobile than the cortical ER and depend upon the actin cytoskeleton for their movement (Allen and Brown, 1988; Collings et al., 1998;

Boevink et al., 1998; Hawes and Satiat-Jeunemaitre, 2001). The tubules of smooth ER overlay the actin cytoskeleton very closely, and specialized domains of the ER appress directly against the microfilaments, suggesting a physical interaction (Allen and Brown, 1988; Lichtscheidl et al., 1990; Staehelin, 1997). The motion of the ER is sensitive to cytochalasin D, a drug that disrupts actin microfilaments (Knebel et al., 1990). In animal cell ER, in contrast, movement and reorganization of the cisternae and tubules depends on microtubules (Cole and Lippincott-Schwartz, 1995).

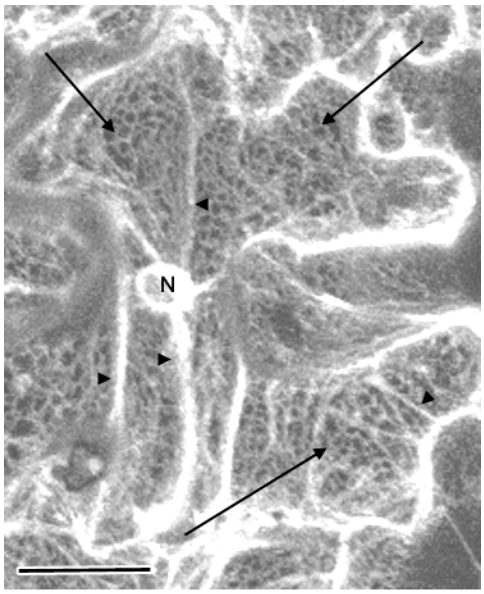

Figure 3. Computer projection of 10 confocal sections through a N. benthamiana cell transformed with mGFP5-ER. The ER is fluoresent throughout the cell, including the nuclear membrane, tubular ER, and the cortical ER. Arrows indicate cortical ER and arrowheads indicate tubular, smooth ER. N= nucleus, horizontal bar = 25 um.

It has recently been shown that the ER ramifies through the nucleus and creates channels through which the cytoskeleton and vesicles can pass (Collings et al., 2000). In *Nicotiana* and onion epidermal cells the tubules were observed to be stable (Collings et al., 2000). Such grooves substantially increase the surface area available for interaction with the cytoplasm. It has previously been shown that animal nuclei contain tubes of ER and invaginations (Fricker et al., 1997) and that the inclusions preferentially associate with nucleoli. It has been suggested that ER channels through the nucleus function in delivering messenger RNA to

ribosomes on nearby rough ER, or function in calcium signaling (Lui et al., 1998a).

In addition to close interactions with the nucleus and actin cytoskeleton, the ER is associated with mitochondria. Both in animal and plant cells, the ER and mitochondria are part of the calcium signaling cascade, and are so closely associated that their interaction has been compared to that of neural synapses (Csordas et al., 1999). One of the best-known examples of this association is muscle contraction, during which calcium is released from the sarcoplasmic reticulum (Alberts et al., 1994).

It has been demonstrated that small mobile particles are associated with the ER in cells of *Acetabularium* (giant algae; Allen and Schumm, 1990). The particles could be equivalent to calciosomes, calsequestrin- containing organelles found in animal cells (Volpe et al., 1998). It was speculated that the particles are functional in signal transduction (Allen and Schumm, 1990). In previous studies small, oval shaped organelles associated with the ER were shown to be ER inclusions contained within the membrane (Haseloff et al., 1997; Gunning, 1998). The inclusions move rapidly along the ER tubules and presumably must interact with the cytoskeleton by transmembrane linker proteins, yet to be characterized (Hawes and Satiat-Jeunemaitre, 2001). In addition, the bodies of the Golgi apparatus (GA) are associated with and move over cortical and tubular ER (Haseloff et al., 1997; Boevink et al., 1998; Gunning, 1998).

The Golgi apparatus is important for cell wall synthesis and post-translational modification of most cellular proteins. The plant Golgi utilizes the same protein machinery that animal and yeast Golgi use for their secretory and biosynthesis functions, but it uses the machinery in novel ways that address the unique needs of plants (Nebenfuehr and Staehelin, 2001; Scales and al., 2000). Plant Golgi bodies are small, compact stacks that are dispersed through out the cytoplasm (Boevink et al., 1998; Horsley et al., 1993). COP-I coated vesicles bud from the Golgi bodies with cargo bound for the lysosome or cell wall (Boyko et al., 2000). COP-I is a vesicle 'coatamer' protein that helps sort vesicle content for targeted delivery (Nebenfuehr, 2001). In addition, the Golgi bodies travel along the actin cytoskeleton by means of a Golgi-specific myosin motor (Boevink et al., 1998). The bodies exhibit stop-and-go motions that are characteristic of specific, directed motility rather than passive riding along with cytoplasmic streaming. This is different from the centralized, microtubule- based location of the animal Golgi apparatus (Nebenfuehr and Staehelin, 2001).

In addition, Golgi body movements along actin cables follow the ER tubules present in the cortical region directly under the plasma membrane (Boevink et al., 1998). This could allow them to sweep up secretory vesicles as they pass sites of protein export from the ER. It has been observed that Golgi bodies in mitotic cells are positioned near the forming cell plate (Nebenfuehr, 2001). These observations suggest that Golgi bodies could be recruited to ER export sites or to locations where their products are needed for cellular growth (Nebenfuehr, 2001) Thus, Golgi could be recruited to sites of virus replication

and packaging to bring structural proteins or host replication components to the viroplasm.

Green fluorescent protein: properties and usage

Chemists and biologists often wish to label a protein with a fluorescent tag in order to study its localization or biochemistry *in vivo*. Traditionally, this meant isolating the protein to be labeled, conjugating a fluorescent chemical dye such as fluorescein to the protein and re-purifying, followed by delivery techniques that involved permeabilization of the plasma membrane or microinjection. Such methods are time consuming, damaging to the cells, and technically complex. In the 1990s, utilization of the green fluorescent protein (GFP) from *Aequoria victoria* as a cell marker revolutionized cell biology (Prasher et al., 1992; Chalfie, 1994; Heim et al., 1994).

GFP is a small 23 kDa protein containing 238 amino acids. In the jellyfish, it is found in small light-emitting organelles, termed lumisomes (Haseloff and Amos, 1995). Inside the lumisomes are two photoproteins, aequorin and GFP. Aequorin was first isolated from *Aequoria aequoria* in 1962 by Osamu Shimomura and generates blue light in the presence of calcium (Shimomura et al., 1962). The light produced by aequorin is absorbed by GFP (Shimomura et al., 1962), which then emits green fluorescence efficiently without the assistance of a cofactor and requiring only molecular oxygen (Heim et al., 1994). GFP was isolated in 1974 and has two excitation peaks, one at 395 nm and a second, smaller peak at 475 nm (Morise et al., 1974). A single emission peak is found at

508 nm. The internal chromophore is composed of a cyclic Ser-Tyr-Gly group at residues 65-67, which oxidizes to produce fluorescence. The reaction is reversible and repeatable (Prasher et al., 1992; Cubitt et al., 1995). The potential to express a stable, non-intrusive fluorescent marker protein *in situ* was enormously exciting to geneticists, biochemists, and cell biologists, and once a clone of the GFP gene was available (Prasher et al., 1992), numerous researchers began screening, mutating, and modifying the protein to make a better molecular reagent.

GFP expressed in *E. coli*, *C. elegans,*(Chalfie et al., 1994) *S. cerevisiae*,(Heim et al., 1994) and *D. melanogaster* (Wang and Hazelrigg, 1994) was fluorescent without additional modification, and appeared to be non-toxic. With that reagent in hand, Cubitt et al. (1995) created the first important mutation of wild-type (wt) GFP, which shifted the primary excitation peak from 395 nm to 488 nm, combining the area under the two peaks into a single larger peak. This change was the result of a single mutation in the chromophore, mutating serine 65 to a threonine (Cubitt et al., 1995). The mutation had several other beneficial effects, including six-fold brighter fluorescence, faster oxidation, and little or no photobleaching of the chromophore (Cubitt et al., 1995). Haseloff et al. (1997) optimized wt GFP for expression in plants by demonstrating that a cryptic intron was efficiently removed from GFP cDNAs between nucleotides 400 and 483 in *Arabidopsis*. The resultant protein was non-fluorescent (Haseloff and Amos, 1995). A modified version of the gene was created that mutated the splice sites and altered codon usage to reduce the AU content of the mRNA. Transgenic

plants stably expressing the modified GFP (mGFP) were created, demonstrating proper expression of the protein in plants (Haseloff et al., 1997). Many other groups optimized and reshaped GFP, creating spectral variants altered in both excitation and emission maxima. The most distinguishable mutant form of GFP features a tyrosine to histidine change at residue 66, resulting in blue fluorescence rather than green (Palm et al., 1997). The existence of two spectrally distinguishable fluorescent proteins made dual-labeling experiments a possibility and spurred the development of additional variants (Davis and Vierstra, 1998). Molecular evolution through DNA shuffling was used by Crameri *et al.* (1996) to generate mutant GFPs with 42-fold greater brightness and increased solubility (which later became the basis of enhanced GFP "eGFP" as sold by BD Biosciences, Palo Alto; Crameri et al., 1996). Eventually, "yellow" (ex. 525 nm em. 540 nm) and "cyan" (ex. 425 nm em. 475 nm) GFPs (Heim and Tsien, 1996) emerged as the most useful variants with regard to brightness, stability, and efficiency (Angres and Green, 1999) and are now commonly available standardized reagents.

GFP as a reporter

GFP retains fluorescence when fused to another protein at either the N- or C- terminus (Leffel et al., 1997). This property makes it an ideal fluorescent tag to monitor subcellular localization of proteins, organelles, and biochemical processes. GFP is efficiently expressed to high levels by the *Cauliflower mosaic*

virus (CaMV) 35S promoter in plants, comprising as much as 0.5% of the total cellular protein (Leffel et al., 1997). These characteristics make GFP a nearly ideal reporter system, and it is the "first truly *in vivo* system to become available for use in whole plants" (Leffel et al., 1997). The earliest uses of GFP as a reporter simply used GFP as a visible marker, a separate co-transformant that identified those individuals that had been successfully transformed, whether transiently or stably (Haseloff et al., 1997; Oparka et al., 1996). Many methods can be used to express GFP along with the gene of interest, including *Agrobacterium*-mediated gene transfer (Zhang et al., 2001), microprojectile bombardment (Kotlizky et al., 2000), transfection (Toth et al., 2001), transformation (Chalfie et al., 1994), and expression from a viral genome (Oparka et al., 1996). Quickly researchers began to use GFP as a translationally fused visible marker, present anywhere the gene of interest was expressed. In addition, GFP was fused to organelle targeting tags. This resulted in GFP localized to subcellular structures including the ER (Haseloff and Amos, 1995), nucleus (Grebenok et al., 1997), mitochondria (Kohler et al., 1997), cytoskeleton (Katz et al., 1998), Golgi apparatus (Boevink, 1998), chloroplasts (Kohler et al., 1997), and peroxisomes (Jedd and Chua, 2002).

GFP is now the favored method of labeling cell components. Traditional methods of cell fractionation and immunoelectron microscopy are being complemented by non-invasive, versatile techniques including confocal microscopy coupled with GFP labeling, deconvolution, and video using CCD cameras. The ability to study live cells without fixation or permeablization has

resulted in new information about cell structure and dynamics (Boevink et al., 1998). In some cases, the use of GFP has revealed previously unknown structures (Collings et al., 2000; Kohler, 1998) or resolved ambiguities in the literature (Gillespie et al., 2001; Heinlein et al., 1998; Oparka et al., 1997).

While GFP has been a boon to cell biology, it is not an appropriate protein tag for all experimental systems. Fusion of GFP to structural proteins can alter their properties, preventing self-interaction as dimers and multimers and leading to loss of fusion protein function and spurious localizations (Katz et al., 1998; Thomas and Maule, 2000). In addition, peptides fused to GFP can be degraded without loss of fluorescence, causing free GFP to accumulate in the cytoplasm and the vacuole, obscuring the true localization of the peptides (Persson et al., 2002). When expressed in the cytoplasm of transgenic plants, GFP can inhibit regeneration of transformants. This could be due to toxicity from fluorescence-related free radicals (Haseloff and Amos, 1995; Haseloff et al., 1997). Finally, the fluorescence of GFP is inhibited at low pH (<6) (Scott et al., 1999) making it inconvenient for studies of the cell wall or vacuole.

Plant virus polymerase localizations

The replication of positive strand RNA viruses takes place in association with host membranes. This membrane localization has been shown to be required for replication (Rohozinski and Hancock, 1996; Carette et al., 2000). The specific type of membrane system utilized in assembling the viral replication complex depends on the individual virus, and is likely to be genetically

determined (Burgyan et al., 1996; Rubino and Russo, 1998). Within the plant virus family *Tombusviridae*, which includes RCNMV, peroxisomes and mitochondria are the sites of replication for *Tomato bushy stunt virus* (TBSV) (Scholthof et al., 1995b) *Carnation Italian ringspot virus* (CIRV) (Rubino et al., 2000) and *Cymbidium ringspot virus* (CymRSV) (Burgyan et al., 1996). No members of the *Tombusviridae* have previously been shown to associate with the endoplasmic reticulum (ER).

In other virus families, it is common to find polymerase proteins associated with the ER, the most abundant membrane form in the plant cell. Very few viruses have been localized to subcellular structures, and it is not yet possible to say whether this likelihood indicates a taxonomic trend or is merely a coincidence. Picorna-like viruses including *Cowpea mosaic virus* (CPMV) (Carette et al., 2000) and *Tobacco etch virus* (TEV) (Schaad et al., 1997) and Alpha-like viruses including *Brome mosaic virus* (BMV) (Oparka et al., 1996), *Tobacco mosaic virus* (TMV) (dos Reis Figureira, 2002; Mas and Beachy, 1999), and *Peanut clump virus* (PCV, family *Pecluvirus)* (Dunoyer et al., 2002) all direct replication proteins to the ER.

Viruses can be found replicating on most other subcellular membranes as well. Invaginations of the chloroplast outer membrane are associated with *Turnip yellow mosaic virus* (TYMV, family *Tymovirus)* replication and assembly (Prod'homme et al., 2001; Rohozinski and Hancock, 1996), while *Alfalfa mosaic virus* (AMV) replication proteins interact at the vacuolar membrane (Van Der Heijden et al., 2001).

Involvement of host factors

Plant viral replication complexes often co-purify with host components, and genetic screens have identified host mutations that impair viral accumulation (Callaway, 1998; Sullivan and Ahlquist, 1997; Mouches et al., 1984; Hayes and Buck, 1990). The proteins encoded in viral genomes are often the core catalytic domains of the polymerase. Viruses rely on recruited host proteins to provide accessory functions, such as separation of transcription and translation or topoisomerase activity (van der Heijden and Bol, 2002). Identification of the host factors involved in virus replication gives greater understanding of the cellular processes that enable virus infection. Unfortunately, very few host factors have been identified, and of those that are known, the role in viral replication is understood for an even smaller number.

The only virus for which the composition of the replication complex is completely known is the bacteriophage Qâ. A model for replication of the phage RNA that includes the phage-encoded core polymerase subunit and four host-encoded proteins has been proposed (Brown and Gold, 1996). The holoenzyme initially includes three host translation factors: ribosomal protein S1, elongation factor Tu (EF-Tu) and elongation factor Ts (EF-Ts) (Blumenthal et al., 1972). A fourth factor, known as host factor (HF-1), is recruited to initiate minus strand synthesis (Barrera et al., 1993). The host proteins apparently function as dual function transcription/translation factors, bringing the necessary components into

proximity for transcription while excluding the translation machinery until it is needed. The same factors later promote translation (Brown and Gold, 1996).

For eukaryotic (+) strand RNA viruses, the manner in which host factors facilitate viral replication is largely unknown. Host factors have been co-purified with the replicase complex of *Turnip yellow mosaic virus,* (Mouches et al., 1984) and *Cucumber mosaic virus*, (Hayes and Buck, 1990), but the identity of these proteins is unknown, and their role in replication unclear. Many of the identified host factors bind to viral RNA, viral proteins, or both. The protein- and RNA-binding proteins are hypothesized to aid replication by separating transcription and translation in time, or by promoting template selection. For example, BMV replication and accumulation in yeast is dependent on *mab1-1*, *mab2-1*, and *mab3-1*. *mab1-1* and *mab2-1* interfere with the ability of BMV 1a to stimulate 2a mRNA and protein accumulation (Ishikawa et al., 1997). The *mab-1* complementation group encodes Lsm1p, a yeast protein related to core RNA splicing factors (Diez et al., 2000). The Lsm1p protein is required for template selection by BMV 1a, the catalytic polymerase subunit. It was suggested that Lsm1p's connection with poly-(A) function indicates an interaction with factors binding RNA 5' ends, which could suggest a mode of interaction with BMV (van der Heijden and Bol, 2002; Diez et al., 2000).

BMV 2a protein associates with barley eukaryotic initiation factor 3 (eIF-3) subunit p41 (Quadt et al., 1993), resulting in a 3-fold stimulation of (-) strand synthesis *in vitro*. The known functions of eIF-3 include binding mRNA and tRNA and stabilization of the ribosome complex (Moldave, 1985). In addition, the yeast

eIF-3 subunit GCD10 (the RNA-binding subunit) binds the methyltransferase domain of TMV126/183 kDa replicase proteins (Osman and Buck, 1997; Taylor and Carr, 2000). Cucumber poly-(A) binding protein specifically interacts with the RdRp of *Zucchini yellow mosaic virus* (Wang et al., 2000) and the TEV-Oxnard strain NIa protein, which can confer host genotype-specific movement functions, interacts with tomato eIF-4E (Schaad et al., 2000). A relationship between protein biosynthesis and viral replication has been proposed based on the presence of functional tRNA-like structures on many viral RNAs (for a review see (Mans et al., 1991)). Host translation factors that are utilized by the virus as RNA binding proteins and transcriptional regulators may be the bridge between the host and the virus.

A second class of identified host proteins includes membrane binding or trafficking proteins like TOM1 from *Arabidopsis* that interacts with the helicase domain of the TMV replicase (Yamanaka et al., 2000). TOM1 has been cloned and is predicted to be a multipass transmembrane protein. TOM1 interacts with membranes in an *in vitro* assay, and may be the membrane anchor for the assembling TMV replication complex (Yamanaka et al., 2000). BMV requires the yeast OLE1 gene, which encodes Ä9 fatty acid desaturase (Lee et al., 2001). It was shown that the proper lipid composition of the membrane is necessary for replication, rather than the OLE1 gene product. Mutant *ole1* yeast blocked BMV replication prior to the initiation of (-) strand synthesis (Lee et al., 2001).

Carette et al. (2002) used a yeast two-hybrid screen to identify two proteins that specifically interact with the CPMV ‘60K’ protein, the nucleotide-

binding domain of the polymerase plus the Vpg. VAP27-1 and VAP27-2 are *Arabidopsis* proteins thought to be SNARE- like proteins that function in vesicle targeting and trafficking (Carette et al., 2002). The two VAP proteins can form multimers in protoplasts, and other SNARE-like proteins are known to form multimers through coiled-coil regions or transmembrane domains (Weir et al., 2001). The VAP27-1 and –2 proteins localized to the ER in a yeast transient expression assay, suggesting that they may play a role in vesicular transport to or from the ER. Proliferation of the ER is characteristic of CPMV infections (Carette et al., 2000), and expression of the '60K' protein induced dramatic vesiculation of yeast membranes (Carette et al., 2002). It has been speculated that 60K interference with VAP protein function could mediate this membrane proliferation.

Even in the instances where the host factors contribute to the localization of the replication complex by serving as the membrane anchor or altering the lipid composition of the membrane, the virus-encoded components of the replication complex independently localize to the proper intercellular membrane (Lee et al., 2001; Yamanaka et al., 2000). Further elucidation of the cellular conditions necessary for productive viral infections may shed light on how the viral and host proteins assemble together on the correct membrane and how the membrane association facilitates replication of the virus and production of progeny virus particles.

Localization of viral genes with GFP

The use of GFP to observe intercellular structures and proteins is still an emerging technology. Many of the subcellular localization studies previously performed on viral proteins utilized biochemical techniques such as tissue and cell fractionation, electron microscopy combined with immunolocalization, or histochemical staining. These methods all have the disadvantage that the cells are disrupted and/or fixed prior to observation, and the risk of preparation artifacts is high (Niwa et al., 1999). It is also impossible to observe the cells in real time as they respond to viral invasion. The use of GFP as a non-invasive label allows observations of subcellular structures via confocal microscopy in live cells. It is possible to tag nearly any protein with GFP (Chalfie et al., 1994), and virus researchers have made use of it to label the MP, CP, and polymerase, as well as other viral accessory proteins. The viruses that have been investigated with this technology do not fall easily into categories. There does not seem to be any correlation between taxonomy and intercellular localization of viral proteins. An overview of some viruses that have been investigated using GFP tags and the results of those investigations is presented.

movement protein:GFP Perhaps the single most intensely studied virus with respect to protein localization is *Tobacco mosaic virus* (TMV). This virus system is also the best example of the potential of GFP as a cell biology tool. The use of GFP in this system has supplanted traditional biochemistry and yielded discoveries that might not have been possible any other way. Research using

TMV MP:GFP from many researchers is presented and discussed to illustrate the effectiveness of GFP as a non-invasive reporter (reviewed in Beachy and Heinlein, 2000). Research using other viral MPs is also discussed to highlight themes in MP localization.

TMV MP:GFP was shown to localize to the cortical ER, plasmodesmata, and microtubules at different times during infection (Heinlein et al., 1998). MP initially localizes to plasmodesmata (Pd), modifying their size exclusion limit (Heinlein et al., 1998). After approximately 12 hours, MP accumulates at the ER, where viral replication and protein synthesis occurs (Mas and Beachy, 1998). The ER localization of the MP:GFP is not required for the MP to function in intercellular movement of viral RNA (Boyko et al., 2000).

Approximately 16 hours post infection, the MP relocates to the underlying microtubule network, where it directs the movement of the viral genome and proteins to adjacent cells and long-distance (Heinlein et al., 1998; Mas and Beachy, 1998). MP targets microtubules and plasmodesmata by independent mechanisms, and intercellular transport of viral RNA (vRNA) depends on the localization of MP to Pd at the leading edge of infection (Boyko et al., 2000).

Tobamovirus MPs bind a specific consensus sequence on microtubules, and may utilize microtubule assembly to drive viral RNA transport within the cell (Boyko et al., 2000). Additionally, it was later found using fusions of TMV MP to both GFP from *Aequoria* and DsRed from *Discosoma* that the MP specifically localizes only to the ER during the early stages of infection, and later transfers from the ER to the underlying microtubule network. A single amino acid mutation

prevents transfer of MP to microtubules. This mutant fails to localize to microtubules while exhibiting enhanced movement. It is possible that the mutant evades a host degradation pathway in which microtubules normally target ubiquitinated MP to the proteasome (Gillespie et al., 2001).

No other virus MPs have been investigated as extensively as the TMV MP. Several virus families are represented among those others that have been investigated, and a few themes emerge. MPs often target to punctate spots at the cell periphery, generally assumed to be plasmodesmata. The MPs of *Apple chlorotic leafspot virus* (ACLV) (Yoshikawa et al., 1999), *Alfalfa mosaic virus* (AlMV) (Huang and Zhang, 1999), and *Cucumber mosaic virus* (CMV) (Itaya et al., 1997) have all been localized to the cell periphery using GFP. In addition, tubules containing MP can form at the periphery of protoplasts, usually projecting from the GFP:MP punctate bodies. ACLV GFP-50kDa (Satoh et al., 2000) and *Cauliflower mosaic virus* (CaMV) MP:GFP fusions (Huang et al., 2001) both produce surface tubules. Some MPs can target the endomembrane system, perhaps for transport to the plasmodesmata. AMV MP:GFP fusions co-localized with the ER of the plant cells but did not induce tubule formation (Huang and Zhang, 1999).

In viruses that have multiple movement proteins, one protein generally traffics to the ER and another targets the periphery. This implies a division of labor and may indicate that the localization is necessary for or dependent upon function. For example, GFP was used to localize the second and third genes of the *Poa semilatent hordeivirus* (PSLV) triple gene block. A TGBp2 15k:GFP

fusion localized to the cortical ER. The TGBp3 18k :GFP fusion protein localized to punctate spots at the periphery of the cells. TGBp2 15k:GFP co-expressed with TGBp3 18k (native) was re-directed to the peripheral bodies. No sequence dependency was found for this targeting. In addition, TGBp2 proteins were shown to effectively target heterologous TGBp2 proteins from to the cell periphery, suggesting that the targeting is part of a generalized mechanism (Solovyev et al., 2000).

There are more examples, but those cited here illustrate that viral MPs use several common mechanisms to solve the problem of how to escape from the initially infected cell. The other viral proteins are not so amenable to analysis, and often there is no discernable pattern to their localizations.

One exception to the pattern of ER/plasmodesmata localization of GFP:MP fusions should be noted. GFP fusions have been used to investigate intra- and intercellular movement of *Maize streak virus* (MSV) movement protein, V1. Geminiviruses are ssDNA viruses. The V1:GFP protein moved from cell-to-cell on bombarded tobacco or maize leaves in the absence of other viral proteins, but did not localize to the Pd in either maize or tobacco (Kotlizky et al., 2000). It is possible that the ER/Pd targeting of MP is a feature of RNA viruses only.

polymerase:GFP Although the positive strand RNA viruses studied to date all utilize intercellular membranes in their replication complexes, the mechanisms of replication are unknown in many viruses, and the factor that indicates which membrane will host replication is equally elusive. As mentioned above in the

discussion of viral polymerases, it is common for polymerase proteins to target the ER, and many that have been investigated with GFP do. CIRV and CymRSV are the only examples of a GFP-polymerase fusion targeting to a membrane other than the ER.

BMV has been studied most extensively, and will serve as the detailed example here. In this case, GFP fusions have served to complement and extend results obtained using traditional methods.

BMV has two replication proteins, 1a and 2a. The two proteins are expressed from separate RNAs, and have been shown to form a 1:1 bimolecular complex *in vitro* (Kao and Ahlquist, 1992b). The interaction of 1a and 2a is necessary for replication (Kao et al., 1992). The sequences required for the 1a protein to bind the 2a protein reside in the C- terminal helicase-like domain of 1a. This domain is highly resistant to proteases, while the 1a N-terminus is rapidly degraded. This protected domain is found in other tripartite virus polymerases and is probably important for the interaction between 1a and 2a and hence for replication (O'Reilly et al., 1995).

GFP was fused to the 1a protein to investigate the interaction of 1a and 2a. The GFP:1a associated with the cytoplasmic face of the ER, with no lumenal protrusions. A region C-terminal to the core methyltransferase was sufficient for ER localization. Additional sequences within 1a acted as modifiers, narrowing the ER domains targeted by 1a (den Boon et al., 2001).

GFP was also fused to the 2b protein. When expressed alone, GFP:2b showed a cytoplasmic distribution similar to free GFP. When expressed in the

presence of BMV 1a, the GFP:2a localized to the ER. The N-terminal 120 aa of 2a that interacts with 1a is necessary and sufficient for directing 2a to the ER. As the interaction between 1a and 2a is essential for RNA replication *in vivo*, these results suggest that BMV 1a directs the assembly and organization of the replication complex (Chen and Ahlquist, 2000; Kao and Ahlquist, 1992b; O'Reilly et al., 1995).

Yeast (*S. cerevisiae*) strains that express BMV 1a, 2a and RNA 3 from expression plasmids have been created. These cells form active BMV replication complexes (Restrepo-Hartwig and Ahlquist, 1999). 1a and 2a were shown to co-localize to the ER in the yeast cells, as they do in plants, establishing the yeast system as a good model for a natural plant infection. 1a and 2a remained in the ER and did not accumulate in the Golgi apparatus. In addition, incorporation of BrUTP showed that nascent vRNA co-localized with BMV 1a. This suggests that the observed sites of 1a and 2a accumulation represented sites of active viral replication (Restrepo-Hartwig and Ahlquist, 1999).

This engineered yeast was used to demonstrate that BMV replication depends on fatty acid synthesis. In yeast, a mutation of the chromosomal *OLE 1* gene severely inhibits BMV replication (Lee et al., 2001). *OLE 1* encodes Δ9 fatty acid desaturase, an ER integral membrane protein and the first enzyme in unsaturated fatty acid synthesis (Stukey et al., 1990). In *ole1* mutant yeast, BMV 1a and 2a still interact and localize to the ER correctly and bind RNA templates, but RNA replication is blocked prior to the initiation of minus strand synthesis. Mutation analysis showed that fatty acids are required for BMV replication rather

than the *OLE1* gene product. This demonstrates that viral RNA synthesis is very sensitive to lipid composition and that the correct membrane fluidity is important for an early step in viral replication (Lee et al., 2001).

Tobacco mosaic virus 126 kDa replicase protein has been shown to be associated with the ER (dos Reis Figueira et al., 2002) via 126 kDa:GFP fusions. Both a nuclear localization signal located in the N-terminal 70 amino acids and an ER-association domain in the C-terminal half of the protein have an effect on localization. The nuclear localization signal appears to modify the ER localization and cause the replicase protein to form inclusions associated with the ER.

In addition to BMV, TEV (Schaad et al., 1997) and PCV (Dunoyer et al., 2002) have been localized to the ER using GFP fusions of polymerase genes. The PCV localization is interesting because multivesicular bodies (MVBs) that contained pinched and broken ER membranes were observed (Dunoyer et al., 2002), suggesting that viral replication caused disruption of the ER membranes.

In an example of a viral polymerase that targets a membrane other than the ER, GFP was fused to the CIRV 36 kDa protein to study the topology of the polymerase complex in association with the mitochondrial membrane. The 36 kDa:GFP fusions were expressed in *S. cerevisiae* to analyze the distribution of 36k in the absence of a virus infection. The fluorescence was observed in a defined part of the cytoplasm, with some fluorescence in structures representing mitochondria (Rubino et al., 2000). The polymerase of a very closely related virus, CymRSV, localizes to the peroxisomes. It was shown that the organelle targeting sequence is located in the 33 kDa (CIRV) or 36 kDa (CymRSV) protein

encoded by ORF 1 (Rubino and Russo, 1998). These proteins have high sequence identity to RCNMV p27. It is possible that p27 performs a similar function.

structural genes:GFP Most often GFP is fused to the coat protein of viruses, resulting in labeled virus particles. The fluorescence is a visible indication of tissues harboring the virus. In some cases, particularly when GFP was first introduced, GFP was simply expressed from the virus, as part of the polyprotein, or from a subgenomic promoter. When expressed this way, GFP is not fused to any viral gene, and simply tracks the movement of the virus. As might be expected, no specific subcellular localization is observed in these studies. In cases where the CP is labeled and expressed independently of the virus, no correlation can be drawn between the taxonomy of the virus and the localization. PVX (Oparka et al., 1996), *Potato leaf roll virus* (PLRV) (Nurkiyanova et al., 2000), and *Lettuce mosaic virus* (LMV-E) (German-Retana et al., 2000) have been studied with GFP, among others.

Concluding remarks

In an effort to increase our understanding of RCNMV replication mechanisms, we undertook a study of the intercellular localization of p27 and p88 (Figure 1). It has previously been shown that p27 and p88 are the viral contribution to the replication complex. In association with host proteins and utilizing a host membrane (Bates et al., 1995) RCNMV produces viral RNA,

proteins, and progeny virus. Knowledge of which membranes are used, how they are modified, and why membranes are required would increase our understanding of viral replication mechanisms and could inspire antiviral compounds or technologies. To investigate our hypothesis that p27 and p88 specifically interact during infection and that such interaction takes place at the ER, it was necessary to label the replicase proteins and observe their location during infection. In order to observe p27 and p88 in live plant cells, fusions were made to the green fluorescent protein of *A. victoria* (Heim et al., 1994). Both p27 and p88 localized specifically and independently to ER in *N. benthamiana* epidermal cells. In addition, p27 and p88 were observed associated with tubules of ER traversing the nucleus. Multi-vesicular bodies formed near the nuclei of cells expressing p27 and p88, and were also observed in the cytoplasm. In general, presence of a viral protein caused thickening and distortion of the ER, as well as brightly fluorescent inclusion bodies. I demonstrated that foreign proteins can enter ER tubules inside the nucleus, which may provide access to transcription factors and other host proteins appropriated by the virus replication machinery.

References

ALBERTS, B., BRAY, D., LEWIS, J., RAFF, M., ROBERTS, K., and WATSON, J. (1994). "Molecular biology of the cell." Garland Publishing, Inc., New York.

ALLEN, N. S., and BROWN, D. (1988). Dynamics of the endoplasmic reticulum in living onion epidermal cells in relation to microtubules, microfilaments and intracellular particle movement. *Cell Motil Cytoskel* **10,** 153-163.

ALLEN, N. S., and SCHUMM, J. H. (1990). Endoplasmic reticulum, calciosomes and their possible roles in signal transduction. *Protoplasma* **154,** 172-178.

ANGRES, B., and GREEN, G. (1999). Dual labeling using eCFP and eYFP in standard fluorescence microscopy. *Clontechniques*, April 1999, 28-9.

BARRERA, I., SCHUPPI, D., SOGO, J., and WEBER, H. (1993). Different mechanisms of recognition of bacteriophage Q beta plus and minus strand RNAs by Q beta replicase. *J Mol Biol* **232,** 512-521.

BATES, A. H., FARJAH, M., OSMAN, T. A. M., and BUCK, K. W. (1995). Isolation and characterization of an RNA-dependent RNA polymerase from *N. clevelandii* plants infected with *Red cover necrotic mosaic dianthovirus*. *J Gen Virol* **76,** 1483-91.

BEACHY, R. N., AND HEINLEIN, M. (2000) Role of P30 in replication and spread of TMV. *Traffic* **1**, 540-544.

BLUMENTHAL, T., LANDERS, T. A., and WEBER, K. (1972). Bacteriophage Q beta replicase contains proteins biosynthesis elongation factors EF Tu and EF Ts. *Proc Natl Acad Sci U S A* **69,** 1313-1317.

BOEVINK, P., OPARKA, K., SANTA CRUZ, S., MARTIN, B., BETTERIDGE, A., and HAWES, C. (1998). Stacks on tracks: the plant Golgi apparatus traffics on an actin/ER network. *Plant Journal* **15,** 441-447.

BOYKO, V., VAN DER LAAK, J., FERRALLI, J., SUSLOVA, E., KWON, M. O., and HEINLEIN, M. (2000). Cellular targets of functional and dysfunctional mutants of tobacco mosaic virus movement protein fused to green fluorescent protein. *J Virol* **74,** 11339-11346.

BROWN, D., and GOLD, L. (1996). RNA replication by Q beta replicase: a working model. *Proc Natl Acad Sci U S A* **93,** 11558-11562.

BUCHANAN, B. B., GRUISSEM, W., JONES, R. L., (2000). Chapter 1: Membrane structure and membranous organelles. First ed. *In* "Biochemistry and molecular biology of plants". Courier Companies, Inc.

BUCK, K. W. (1996). Comparison of the replication of positive-stranded RNA viruses of plants and animals. *Adv Virus Res* **47,** 159-213.

BURGYAN, J., RUBINO, L., and RUSSO, M. (1996). The 5' terminal region of a tombusvirus determines the origin of multivesicular bodies. *J Gen Virol* **77,** 1967-1974.

CALLAWAY, A. S. (1998). PhD. A genetic approach to study host factors of Arabidopsis thaliana that influence susceptibility to Cauliflower mosaic virus. Cornell University, Ithaca, NY.

CARETTE, J. E., STUIVER, M., VAN LENT, J., WELLINK, J., and VAN KAMMEN, A. (2000). Cowpea mosaic virus infection induces a massive proliferation of endoplasmic reticulum but not Golgi membranes and is dependent on de novo membrane synthesis. *J Virol* **74,** 6556-6563.

CARETTE, J. E., VERVER, J., MARTENS, J., VAN KAMPEN, T., WELLINK, J., and VAN KAMMEN, A. (2002). Characterization of plant proteins that interact with cowpea mosaic virus '60K' protein in the yeast two-hybrid system. *J Gen Virol* **83,** 885-893.

CHALFIE, M., TU, Y., EUSKIRCHEN, G., WARD, W. W., and PRASHER, D. (1994). Green fluorescent protein as a marker for gene expression. *Science* **263,** 802-805.

CHECK, E. (2002). Will the real Golgi please stand up. *Nature* **416,** 780-781.

CHEN, J., and AHLQUIST, P. (2000). Brome mosaic virus polymerase-like protein 2a is directed to the endoplasmic reticulum by helicase-like viral protein 1a. *J Virol* **74,** 4310-4318.

COLE, N. B., and LIPPINCOTT-SCHWARTZ, J. (1995). Organization of organelles and membrane traffic by microtubules. *Curr Opin Cell Biol* **7,** 55-64.

COLLINGS, D., ASADA, T., ALLEN, N., and SHIKOBA, H. (1998). Plasma-membrane associated actin in bright yellow 2 tobacco cells. Evidence for interaction with microtubules. *Plant Physiol* **118,** 917-928.

COLLINGS, D. A., CARTER, C. N., RINK, J. C., SCOTT, A. C., WYATT, S., and ALLEN, N. S. (2000). Plant nuclei can contain extensive grooves and invaginations. *Plant Cell* **12,** 2425-2439.

CRAMERI, A., WHITEHORN, E. A., TATE, E., and STEMMER, W. P. C. (1996). Improved green fluorescent protein by molecular evolution using DNA shuffling. *Nature Biotechnol* **14,** 315-319.

CSORDAS, G., THOMAS, A. P., and HANJANOCKY, G. (1999). Quasi-synaptic calcium signal transmission between endoplasmic reticulum and mitochondria. *EMBO J* **4,** 96-108.

CUBITT, A. B., HEIM, R., ADAMS, S. R., BOYD, A. E., GROSS, L. A., and TSIEN, R. Y. (1995). Understanding, improving and using green fluorescent proteins. *TIBS* **November,** 449-455.

DAVIS, S. J., and VIERSTRA, R. D. (1998). Soluble, highly fluorescent variants of green fluorescent protein (GFP) for use in higher plants. *Plant Mol Biol* **36,** 521-528.

DEN BOON, J. A., CHEN, J., and AHLQUIST, P. (2001). Identification of sequences in brome mosaic virus replicase protein 1a that mediate association with endoplasmic reticulum membranes. *J Virol* **75,** 12370-12381.

DIEZ, J., ISHIKAWA, M., KAIDO, M., and AHLQUIST, P. (2000). Identification and characterization of a host protein required for efficient template selection in viral RNA replication. *Proc Natl Acad Sci U S A* **97,** 3913-3918.

DOS REIS FIGUEIRA, A., GOLEM, S., GOREGAOKER, S. P., AND CULVER, J. S. (2002). A nuclear localization signal and a membrane association domain contribute to the localization of the *Tobacco mosaic virus* 126-kDa replicase protein. Virology **301**, 81-89

DUNOYER, P., RITZENTHALER, C., HEMMER, O., MICHLER, P., and FRITSCH, C. (2002). Intracellular localization of the *Peanut clump virus* replication complex in tobacco BY-2 protoplasts containing green fluorescent protein-labeled endoplasmic reticulum or golgi apparatus. *J Virol* **76,** 865-874.

ELLENBERG, J., SIGGIA, E., MORIERA, J. E., SMITH, C., PRESLEY, J., WORMAN, H., and LIPPINCOTT-SCHWARTZ, J. (1997). Nuclear membrane dynamics and reassembly in living cells: targeting of an inner nuclear membrane protein in interphase and mitosis. *J Cell Biol* **136,** 1193-1206.

FRANCKI, R., MILNE, R., and HATTA, T. (1985). "Atlas of plant viruses.", II CRC Press, Boca Raton, FL.

FRICKER, M., HOLLINSHEAD, M., WHITE, N., and VAUX, D. (1997). Interphase nuclei of many mammalian cell types contain deep, dynamic, tubular membrane-bound invaginations of the nuclear envelope. *J Cell Biol* **136,** 531-544.

FUJIWARA, T., GEISMAN-COOKMEYER, D., DING, B., LOMMEL, S. A., and LUCAS, W. J. (1993). Cell-to-cell trafficking of macromolecules through plasmodesmata potentiated by the red clover necrotic mosaic virus protein. *Plant Cell* **5,** 1783-1794.

GEISMAN-COOKMEYER, D., SILVER, S., VAEWHONGS, A. A., LOMMEL, S. A., and DEOM, C. M. (1995). Tobamovirus and dianthovirus movement proteins are functionally homologous. *Virology* **213,** 38-45.

GERMAN-RETANA, S., CANDRESSE, T., ALIAS, E., DELBOS, R. P., and LE GALL, O. (2000). Effects of green fluorescent protein or beta-glucuronidase tagging on the accumulation and pathogenicity of a resistance-breaking Lettuce mosaic virus isolate in susceptible and resistant lettuce cultivars. *Mol Plant Microbe Interact* **13,** 316-324.

GILLESPIE, T., TOTH, R. L., HAUPT, S., BOEVINK, P., ROBERTS, A. G., CHAPMAN, S., and OPARKA, K. (2001). *Plasmodesma 2001 Fourth International Conference, Capetown South Africa*.

GRABSKI, S., FEIJTER, A. W., and SCHINDLER, M. (1993). Endoplasmic reticulum forms a dynamic continuum for lipid diffusion between contiguous soybean root cells. *Plant Cell* **5,** 25-38.

GREBENOK, R., LAMBERT, G., and GALBRAITH, D. W. (1997). Characterization of the targeted nuclear accumulation of GFP within the cells of transgenic plants. *Plant J* **12,** 685-696.

GUNNING, B. (1998). The identity of mystery organelles in *Arabidopsis* plants expressing GFP. *Trends Plant Sci* **3,** 417.

HAMILTON, R. I., and TREMAINE, J. H. (1996). Dianthoviruses: properties, molecular biology, ecology and control. *In* "The Plant Viruses, Volume 5: Polyhedral virions and bipartite RNA genomes" (B. D. Harrison, and A. F. Murant, Eds.), Vol. 5, pp. 251-281. Plenum Press, New York.

HARRIS, N. (1979). Endoplasmic reticulum in developing seeds of *Vicia faba*. A high voltage electron microscope study. *Planta* **146,** 63-69.

HASELOFF, J., and AMOS, B. (1995). GFP in plants. *Trends Genetics* **11,** 328-329.

HASELOFF, J., SIEMERING, K. R., PRASHER, D., and HODGE, S. (1997). Removal of a cryptic intron and subcellular localization of green fluorescent protein are required to mark transgenic *Arabidopsis* plants brightly. *Proc Natl Acad Sci U S A* **94,** 2122-2127.

HAWES, C., and SATIAT-JEUNEMAITRE, B. (2001). Trekking along the cytoskeleton. *Plant Physiol* **125,** 119-122.

HAYES, R., and BUCK, K. W. (1990). Complete replication of a eukaryotic virus RNA *in vitro* by a purified RNA dependent RNA polymerase. *Cell* **63,** 363-368.

HEIM, R., PRASHER, D., and TSIEN, R. Y. (1994). Wavelength mutations and posttranslational oxidation of green fluorescent protein. *Proc Natl Acad Sci U S A* **91,** 12501-12504.

HEIM, R., and TSIEN, R. Y. (1996). Engineering green fluorescent protein for improved brightness, longer wavelengths and fluorescence resonance energy transfer. *Curr Biol* **6,** 178-182.

HEINLEIN, M., PADGETT, H. S., GENS, J. S., PICKARD, B. G., CASPER, S. J., EPEL, B. L., and BEACHY, R. N. (1998). Changing patterns of localization of the tobacco mosaic virus movement protein and replicase to the endoplasmic reticulum and microtubules during infection. *Plant Cell* **10,** 1107-1120.

HEPLER, P. K. (1981). The structure of the endoplasmic reticulum revealed by osmium tetroxide-potassium ferricyanide staining. *Eur J Cell Biol* **26,** 102-110.

HEPLER, P. K., PALEVITZ, B. A., LANCELLE, S. A., MCCAULEY, M. M., and LICHTSCHLEIDL, I. (1990). Cortical endoplasmic reticulum in plants. *J Cell Sci* **96,** 355-373.

HORSLEY, D., COLEMAN, J., EVANS, D., CROOKS, K., PEART, J., SATIAT-JEUNEMAITRE, B., and HAWES, C. (1993). A monoclonal antibody, JIM 84, recognises the golgi apparatus and plasma membrane in plant cells. *J Exp Bot* **44,** 223-229.

HUANG, M., and ZHANG, C. L. (1999). Association of the movement protein of alfalfa mosaic virus with the endoplasmic reticulum and its trafficking in epidermal cells of onion bulb scales. *Mol Plant-Microbe Interact* **12,** 680-90.

HUANG, Z., HAN, Y., and HOWELL, S. H. (2001). Effects of movement protein mutations on the formation of tubules in plant protoplasts expressing a fusion between the green fluorescent protein and Cauliflower mosaic virus movement protein. *Mol Plant Microbe Interact* **14,** 1026-31.

HULL, R. (2002). "Matthews' Plant Virology." 4 ed. Academic Press, New York.

ISHIKAWA, M., DIEZ, J., RESTREPO-HARTWIG, M., and AHLQUIST, P. (1997). Yeast mutations in multiple complementation groups inhibit brome mosaic virus RNA replication and transcription and perturb regulated expression of the viral polymerase-like gene. *Proc Natl Acad Sci U S A* **94,** 13810-13815.

ITAYA, A., HICKMAN, H., BAO, Y., NELSON, R. S., and DING, B. (1997). Cell-to-cell trafficking of cucumber mosaic virus movement protein:green fluorescent protein fusion produced by biolistic gene bombardment in tobacco. *Plant J* **12**(5)**,** 1223-1230.

JEDD, G., and CHUA, N. H. (2002). Visualization of peroxisomes in living plant cells reveals acto-myosin-dependent cytoplasmic streaming and peroxisome budding. *Plant Cell Physiol* **43,** 384-392.

KAO, C. C., and AHLQUIST, P. (1992b). Identification of the domains required for direct interaction of the helicase-like and polymerase-like RNA replication proteins of brome mosaic virus. *J Virol* **66,** 7293-7302.

KAO, C. C., QUADT, R., HERSHBERGER, R., and AHLQUIST, P. (1992). Brome mosaic virus RNA replication proteins 1a and 2a form a complex in vitro. *J Virol* **66,** 6322-6329.

KATZ, B., KRYLOV, D., AOTA, S., OLIVE, M., VINSON, C., and YAMADA, K. (1998). Green fluorescent protein labeling of the cytoskeletal structures- novel targeting approach based on leucine zippers. *Biotechniques* **25,** 289-304.

KIM, K. H., and LOMMEL, S. A. (1994). Identification and analysis of the site of -1 ribosomal frameshifting in red clover necrotic mosaic virus. *Virology* **200,** 574-582.

KNEBEL, W., QUADER, H., and SCHNEPF, E. (1990). Mobile and immobile endoplasmic reticulum in onion bulb epidermis cells: short- and long-term observations with a confocal laser scanning microscope. *Eur J Cell Biol* **52,** 328-340.

KOENIG, R., LESEMANN, D., and BURGERMEISTER, W. (1988). Isolation of carnation ringspot virus from a canal near a sewage plant: cDNA hybridization analysis, serology and cytopathology. *J Phytopathol* **121,** 346.

KOHLER, R. H. (1998). GFP for *in vivo* imaging of subcellular structures in plant cells. *Trends Plant Sci* **3,** 317-20.

KOHLER, R. H., CAO, J., ZIPFEL, W. R., WEBB, W. W., and HANSON, M. R. (1997). Exchange of protein molecules through connections between higher plant plastids. *Science* **276,** 2039-2042.

KOONIN, E. V. (1991). The phylogeny of RNA-dependent RNA polymerases of positive strand RNA viruses. *J Gen Virol* **72,** 2197-2206.

KOTLIZKY, G., BOULTON, M. I., PITAKSUTHEEPONG, C., DAVIES, J. W., and EPEL, B. L. (2000). Intracellular and intercellular movement of maize streak geminivirus V1 and V2 proteins transiently expressed as green fluorescent protein fusions. *Virology* **274,** 32-38.

LEE, W.-M., ISHIKAWA, M., and AHLQUIST, P. (2001). Mutation of Host delta-9 fatty acid desaturase inhibits brome mosaic virus RNA replication between template recognition and RNA synthesis. *J Virol* **75,** 2097-2106.

LEFFEL, S. M., MABON, S. A., and STEWART, C. N., JR. (1997). Applications of green fluorescent protein in plants. *Biotechniques* **23,** 912-918.

LICHTSCHEIDL, I. K., LANCELLE, S. A., and HEPLER, P. K. (1990). Actin-endoplasmic reticulum complexes in Drosera: their structural relationship with the plasmalemma, nuclei and organelles. *Protoplasma* **155,** 116-126.

LOMMEL, S. A., WESTON-FINA, M., and LOMOMOSSOFF, G. P. (1988). The nucleotide sequence and gene organization of red clover necrotic virus RNA-2. *Nucleic Acids Res* **16,** 8587-8602.

LUI, P., KONG, S. K., KWOK, T. T., and LEE, C. Y. (1998a). The nucleus of HeLa cells contains tubular structures for calcium signaling. *Biochem Biophys Res Commun* **247,** 88-93.

MANS, R., PLEIJ, C., and BOSCH, L. (1991). t-RNA like structures. Structure, function and evolutionary significance. *Eur J Biochem* **201,** 303-324.

MAS, P., and BEACHY, R. N. (1998). Distribution of TMV movement protein in single living protoplasts immobilized in agarose. *Plant J* **15,** 835-842.

MAS, P., and BEACHY, R. N. (1999). Replication of tobacco mosaic virus on endoplasmic reticulum and role of the cytoskeleton in intercellular distribution of viral RNA. *J Cell Biol* **147,** 945-958.

MATTHEWS, R. E. F. (1991). "Plant Virology." Academic Press, Inc., San Diego, CA.

MILLER, D., SCHWARTZ, M., and AHLQUIST, P. (2001). Flock house virus RNA replicates on outer mitochondrial membranes in Drosophila cells. *J Virol* **75,** 11664-11667.

MIZUMOTO, H., HIKICHI, Y., and OKUNO, T. (2002). The 3'-untranslated region of RNA 1 as a primary determinant of temperature sensitity of Red clover necrotic mosaic virus Canadian strain. *Virology* **293,** 320-327.

MOLDAVE, K. (1985). Eukaryotic protein synthesis. *Annu Rev Biochem* **54,** 1109-1149.

MORISE, H., SHIMOMURA, O., JOHNSON, F. H., and WINANT, J. (1974). Intermolecular energy transfer in the bioluminescent system of *Aequoria*. *Biochemistry* **13,** 2656-2662.

MOUCHES, C., CANDRESSE, T., and BOVE, J. (1984). Turnip yellow mosaic virus RNA-replicase contains host and virus-encoded subunits. *Virology* **134,** 78-90.

MURPHY, F., FAUQUET, C., BISHOP, D., GHABRIAL, S., JARVIS, A., MARTELLI, G. P., MAYO, M. A., and SUMMERS, M. (1995). Virus Taxonomy, 6th report of the International Committee on the Taxonomy of Viruses.

NEBENFUEHR, A. (2001). Redistribution of Golgi stacks and other organelles during mitosis and cytokinesis in plant cells. *Plant Physiol* **124,** 135-151.

NEBENFUEHR, A., and STAEHELIN, L. A. (2001). Mobile factories: Golgi dynamics in plant cells. *Trends Plant Sci* **6,** 1360-1385.

NIWA, Y., HIRANO, T., YOSHIMOTO, K., SHIMIZU, M., and KOBAYASHI, H. (1999). Non-invasive quantitative detection and applications of non-toxic, S65T- type green fluorescent protein in living plants. *Plant J* **18,** 455-63.

NURKIYANOVA, K. M., RYABOV, E. V., COMMANDEUR, U., DUNCAN, G. H., CANTO, T., GRAY, S. M., MAYO, M. A., and TALIANSKY, M. E. (2000). Tagging potato leafroll virus with the jellyfish green fluorescent protein gene. *J Gen Virol* **81,** 617-26.

OPARKA, K., BOEVINK, P., and CRUZ, S. S. (1996). Studying the movement of plant viruses using green fluorescent protein. *Trends Plant Sci* **1,** 412-418.

OPARKA, K., ROBERTS, A. G., CRUZ, S. S., BOEVINK, P., PRIOR, D. A., and SMALLCOMBE, A. (1997). Using GFP to study virus invasion and spread in plant tissues. *Nature* **388,** 401-402.

O'REILLY, E. K., TANG, N., AHLQUIST, P., and KAO, C. C. (1995). Biochemical and genetic analyses of the interaction between the helicase-like and polymerase-like proteins of the brome mosaic virus. *Virology* **214,** 59-71.

OSMAN, T. A. M., and BUCK, K. W. (1990). Double-stranded RNAs isolated from plant tissue infected with red clover necrotic mosaic virus correspond to genomic and subgenomic single-stranded RNAs. *J Gen Virol* **71,** 945-948.

OSMAN, T. A. M., and BUCK, K. W. (1997). The tobacco mosaic virus RNA polymerase complex contains a plant protein related to the RNA-binding subunit of yeast eIF-3. *J Virol* **71,** 6075-6082.

PAJE-MANALO, L. L., and LOMMEL, S. A. (1989). Independent replication of red clover necrotic mosaic virus RNA-1 in electroporated host and non-host Nicotiana species protoplasts. *Phytopathology* **79,** 457-461.

PALM, G. J., ZDANOV, A., GAITANARIS, G. A., STAUBER, R. H., PAVLAKIS, G. N., and WLODAWER, A. (1997). The structural basis for spectral variations in green fluorescent protein. *Nat Struct Biol* **4,** 361-365.

PERSSON, S., LOVE, J., TSOU, P., ROBERTSON, D., THOMPSON, W. F., and BOSS, W. F. (2002). When a day makes a difference. Interpreting data from edoplasmic reticulum-targeted green fluorescent protein fusion in cells grown in tissue culture. *Plant Physiol* **128,** 341-344.

PRASHER, D., ECKENRODE, V. K., WARD, W. W., PRENDERGAST, F. G., and CORMIER, M. J. (1992). Primary structure of the *Aequoria victoria* green-fluorescent protein. *Gene* **111,** 229-233.

PROD'HOMME, D., LE PANSE, S., DRUGEON, G., and JUPIN, I. (2001). Detection and subcellular localization of the turnip yellow mosaic virus 66K replication protein in infected cells. *Virology* **281,** 88-101.

QUADT, R., KAO, C. C., BROWNING, K. S., HERSHBERGER, R. P., and AHLQUIST, P. (1993). Characterization of a host protein associated with brome mosaic virus RNA-dependent RNA polymerase. *Proc Natl Acad Sci U S A* **90,** 1498-1502.

RAGETLI, H. W. J., and ELDER, M. (1976). Characteristics of clover primary leaf necrosis virus, a new spherical isolate from *Trifolium pratense*. *Can J Bot* **55,** 2122-2136.

RESTREPO-HARTWIG, M., and AHLQUIST, P. (1999). Brome Mosaic Virus RNA replication proteins 1a and 2a colocalize and 1a independently localizes on the yeast endoplasmic reticulum. *J Virol* **73**(12)**,** 10303-10309.

ROHOZINSKI, J., and HANCOCK, J. M. (1996). Do light induced pH changes within the chloroplast drive turnip yellow mosaic virus assembly? *J Gen Virol* **77,** 163-165.

RUBINO, L., DI FRANCO, A., and RUSSO, M. (2000). Expression of a plant virus non-structural protein in *S. cerevisiae* causes membrane proliferation and altered mitochondrial morphology. *J Gen Virol* **81,** 279-286.

RUBINO, L., and RUSSO, M. (1998). Membrane targeting sequences in tombusvirus infections. *Virology* **252,** 431-437.

SATOH, H., MATSUDA, H., KAWAMURA, T., ISOGAI, M., YOSHIKAWA, N., and TAKAHASHI, T. (2000). Intracellular distribution, cell-to-cell trafficking and tubule- inducing activity of the 50 kDa movement protein of Apple chlorotic leaf spot virus fused to green fluorescent protein. *J Gen Virol* **81,** 2085-2093.

SCALES, S., and AL., E. (2000). Coat proteins regulating membrane traffic. *Int Rev Cytol* **195,** 67-144.

SCHAAD, M. C., ANDERBERG, R., and CARRINGTON, J. C. (2000). Strain-specific interaction of the tobacco etch virus NIa protein with the translation initiation factor eIF4E in the yeast two-hybrid system. *Virology* **273,** 300-306.

SCHAAD, M. C., JENSEN, P. E., and CARRINGTON, J. C. (1997). Formation of plant RNA virus replication complexes on membranes: role of an endoplasmic reticulum-targeted viral protein. *EMBO J* **16,** 4049.

SCHOLTHOF, K.-B. G., SCHOLTHOF, H. B., and JACKSON, A. O. (1995b). The tomato bushy stunt virus replicase proteins are coordinately expressed and membrane associated. *Virology* **208,** 365-369.

SCHWARTZ, M., CHEN, J., JANDA, M., SULLIVAN, M., DEN BOON, J. A., and AHLQUIST, P. (2002). A positive-strand RNA virus replication complex parallels form and function of retrovirus capsids. *Molecular Cell* **9,** 505-514.

SCOTT, A. C., WYATT, S., TSOU, P., ROBERTSON, D., and ALLEN, N. S. (1999). Model system for plant cell biology: GFP imaging in living onion epidermal cells. *Biotechniques* **26,** 1125-1132.

SHIMOMURA, O., JOHNSON, F. H., and SAIGA, Y. (1962). Extraction, purification and properties of aequorin, a bioluminescent protein from the luminous hydromedusan, *Aequoria*. *J Cell Comp Physiol* **59,** 223.

SIT, T. L., VAEWHONGS, A. A., and LOMMEL, S. A. (1998). RNA-mediated trans-activation of transcription from a viral RNA. *Science* **281,** 829-832.

SOLOVYEV, A. G., STROGANOVA, T. A., ZAMYATNIN, A. A., JR., FEDORKIN, O. N., SCHIEMANN, J., and MOROZOV, S. Y. (2000). Subcellular sorting of small membrane-associated triple gene block proteins: TGBp3-assisted targeting of TGBp2. *Virology* **269,** 113-127.

STAEHELIN, L. A. (1997). The plant ER: a dynamic organelle composed of a large number of discrete functional domains. *Plant Journal* **11,** 1151-1165.

STUKEY, J., MCDONOUGH, M., and MARTIN, C. (1990). The OLE 1 gene of S. cerevisiae encodes the delta 9 fatty acid gene and can be functionally replaced by the rat stearoyl-CoA desaturase gene. *J Biol Chem* **265,** 20144-20149.

SULLIVAN, M., and AHLQUIST, P. (1997). cis-Acting signals in bromovirus RNA replication and gene expression: Networking with viral proteins and host factors. *Semin Virol* **8,** 221-230.

TAYLOR, D., and CARR, J. (2000). The GCD10 subunit of yeast eIF-3 binds the methyltransferase-like domain of the 126 and 183kDa replicase proteins of tobacco mosaic virus in the yeast two-hybrid system. *J Gen Virol* **81,** 1587-1591.

THOMAS, C. L., and MAULE, A. J. (2000). Limitations on the use of fused green fluorescent protein to investigate structure-function relationships for the cauliflower mosaic virus movement protein. *J Gen Virol* **81,** 1851-1855.

TOMENIUS, K., CLAPHAM, D., and MESHI, T. (1987). Localization by immunogold cytochemistry of the virus-encoded 30K protein in plasmodesmata of leaves infected with tobacco mosaic virus. *Virology* **160,** 363-371.

TOTH, R. L., CHAPMAN, S., CARR, F., and SANTA CRUZ, S. (2001). A novel strategy for the expression of foreign genes from plant virus vectors. *FEBS Lett* **489,** 215-219.

TURNER, R., and BUCK, K. W. (1999). Mutational analysis of *cis*-acting sequences in the 3'- and 5'-untranslated regions of RNA2 of red clover necrotic mosaic dianthovirus. *Virology* **253,** 115-124.

VAEWHONGS, A. A., and LOMMEL, S. A. (1995). Virion Formation is required for the long-distance movement red clover necrotic mosaic virus in movement protein transgenic plants. *Virology* **212,** 607-613.

VAN DER HEIJDEN, M., and BOL, J. F. (2002). Composition of alphavirus-like replication complexes: involvement of virus and host-encoded proteins. *Arch Virol* **147,** 875-898.

VAN DER HEIJDEN, M., CARETTE, J. E., REINHOUD, P., HAEGI, A., and BOL, J. F. (2001). Alfalfa Mosaic Virus replicase proteins P1 and P2 interact and colocalize at the vacuolar membrane. *J Virol* **75,** 1879-1887.

VOLPE, P., KRAUSE, K., HASHIMOTO, S., ZORZATO, F., POZZAN, T., MELODESI, J., and LEW, D. (1998). Calcisome, a cytoplasmic organelle: the inositol-1, 4, 5-triphosphate-senstitive Ca++ store of nonmuscle cells? *Proc Natl Acad Sci U S A* **85,** 1091-1095.

WANG, H.-L., WANG, Y., GEISMAN-COOKMEYER, D., LOMMEL, S. A., and LUCAS, W. J. (1998). Mutations in viral movement protein alter systemic infection and identify an intracellular barrier to entry into the phloem long-distance transport system. *Virology* **245,** 75-89.

WANG, S., and HAZELRIGG, T. (1994). Implications for bcd mRNA localization from spatial distribution of exu protein in Drosophila oogenesis. *Nature* **369,** 400-403.

WANG, X., ULLAH, Z., and GRUMET, R. (2000). Interaction between zucchini yellow mosaic potyvirus RNA-dependent RNA polymerase and host poly-(A) binding protein. *Virology* **275,** 433-43.

WEINTRAUB, M., RAGETLI, H. W. J., and LEUNG, E. (1975). Abnormal nuclear structures in mesophyll cells infected with carnation ringspot virus. *Phytomorphology* **25,** 288.

WEIR, M., XIE, H., KLIP, A., and TRIMBLE, W. (2001). VAP-A binds promiscuously to both v- and tSNAREs. *Biochem Biophys Res Commun* **286,** 616-621.

XIONG, Z., KIM, K. H., KENDALL, T. L., and LOMMEL, S. A. (1993). Synthesis of putative red clover necrotic mosaic virus RNA polymerase by ribosomal frameshifting *in vitro*. *Virology* **193,** 213-221.

XIONG, Z., and LOMMEL, S. A. (1989). The complete nucleotide sequence and genome organization of red clover necrotic mosaic virus RNA-1. *Virology* **171,** 543-554.

XIONG, Z., and LOMMEL, S. A. (1991). Red clover necrotic mosaic virus infectious transcripts synthesized *in vitro*. *Virology* **182,** 388-392.

YAMANAKA, T., OHTA, T., TAKAHASHI, M., SCHMIDT, R., DEAN, C., SATOSHI, N., and ISHIKAWA, M. (2000). *TOM1*, an *Arabidopsis* gene required for efficient multiplication of a tobamovirus, encodes a putative membrane protein. *Proc Natl Acad Sci U S A* **97,** 10107-10112.

YOSHIKAWA, N., LIDA, H., GOTO, S., MAGOME, H., TAKAHASHI, T., and TERAI, Y. (1999). Apple chlorotic leafspot virus 50 kDa protein is targeted to plasmodesmata and accumulates in sieve elements in transgenic plant leaves. *Arch Virol* **144,** 2475-2483.

ZAVRIEV, S. K., HICKEY, C. M., and LOMMEL, S. A. (1996). Mapping of the red clover necrotic mosaic virus subgenomic RNA. *Virology* **216,** 407.

ZHANG, C. L., CHEN, D. F., MCCORMAC, A. C., SCOTT, N. W., ELLIOTT, M. C., and SLATER, A. (2001). Use of the GFP reporter as a vital marker for Agrobacterium-mediated transformation of sugar beet (Beta vulgaris L.). *Mol Biotechnol* **17,** 109-117.

Chapter 2

Red Clover Necrotic Mosaic Virus Replication Proteins Accumulate at the Endoplasmic Reticulum

KATHERINE A. TURNER[1], TIM L. SIT[3], ANTON S. CALLAWAY[2],

NINA S. ALLEN[2], and STEVEN A. LOMMEL[1, 3]

Departments of [1]Genetics, [2]Botany, and [3]Plant Pathology

North Carolina State University, Raleigh North Carolina 27695-7616

Red Clover Necrotic Mosaic Virus Replication Proteins Accumulate at the Endoplasmic Reticulum

Abstract

The replication of positive strand RNA viruses requires association with host membranes and results in membrane proliferation and rearrangement. The fact that widely divergent virus families share form and function of replication strategies is likely due to common evolutionary origin and suggests that elucidating the reproduction strategies of one virus may provide insight to virus life cycles in general. *Red clover necrotic mosaic virus* (RCNMV) is a positive-strand RNA virus in the *Tombusviridae* family. RCNMV encodes two N-terminally overlapping proteins of 27 kDa and 88 kDa (p27 and p88). p88 contains motifs characteristic of RNA-dependent RNA polymerases and is the catalytic portion of the replication complex. While the function of p27 is unclear, it is very likely to be part of the RCNMV replication complex (Bates et al., 1995). We have investigated the localization of the putative RCNMV replicase proteins in plant cells using green fluorescent protein (GFP) fusions observed in live cells using confocal microscopy.

The GFP:p27 and GFP:p88 fusions were expressed in *N. benthamiana* epidermal cells and protoplasts. GFP:p27 consistently localized to the endoplasmic reticulum (ER) and caused membrane restructuring and proliferation. GFP:p88 also localized to the ER and co-localized with GFP:p27.

In addition, GFP:p27 and GFP:p88 were associated with invaginations of the nuclear membrane. Fractionation of virus-inoculated leaves demonstrated the association of p27 with isolated ER membranes. Additionally, GFP:p27 co-localized with ER-targeted YFP.

GFP:p88 co-localized with GFP:p27 in two expression systems. This and the fact that GFP:p27 localized to the ER in the presence of heterologous and homologous viral genomes as well as in the absence of any viral proteins suggests that the two proteins co-localize to the cortical ER, the nuclear envelope, and cytoplasmic ER domains. The fact that both proteins independently accumulated in the ER and perturbed the ER morphology suggests that the proteins function together, as part of a larger replication complex. The data suggest that the virus remodels ER structure to create aggregates containing active viral replication complexes. This is the first report of a member of the *Tombusviridae* replicating in association with the ER.

Introduction

Viral replication is a critical step in the infection cycle, and as such is often the target of anti-viral strategies. Much research focuses on the conserved aspects of replication, including viral factors, host factors, and cellular localization. Some virus genera such as the *Noda-* and *Bromoviruses* replicate in hosts from multiple kingdoms (plant, insect, and yeast cells) (Miller et al., 2001; Restrepo-Hartwig and Ahlquist, 1999), suggesting that the host components that contribute to the replication complex are conserved across kingdoms and must

function in critical pathways. Additionally, a recent study demonstrated that the *Brome mosaic virus* (BMV) replication proteins 1a and 2a, along with essential *cis*-acting replication signals, duplicate the functions of *Gag*, *Pol* and RNA packaging signals in Retrovirus and *Foamy virus* cores (Schwartz et al., 2002). The fact that widely divergent virus families share form and function of replication strategies is likely due to a common evolutionary origin (Schlegel et al., 1996; Buck, 1996; Schwartz et al., 2002), and suggests that elucidating the reproduction strategies of one virus will provide insight to virus life cycles in general.

One feature common among positive strand RNA viruses is a requirement for replication in association with host membranes (Rohozinski and Hancock, 1996; Carette et al., 2000; Miller et al., 2001; Lee et al., 2001). The presence of a replicating virus frequently induces proliferation and rearrangement of the host membranes (Reichel and Beachy, 1998; Rubino et al., 2000; Rohozinski and Hancock, 1996; Bong et al., 1999), and can also be required for viral assembly (Rohozinski and Hancock, 1996).

The specific type of membrane system utilized in assembling the viral replication complex depends on the individual virus, and is likely to be genetically determined (Burgyan et al., 1996; Rubino and Russo, 1998). It is most common to find polymerase proteins associated with the endoplasmic reticulum (ER), the most abundant membrane form in the plant cell. Picorna-like viruses including the plant *Comoviruses* (Carette et al., 2000) and *Potyviruses* (Schaad et al., 1997) and Alpha-like viruses including *Bromoviruses* (Oparka et al., 1996),

Tobamoviruses (dos Reis Figueira, et al., 2002; Mas and Beachy, 1999), and *Pecluviruses* (Dunoyer et al., 2002) direct replication proteins to the ER. Reports in the literature indicate that replication complexes also target most other subcellular membranes.

Within the family *Tombusviridae*, which includes RCNMV, mitochondria and peroxisomes are the sites of replication for *Tomato bushy stunt virus* (TBSV) (Scholthof et al., 1995b) *Carnation Italian ringspot virus* (CIRSV) (Weber-Lotfi et al., 2002; Rubino et al., 2000; Rubino et al., 2001) and *Cymbidium ringspot virus* (CyRSV) (Burgyan et al., 1996). In other families, invaginations of the chloroplast outer membrane are associated with *Tymovirus* replication and assembly (Prod'homme et al., 2001; Rohozinski and Hancock, 1996), and *Alfalfa mosaic virus* (AMV) replication proteins interact at the vacuole membrane (Van Der Heijden et al., 2001).

In animal cells, Nodaviruses replicate in association with mitochondrial outer membranes (Miller et al., 2001), while polioviruses generate vesicles containing membranes from ER, the Golgi apparatus, and lysosomes (Dunoyer et al., 2002; Schlegel et al., 1996). Although membrane association is a common feature of viral replication, in most cases the mechanism of membrane targeting is unknown and there is no correlation between phylogenetic relationships and which membranes are recruited for replication.

RCNMV is a positive-strand RNA virus in the *Dianthovirus* genus, *Tombusviridae* family. The RCNMV genome is comprised of 2 RNA molecules (Xiong and Lommel, 1989) (Figure 1). RNA-1 replicates independently of RNA-2

in protoplasts, but both RNAs are required for movement and plant infection (Osman and Buck, 1987; Sit et al., 1998). The RNA-1 of RCNMV encodes two N-terminally overlapping proteins of 27 kDa and 88 kDa (p27 and p88). p88 is generated via a –1 ribosomal frameshifting event (Xiong et al., 1993), and contains the GDD motif characteristic of RNA-dependent RNA polymerases (Bates et al., 1995; Xiong et al., 1993). Both p27 and p88 have a high degree of sequence identity with replicases from other species in the *Tombusviridae* (Xiong and Lommel, 1989). While the role of p27 during infection is unclear, it is very likely to be part of the RCNMV replication complex. Both p27 and p88 are immunoprecipitated from functional, membrane-bound template-dependent polymerase preparations isolated from RCNMV-infected *Nicotiana benthamiana* and are required for viral replication (Xiong and Lommel, 1991). RNA-1 also encodes the capsid protein of the virus, which is not required for replication (Xiong and Lommel, 1991).

To gain insight into the mechanism of viral replication in the host and how the virus causes disease, we have investigated the localization of the RCNMV replicase proteins in plant cells using green fluorescent protein (GFP) fusions. Laser scanning confocal microscopy allowed the subcellular localization of fluorescence from the GFP:p27 and GFP:p88 fusions to be observed in real time and at high resolution. In this study, we demonstrate that RCNMV p27 and p88 localize to the ER and modify the morphology of the cortical and cytoplasmic ER domains.

Materials and methods

RCNMV RNA-1 expressing only p88. An RCNMV cDNA clone of RNA-1 was created that expressed only the 88 kDa protein from the 5' terminal ORF. The cDNA sequence that represents the wild-type (wt) RCNMV sequence surrounding the –1 frameshift is 5'GAGGATTT**TTA**GGCGGC 3'. The ribosome slips backward from the bold p27 termination codon to the underlined codon and continues translation in the –1 frame (Kim and Lommel, 1994). To eliminate the frameshift and create one continuous ORF we used site-directed mutagenesis to insert one nucleotide (bold) into the wt sequence, which would then be 5'GAGGATTTTTT**T**AGGCGGC 3'. This changed the terminator codon at the 3' end of the p27 gene to a tyrosine codon. Site directed mutagenesis was performed using the long-PCR method of Callaway (Callaway, 1998) with primers FpRC169p88 and RpRC169p88 (Table 1).

GFP:p27 expressed from RCNMV RNA-1. A cDNA copy of RCNMV RNA-1, termed R16sG3, was engineered to express a synthetic copy of GFP from *Aequoria victoria* [sGFP, courtesy of Jen Sheen (Chiu, et al., 1996)] from the capsid protein subgenomic promoter. Genes ligated to the 3' end of sGFP in R1s6G3 are produced as translational fusions with GFP. The sGFP was amplified by PCR (Stratagene) with primers sGFP 3' ΔNM and sGFP 5' 6xHIS (Table 1) and ligated into a construct coding for RNA-1 replacing the CP ORF. RCNMV p27 was amplified by PCR with primer p27-5'ClaI/NcoI and primer p27-3'XhoI/MluI (Table 1). The PCR product was digested and cloned in frame

behind the sGFP, creating R1-G27. These constructs were verified by sequencing the 5' end of the sGFP and p27 ORFs, and western blot analysis was performed using anti-p27 (Xiong et al., 1993) to verify that the constructs produced full-length fusion proteins.

GFP:p27 and GFP:p88 expressed from the CaMV 35S promoter. In order to label p27 independently from p88 without compromising the replication capacity of RNA-1, a previously engineered plant expression vector for translational fusions (pRTL2, Topfer et al., 1987) was used to drive production of GFP:p27 and GFP:p88 from the CaMV 35S promoter. sGFP (Chiu et al., 1996) was amplified by PCR with primers sGFP 5' 6xHIS and sGFP 3' MKSX (Table 1), digested with *Nco*I and *Xba*I and ligated to pRTL2 to produce pSX, which expresses sGFP. p27 was amplified by PCR with primers P88-5'Mlu/Kpn and p27-3'Xba/Bam (Table 1), digested with *Mlu*I and *Xba*I and ligated to pSX to produce pRTL2-GFP:p27.

In addition, p88 was amplified from RC169-p88 that expresses only the 88 kDa protein from the RCNMV N-terminal ORF by PCR with primers p88-5'Mlu/Kpn and p88-3' Not/Spe (Table 1), digested with *Mlu*I and *Spe*I, and ligated to pSX to produce pSX-GFP:p88. These clones were verified by sequencing.

GFP: p27 expressed from a TBSV vector. To uncouple the localization of p27 from its role in viral replication, we used a heterologous viral RNA vector. An infectious cDNA clone of *Tomato bushy stunt virus* (TBSV) was previously

engineered to allow transcription of foreign sequences from the CP subgenomic promoter (pHST2; Scholthof and Scholthof, 1996). The GFP:p27 cassette previously engineered for expression from RCNMV RNA-1 was digested with *Cla*I and *Mlu*I and cloned into a similarly digested pHST2-sGFP backbone. The resultant construct (pHST2-G27) expresses the GFP:p27 fusion to high levels in inoculated leaves of *N. benthamiana*. The clone was verified by sequencing.

To verify co-localization of the ER and p27, a control construct was created that expresses the yellow fluorescent protein (YFP, BD BioSciences, Palo Alto, CA) and includes an ER targeting signal sequence and the cognate 'KDEL' ER-retention peptide. The ER:YFP was amplified by PCR using primers ERYFP 5'Sna/Xho and ER YFP 3' Sca/Xba (Table 1), digested with *Xho*I and *Sac*I, and ligated into pHST2. The clone was verified by sequencing.

To ensure that GFP and YFP were both expressed in a single cell, a movement-defective version of pHST2-G27 was created. The p22 movement protein of TBSV was digested with *NcoI* and *Eco RI*, and a small fragment was removed. The overhanging ends were filled in with the Klenow fragment of DNA polymerase I (Promega, Madison WI) and re-ligated. The resultant clone, pHST2-g27ΔAH, does not produce the p22 movement protein and transcripts produced from this template cannot traffic out of the inoculated cell. The integrity of this clone was verified by sequencing.

Microprojectile bombardment. 1 μm gold particles (Bio-Rad, Hercules, CA) were coated with pRTL2-sGFP, pPRTL2-GFP:27, or pRTL2-GFP:p88 DNA alone

or in combination following the manufacturer's directions. Particles were delivered into *Nicotiana benthamiana* epidermal cells on detached leaves using the Biolistic PDS-1000/He system (Bio-Rad) with 1100 psi rupture disks under vacuum of 27 inches of Hg. After bombardment, the cut petioles of leaves were wrapped in damp kimwipes (Fisher Scientific Co., Pittsburg, PA) and the leaves sealed in plastic Petri dishes. Leaves were incubated at room temperature overnight before being imaged via fluorescence microscopy.

Live cell microscopy. Plant cells were observed and selected for further confocal observation using an epifluorescence microscope (Zeiss Axiopohot) equipped with a long-pass FITC filter set. Confocal microscopy was carried out on a Leica DMIRBE inverted microscope equipped with a spectral scanning head and a 63X 1.2 N.A. water-immersion lens. An argon laser (488- and 514 nm lines) was used to discriminate between the GFP and YFP fluorochromes. In experiments where both fluorochromes were analyzed, the emission signal from GFP was collected via photomultiplier tube from 500-515 nm, and the emission from YFP was collected from 530-565 nm. In single-label experiments the signal from GFP was collected from ca. 500-565 nm. The GFP channel was assigned false green and the YFP channel false red color. Images were processed using Photoshop 4.0 software (Adobe Systems, Mountain View, CA) and overlaid using MetaMorph (Universal Imaging Corp.).

Plant inoculations. RCNMV and TBSV RNAs were transcribed from *Sma*I linearized templates as previously described (Geisman-Cookmeyer and Lommel, 1993; Scholthof et al., 1995b; Xiong and Lommel, 1991). RNA in 10 mM phosphate buffer was used to inoculate four leaves of *N. benthamiana* plants at the six- to eight-leaf stage. The plants were grown in a glasshouse at 21°C. Each construct was inoculated to two plants and each experiment was repeated at least three times.

Protoplast preparation. Protoplasts were prepared from young *N. benthamiana* plants and *N. benthamiana* suspension cell culture (a kind gift from Dr. Linda Hanely-Bowdoin) and inoculated essentially as described in Negrutiu *et al.* 1987, with modifications described in Brough *et al.* 1992. Briefly, after preparation, the protoplasts were inoculated with 5 μg of DNA in the presence of PEG 4000 (Fluka) to permeablize the membranes, washed with buffer, and allowed to recover overnight before being imaged by fluorescence microscopy.

Membrane fractionation. Equal weights of *N. benthamiana* leaves inoculated with wt RCNMV and mock-inoculated leaves were ground in buffer A (50 mM Tris HCl pH 7.4, 15 mM $MgCl_2$, 10 mM KCl, 0.1%β -mercaptoethanol, 1 μm pepstatin, 0.1 mM PMSF, 20% glycerol) using a mortar and pestle. The slurries were filtered through cheesecloth, and equal volumes of the filtrates were applied to the tops of sucrose density gradients ranging from 51% sucrose at the bottom to 40% sucrose at the top. The gradients were equilibrated by centrifugation at

15,000 X g in a tabletop microfuge. The membrane fraction floating on top of the 40% sucrose fraction was identified by the bright green color due to the presence of chloroplast membranes and designated the “supernatant.” The pellet at the bottom of the tube contained cell debris, nuclei, and heavier plastids (den Boon et al., 2001). The pellet was washed and designated “pellet”. Volumes equivalent to the volume of applied homogenate were collected from the pellet and supernatant.

Western Blots. Protein extracts from ground leaves were prepared as described (Petty et al., 1989) and quantified using the Bradford Assay (Bio-Rad). Samples of the leaf extracts were applied to either 15% acrylamide hand-cast or 12.5% acrylamide pre-cast (BioRad) SDS-PAGE gels and separated at 100V for 1.5 hours in Laemmli running buffer (Laemmli, 1970) in a Bio-Rad Protean II apparatus. The proteins were transferred to PVDF membranes (Millipore, Bedford, MA) in transfer buffer (25mM Tris 40 mM glycine, 10%methanol) using a BioRad trans-blotter. GFP was detected using an anti-GFP antibody (Clontech) and p27/p88 was detected using a polyclonal anti-p27 antibody (Xiong et al., 1993). BiP was detected using a polyclonal anti-BiP antibody kindly provided by Dr. Rebecca Boston (Fontes et al., 1991). Primary antibodies were detected with alkaline phosphatase-conjugated secondary antibodies (Bio-Rad, Hercules, CA), and the labeled proteins were visualized using the CDP-Star chemiluminescence kit (Novagen) as directed by the manufacturer, and exposed to Kodak BioMax MS film.

Densitometry. The exposed films were quantified using ImageQuant Mac software version 1.2 (Molecular Dynamics) with constant areas selected between bands, and background subtraction performed by the software.

Results

GFP:p27 expressed from RCNMV RNA-1

To localize RCNMV p27 within living plant cells during a natural infection, we constructed plasmids in which a cDNA copy of RCNMV RNA-1 was used as a vector. The coding sequence of the CP gene was removed, facilitating insertion of foreign gene sequences. Absence of the CP does not impair normal replication of the virus (Xiong and Lommel, 1989). The coding sequence of *Aequoria victoria* green fluorescent protein (GFP) was fused to the RCNMV p27 gene (pre-frameshift) and the fusion was inserted in RNA-1 to produce GFP:p27 from the subgenomic promoter (Figure 1A). The fusion proteins were expressed in *N. benthamiana* epidermal and mesophyll cells along with the entire unlabelled RCNMV genome as part of the replication cycle of RCNMV during a local infection. Infectious transcripts of the modified virus were generated and inoculated to leaves (Xiong and Lommel, 1991). This infection resulted in the accumulation of wt levels of unlabelled p27 and much higher levels of GFP:p27, presumably equal to the levels of CP in a natural infection.

The construct generated a productive infection that moved cell-to-cell and expressed GFP:p27. The GFP:p27 fusion protein was associated with the endoplasmic reticulum (ER) throughout the cell. A web-like, reticular network of relatively stationary interconnected tubules is characteristic of the ER in the cortical region of plant and animal cells (Terasaki and Reese, 1992; Staehelin, 1997; Knebel et al., 1990). Fluorescence was observed in such a polygonal network of cortical ER (Fig. 2A and B, arrows) but was also seen in thick, flowing, tubular ER (Fig. 2A and 2B, darts) and several sub-domains, including the nuclear envelope (Fig. 2A, small arrow). In addition, fluorescence was observed in large, amorphous aggregates that flowed along or within the tubular cytoplasmic ER (Fig. 2B, small arrow). The membranous aggregates were seen to fuse with the nuclear membrane and then detach again, flowing around the periphery of the nucleus, likely as a result of cytoplasmic streaming. The aggregates represented a distortion of normal ER structure, and likely indicate that the virus caused proliferation of ER cisternae (Carette et al., 2000; Rubino et al., 2000). In order to determine the localization of p88, another experiment was needed.

GFP:p27 and GFP:p88 expressed from the CaMV 35S promoter

We wanted to determine the localization of the core polymerase p88 independently of p27. We therefore performed a second set of experiments in which a previously engineered plant expression vector for translational fusions

(pRTL2, Topfer et al., 1987) was used to drive production of GFP:p27 and GFP:p88 from the CaMV 35S promoter.

Epidermal cells. We assumed that it was not possible to fuse GFP to the p88 post-frameshift protein without destroying the replication ability of the RCNMV vector. We had previously attempted to fuse GFP to the N-terminus of p27 in RCNMV RNA-1, but that construct did not generate an infection. As a consequence we constructed a plasmid containing GFP fused to a mutated p88 gene in which the frameshift signal had been abolished, creating an uninterrupted ORF expressing the 88kD protein (Figure 1B). In addition, we constructed a plasmid containing GFP fused to the p27 gene (Fig. 1B). The fusion proteins were expressed in *N. benthamiana* leaf epidermal cells via microprojectile bombardment (Sanford et al., 1993). 24 hours after bombardment, the cells were examined by confocal microscopy. In cells that had been bombarded with GFP:p27, fluorescence was observed associated with the ER throughout the cell (Fig. 2, C, D, E, F, G, H, and O) . Fluorescence was seen in the cortical ER, similar to the patterns observed in R1G27.1 inoculated cells (Fig. 2 D and F, arrows), as well as in the nuclear envelope (Fig. 2F and H, arrowheads). The patterns of fluorescence in R1G27.1 inoculated cells were nearly identical to the patterns in pRTL2 inoculated cells. The cortical ER is not as bright in the R1G27.1 inoculated cells, due to overexpression of GFP:p27 in the bombarded cells.

In addition to regular endomembrane patterns, fluorescence was also seen in large aggregates of membranes or proteins (Fig. 2C, D and E, labeled

‘A’) and numerous small, motile bodies (Fig. 2C, F and H, small arrows), which flowed along the tubules of ER. These aggregates are again suggestive of membrane proliferation. Spherical membranous structures were seen associated with the tubular ER; these appeared to be composed of ER containing the GFP:p27 fusion (Fig. 2H, doubled dart). During short observation periods (20 minutes or less) the structures were immobile. In addition, fluorescence was sometimes detected within the nucleus (Fig. 2D, small arrowheads and enlargment 2O). In cells where fluorescence was apparent within the nucleus, the characteristic reticular pattern of ER was still present, indicating that the fusion had acquired a secondary localization in addition to its ER localization rather than reverting to a cytosolic localization. It was often possible to see strands or tubes of fluorescent material within the nucleus (Fig. 2D, small arrowheads and 2O). The cells which showed large aggregate bodies also had very fine strands of membrane stretched between the aggregates, suggesting that they were contained within the endomembrane system (Fig. 2F and H). These large bodies were rarely motile. In all cases, the fluorescence patterns observed were distinct from the diffuse cytoplasmic fluorescence observed in cells bombarded with GFP alone (Fig. 2 I and J).

The GFP:p88 fusion protein was also associated with the endomembrane system throughout the cell. Specifically, fluorescence was detected in the reticular network of the cortical ER (Fig. 2K and L, arrows), in smooth ER tubules bundled along the actin (Staehelin, 1997) cytoskeleton (Fig. 2L, small arrow) and in large membrane or protein aggregates (Fig. 2K and L, labeled ‘A’).

Some cells also showed apparent nuclear localization of GFP:p88 (Fig. 2M, N). There are no identifiable nuclear targeting signals in either p27 or p88, and the GFP:p88 fusion protein is ca 115 kDa, far too large to diffuse into the nucleus passively. As with the GFP:p27 fusion proteins, it is possible to see strands or fluorescent tubules within the nucleus (Fig. 2K, dart and enlargement 2P) as well as large, densely fluorescent bodies pressed against the nucleus (aggregates, labeled 'A' in Fig 2 K and L). These are likely multivesicular bodies, common to Tombusvirus infections (Burgyan et al., 1996). In some cells expressing GFP:p88, the characteristic polygonal pattern of the ER appeared diffuse and faint, resembling the cytoplasmic distribution of fluorescence in cells expressing unfused GFP only (compare Fig. 2M, N with Fig. 2I, J). This appearance is particularly pronounced in computer projections of multiple confocal scans of leaf epidermal cells. The overall fluorescence level of the epidermal cells' expression GFP:p88 was very low compared to the expression of free GFP controls. In order to more efficiently identify cells expressing GFP:p88 and GFP:p27, protoplasts were made from inoculated leaves.

Protoplasts. The same CaMV 35S constructs were PEG-inoculated to protoplasts to study the expression of p27 and p88 in a more optically favorable cell type. Twenty-four hours after inoculation with pRTL2-GFP:p27, fluorescence was observed in punctate spots throughout the cytoplasm of the protoplasts (Fig. 3B). The aggregates were connected by a network of finely stretched membranes, suggesting that they were derived from ER or contained

within it (Fig. 3B). This fluorescence pattern strongly resembles the early stages of ER disruption by brefeldin A (Figure 4 L).

Fluorescence generated from the GFP:p88 fusion protein was detected throughout the cytoplasm and appeared to localize to the nucleus (Fig. 3C). In addition, fluorescent aggregates associated with the endomembrane system in a pattern similar to that seen for GFP:27 (data not shown). Approximately 22% (62/283) of the cells expressing GFP:p88 showed the punctate pattern of fluorescence, with the remainder showing diffuse fluorescence. In many cells, fluorescent protein appeared to occupy the entire cytoplasmic volume of the cell, suggesting that overexpression of the GFP:p88 was causing distortion of the ER, or that once the ER had exceeded its storage capacity, additional proteins were shunted into the nucleus or remained untargeted in the cytoplasm (Fig. 3C and D).

In protoplasts inoculated with both pRTL2-GFP:p27 and pSX:p88 three distinct fluorescence patterns were observed. The first resembled the pattern of GFP:p27 alone (aggregates in the ER, seen in ca. 4% (9/216) of the fluorescent cells), the second resembled the pattern of p88 alone (GFP in the entire cell, seen in about 16% (35/216)), and the third had elements of both (seen in ca. 80% (172/216) of the cells, Fig. 3D). In the protoplasts inoculated with both constructs, fluorescence was observed in aggregates throughout the endomembrane system, which was swollen and distorted. It is also likely that proliferation of the ER membranes was induced, creating even more volume to distort the normal ER morphology. In addition, fluorescence could be detected

from within the nucleus (Fig. 3D, E, F), in strands and aggregates. It has been demonstrated that the ER forms grooves and tunnels throughout the nucleus in plant cells (Collings et al., 2000) including *N. benthamiana*, suggesting that the fluorescence observed in the nucleus is actually GFP:p88 and GFP:p27 localized to the ER. In all cases, the percentage of protoplasts that survived inoculation with the RCNMV fusions was very low, and the cells often appeared stressed. The fluorescence output per cell was also low compared with free GFP controls. Consequently, in another attempt to express the fusions efficiently in healthy cells, a heterologous viral vector was used.

GFP:p27 expressed from pHST2

To further localize GFP:p27 in plant cells that retained normal ER structure, GFP:p27 was engineered to be expressed from the CP subgenomic promoter (sgp) of *Tomato bushy stunt virus* (TBSV). *In vitro* transcripts of the pHST2-GFP:p27 construct were mechanically inoculated onto *N. benthamiana*. Two days after inoculation, the leaves exhibited hundreds of brightly fluorescent foci. The cells were imaged using the laser scanning confocal microscope. Similar to the GFP:p27 expressed from the RCNMV sub genomic promoter, the fluorescence was localized to the ER, particularly the cortical ER (Fig. 4A), the perinuclear ER (Fig. 4B, arrow) and thick cytoplasmic tubes of ER (Fig. 4B, arrowhead). In addition, numerous tiny (ca. 1μm), highly fluorescent bodies were present along the tubular ER and associated with the polygonal cortical ER network. The tiny bodies moved quickly along the ER tubules, often in a

coordinated fashion, and additionally displayed discontinuous movements, including reversing direction and stopping entirely for a brief time before resuming motion (Fig. 4B, small arrow, and supplemental video). The cells expressing GFP:p27 appeared healthy and maintained wild-type ER structure, as well as rapid cytoplasmic streaming.

In order to confirm the ER localization of the GFP:p27, a co-localization experiment was performed. A second pHST2 construct was created that expressed YFP (BD Biosciences) modified with a calreticulin ER targeting signal peptide and cognate 'KDEL' ER retention signal (Fliegel, 1989). In addition, a third pHST2 construct was produced, based on the pHST2-GFP:p27 clone, in which the p22 movement protein of TBSV had been partially deleted. This clone, termed pHST2-GFP:p27ΔAH, was unable to escape the initial inoculated cell unless it was complemented by a functional p22 movement protein expressed from the ER-YFP clone. In this manner, it was guaranteed that both constructs were present in cells located in foci of green fluorescence-expressing cells. *In vitro* transcripts of the pHST2 ER-YFP construct were co-inoculated with pHST2-GFP:p27ΔAH to *N. benthamiana* leaves and the resultant foci imaged with the confocal microscope. Although the spectra of GFP and YFP overlap considerably, care was taken with the microscope settings to minimize crosstalk between the fluorochromes (see materials and methods). The resultant images were pseudo-colored green for the GFP:p27 signal and red for the ER YFP signal and digitally overlaid. Areas where the two signals overlapped appeared yellow due to the mix of red and green pixels.

When the co-inoculated cells were observed with 514 nm (green) light, yellow fluorescence from YFP was observed throughout the endomembrane system. The cortical ER was clearly visible (Fig. 4 E, arrow) as were tubes of cytoplasmic ER (Fig. 4 E, arrowheads). In all cases, the YFP was observed within the nucleus as well as in the lumen of the nuclear envelope, which is contiguous with the lumen of the ER (Fig. 4 C). This was an unexpected result. The ER targeting signal sequence in this construct was derived from rabbit calreticulin (Fliegel, 1989; Clontechniques, April 1999). Although calreticulin is conserved throughout eukaryotes, in the virus-based system the signal peptide that provides ER localization properly in mammals does not have the same stringency as in plants. It is possible that the rabbit signal peptide is in a slightly different context or has a slightly different structure than that needed for the signal sequence to correctly direct proteins to the plant ER alone. The YFP also used a 'KDEL' ER retention signal (Angres and Green, 1999) rather than the HDEL signal often found in plants (Gomord et al., 1997). The YFP may have been correctly directed to the ER, but inefficiently retained.

When the same cells were observed under 488 nm (blue) light, green fluorescence from GFP was observed associated with the endomembrane system throughout the cell, in identical patterns to those observed with pHST2-GFP:p27, discussed above (Fig. 4 D). It could be clearly seen in the pseudo-color overlays of ER YFP and GFP:p27 that the fusion proteins co-localized, suggesting the GFP:p27 accumulated predominantly within the cortical and tubular ER (Fig. 4 E). In most co-inoculated cells the interior of the nucleus

exhibited red pseudo-color from the mistargeted ER YFP, while signal from both fluorochromes was apparent within the nuclear envelope (Fig. 4 C) in some cases, signal from GFP:p27 was also seen within the nucleus. It is not clear whether this is due to fluorescence associated with intranuclear ER tubules or a side effect of the mistargeting of ER YFP. The fluorophores were scanned independently to minimize crossover between the two channels.

ER response to viral infection

Transgenic *N. benthamiana* plants expressing GFP targeted to the ER (seed lines courtesy of Dr. David Baulcombe, John Innes Institute, Norwich, UK) were employed to observe the effect of viral infection on the ER. The only fluorescence in this system was derived from GFP with an ER-targeting signal sequence and cognate 'HDEL' ER retention signal, completely contained within the ER lumen (Fig. 4 G). These transgenic plants (GFP-ER *N. benth*) were inoculated with each of the TBSV constructs described above. pHST2, the TBSV vector, caused aggregations of ER to appear in the cortical region, and caused thickening of the smooth ER strands that transverse the cell (Fig. 4 H) Some of the aggregates were in the perinuclear area (Fig. 4 H, dart). pHST2-p27 caused similar changes in ER structure, to a slightly more severe extent (Fig. 4 I). The aggregates of ER were larger and the smooth strands were thicker and more evident in the cortical region. This suggests proliferation of ER membranes (Fig. 4 I). The aggregates were also in the perinuclear region (Fig. 4 I, dart). In GFP-ER *N. benth* cells inoculated with wt RCNMV, the perinuclear aggregates

were very large, while the cortical aggregates were reduced in size and increased in number. The smooth ER strands were thickened and proliferated (Fig. 4 K). The structure of the ER in RCNMV-inoculated GFP-ER plants was very similar to the fluorescence pattern observed in epidermal cells bombarded with GFP:p27 and GFP:p88, as well as to the pattern in epidermal cells expressing GFP:p27 from the RCNMV subgenomic promoter (compare Fig. 2 A, C, E, G, and K with Fig. 4 K). The cytoplasmic aggregates observed in a wt RCNMV infection were not as large as those in the engineered infections, but the perinuclear aggregates were similar in size. Overall, the distortion of the ER in the wt RCNMV infection was less severe than that observed in a engineered infection, which is likely a consequence of the overexpression of the proteins.

In both the TBSV construct inoculations and RCNMV inoculation, the reticular web of cortical ER in the GFP-ER transgenic plants remained visible and relatively normal, with the aggregates and thickened strands superimposed upon it. Interestingly, in transgenic cells inoculated with pHST2- ER YFP, large aggregates of ER formed in the perinuclear and cortical regions (Fig. 4 J, dart), as well as very small aggregates, similar to those seen with RCNMV (Fig. 4 K). The cortical ER was not as evident in the cells, and the smooth ER strands were thickened and distorted (Fig. 4 J, arrow). It was not immediately apparent why the presence of ER YFP would perturb the ER structure beyond the changes caused by the viral vector alone.

Cell Fractionation

Cellular fractionation experiments were performed to physically verify the membrane association of p27. Equal weights of leaf tissue from *N. benthamiana* inoculated with wt RCNMV and mock-inoculated were homogenized and separated on sucrose gradients. The pellet and supernatant fractions were separated by SDS-PAGE, transferred to PVDF, and analyzed by western blot. Antibodies to p27 and BiP, an ER-resident protein (Wrobel, 1997; Terasaki and Reese, 1992), were used to identify fractions containing those proteins. BiP was associated with the supernatant fraction containing cellular membranes in both RCNMV- and mock-inoculated control tissues (Fig. 5). Interestingly, the BiP signal was much stronger in RCNMV inoculated tissue, suggesting that viral infection stimulates BiP production. BiP is a chaperonin, a protein the cell deploys to help other proteins fold correctly inside the ER (Wrobel, 1997; Terasaki and Reese, 1992). Elevated levels of BiP could indicate that the cell has proliferated ER, or that increased levels of chaperonins are needed in response to viral infection. Densitometry of the exposed films indicated that at least 20% more BiP signal was present in the RCNMV inoculated tissue (compare Fig. 5B Mock (T) with RCNMV (T)). p27 was also predominantly located in the supernatant of RCNMV-inoculated tissue, with some signal remaining in the pellet. It is likely that the p27 associated with the nuclear envelope and in large, dense protein aggregates is responsible for detection of signal in the pellet fraction. No p27 signal is detectable in mock-inoculated tissue.

Discussion

Eukaryotic (+) stranded RNA viruses replicate in association with intercellular membranes. This holds true for both plant and animal viruses, even for those that are non-enveloped and do not use glyco- or phospholipids for assembly or transmission (Ahlquist et al., 1994; Schlegel et al., 1996; Schwartz et al., 2002, and references therein). It is remarkable for such a requirement to be nearly universal across so many virus families with different protein expression, packaging, and replication strategies. Even more remarkable, with a few exceptions (Lee et al., 2001; Schwartz, 2002), the replication mechanism that underlies the requirement for association with a cellular membrane remains unknown. In this study, we investigated the intercellular localization of the RCNMV p27 and p88 replication proteins. In three different expression systems, GFP:p27 was found to accumulate in the ER of inoculated cells and to distort normal ER morphology, likely due to induced proliferation of ER membranes. Wild-type RCNMV caused morphological changes in the ER of GFP-ER transgenic plants similar to those observed in the GFP:p27 and GFP:p88 expressing cells, including thickening of ER tubules and formation of large fluorescent aggregates near the nucleus. p27 and p88 were found primarily in the membrane fractions of infected *N. benthamiana* leaves, and RCNMV infected cells displayed elevated levels of ER resident binding protein BiP, a chaperonin, consistent with ER proliferation and pathology (Fig. 5). In addition, GFP:p88 co-localized with GFP: p27 in the ER of inoculated *N. benthamiana* epidermal cells

and protoplasts. Both p27 and p88 independently localized to the ER and caused morphological changes, suggesting that both proteins work to establish a replication site within the cell. Because p27 and p88 independently localized to the ER, both the pre- and post-readthrough portions must share an N-terminal localization domain or have distinct ER targeting properties. This suggests that the targeting of one protein is not dependent upon the targeting of the other. It has been hypothesized that one component of bipartite viral polymerases functions as a membrane anchor, while the other components assemble the holoenzyme around the anchor (Schaad et al., 1997). RCNMV may be a case of a replication complex that assembles without an anchor, each component associating with membranes or other components through hydrophobic interactions.

P27 expressed from RCNMV RNA-1 localizes to ER

In this study, we used a variety of techniques to demonstrate that p27 and p88 accumulate in the ER of infected *N. benthamiana*. GFP:p27 was first produced from the subgenomic promoter of RCNMV RNA-1. Fluorescence was observed in the nuclear envelope, the cortical ER, and in strands of cytoplasmic ER. Fluorescence in the nuclear envelope that does not enter the nucleus interior (giving the appearance of a 'ring' around the nucleus in optical sections) and a web-like reticular pattern evident just under the plasma membrane are widely considered to be canonical indicators of ER (Allen and Schumm, 1990; Cole and Lippincott-Schwartz, 1995; Staehelin, 1997; Terasaki and Reese,

1992). The GFP:p27 inoculated cells exhibited cytoplasmic streaming and movement of ER inclusions, indicating relative good health.

GFP:p27 was also associated with the ER in isolated membrane fractions of RCNMV-inoculated *N. benthamiana* leaves. Inoculated leaves appeared to have increased relative levels of BiP, a molecular chaperone confined to the ER lumen (Boston et al., 1991; Terasaki and Reese, 1992). An effort was made to standardize the amount of membrane loaded on the gels by loading slurry prepared from equivalent tissue weights. Increased signal from the anti-BiP could reflect either a greater amount of membrane loaded or an increased ratio of BiP to membrane volume. Since virus-infected plants appear to have relatively more membranes, it is likely that any ER marker used as a loading control will give increased signal, and would be no more informative than BiP. Increased levels of ER resident proteins are consistent with ER proliferation as a result of RCNMV replication. This behavior is also consistent with other tombusviruses, which induce membrane proliferation and distortion during replication (Burgyan, et al. 1996; Rubino et al., 2000; Rubino et al., 2001).

The technique of expressing GFP:p27 from the RCNMV subgenomic promoter is limited in that it produces extremely high amounts of GFP:p27 in addition to the unlabelled p27 normally produced during infection. The presence of an unlabelled copy of p27 in the cells simultaneously with GFP:p27 makes it impossible to guarantee that this localization is biologically relevant. The ER may be distorted simply as a result of increased protein production, and the localization of GFP:27 could reflect the cell's attempt to sequester the viral

proteins prior to degradation, rather than any activity of the virus. To address these concerns, a heterologous vector system was devised.

GFP:p27 and GFP:p88 expressed from CaMV 35S promoter localize to ER

The RCNMV replicase does not complement replication in *trans* (Kim and Lommel, 1998). In order to genetically uncouple the expression of p88 from that of p27, we generated CaMV 35S constructs that produce GFP:p27 and GFP:p88. The constructs were used to inoculate both whole leaves and protoplasts. In epidermal cells both proteins independently localize to the cortical ER, the nuclear envelope, and tubular ER. In addition, tubular projections of fluorescence could be observed within the nucleus. While sequence analysis indicates that there are no recognized ER or nuclear targeting or retention signals present in p27 or p88, both proteins localize to the ER in the absence of any other RCNMV proteins. A general feature of *Tombusvirus* infections is the appearance of multi-vesicular bodies (MVB), large aggregates of viral proteins and proliferated, vesiculated membranes (Burgyan et al., 1996). The large aggregates seen in the ER and near the nucleus in cells expressing p27 and p88 are a form of MVB, although the fluorescence intensity is too great to discern any internal structures. With other Tombusviruses nascent RNA synthesis often takes place in MVB (Burgyan et al., 1996; Rubino and Russo, 1998), and this is likely to occur with RCNMV as well.

In inoculated protoplasts, p27 and p88 accumulated in distorted ER, and fluorescent aggregates could be observed within the nucleus. Particularly in

protoplasts, the pathological condition induced by over-expression of p27 and p88, as well as damage done to the cells during preparation and inoculation perturbed the ER to such a degree that the typical reticular structure and streaming were not evident. In many cells, the entire cell volume was filled with fluorescence. In this condition, the cells were not amenable to observation of subcellular structures. The ER often appeared vesiculated and patchy, and the nuclear envelope was not evident.

Collings et al. (2000) demonstrated that plant nuclei may have extensive grooves and invaginations that are contiguous with the ER membranes. These tubes ramify throughout the nucleus of plant and animal cells (Collings et al., 2000; Fricker et al., 1997). Such an intimate connection between the nuclear interior and the ER could provide increased surface area for translation, or could provide isolated domains for assembly of protein complexes destined to be transported by the secretory pathway (Fricker et al., 1997; Lui et al., 1998a). It is consistent with this observation that fluorescence from p27 and p88 could be associated with the ER while appearing to be inside the nucleus.

In protoplasts inoculated with both GFP:p27 and GFP:p88, three patterns of fluorescence were evident: one similar to GFP:p27 alone, one similar to GFP:p88 alone, and one pattern that had characteristics of both. Since the two constructs were on separate plasmids, it was impossible to guarantee that each protoplast received both constructs. It is likely, therefore, that the range of patterns reflected cells that received one or the other construct, or both. The

protoplasts that had characteristics of both patterns were assumed to express both p27 and p88, and were selected for further study.

In epidermal cells and protoplasts the fluorescence pattern of overexpressed GFP:p88 was variable and included large aggregates, the web of cortical ER, and diffuse fluorescence that could not be unambiguously attributed to any organelle. In previous tombusvirus studies it has been shown that GFP-labeled viral proteins cannot localize to chloroplasts if there are no chloroplasts in the infected cell, regardless of targeting signals (Burgyan et al., 1996). It follows that if the normal ER structure were absent from the GFP:p88 inoculated cells, the fluorescence pattern would reflect that lack. In addition, in studies of poliovirus, it has been found that cellular markers for the ER, Golgi and lysosomes are equally represented in the membranous bodies produced during infection, even though electron micrographs show direct budding of poliovirus-induced membranes from rough ER and brefeldin A inhibits poliovirus RNA replication (Schlegel et al., 1996), strongly suggesting the ER membranes as the source of MVB. These contradictory data could indicate that virus infection perturbs the lipid balance of the entire secretory pathway, or even of the whole cell. It has been shown that some RNA viruses require a specific lipid environment for replication (Bong et al., 1999; Carette et al., 2000; Lee et al., 2001). The diffuse fluorescence pattern in GFP:p88 inoculated cells is likely due to degradation of the normal reticular ER structure, and may be indicative of general membrane reorganization in the cell.

GFP:p27 expressed from TBSV localizes to ER and co-localizes with ER YFP

A heterologous viral vector based on TBSV, a species in the same virus family as RCNMV, was used to uncouple the expression of p27 and p88 from replication while avoiding the excessive damage caused by protoplasting. Expression of GFP:p27 from the vector confirmed the results obtained with RCNMV. p27 accumulated in the ER of inoculated cells. Fluorescence was observed throughout the ER, including the nuclear envelope and cortical ER. In this system, the cells were able to tolerate high levels of GFP:27 expression without apparent pathology. While the ER network appeared thicker and more prolific than in control plants (compare Fig. 4 G and I), the cortical ER was crisp, with detailed structures. Numerous tiny motile bodies displayed intense fluorescence and directed movement. Golgi are associated with and move over cortical and tubular ER (Boevink et al., 1998; Haseloff et al., 1997). The tiny, bright fluorescent bodies in GFP:27 inoculated cells greatly resemble Golgi bodies. The larger fluorescent aggregates appearing in inoculated cells are more stationary, and are likely related to the ER inclusions studied by Haseloff (1997). Both types of ER-associated bodies must use transmembrane linker proteins to travel along the actin cytoskeleton and are perfectly positioned to play a role in intercellular communication or protein synthesis.

In order to verify the ER localization of GFP:p27 and GFP:p88, a co-inoculation experiment was performed. GFP:p27 co-inoculated with ER YFP co-localized with the ER targeted yellow fluorescence in the cortical and cytoplasmic

ER. Unexpectedly, the ER YFP was also visualized in the interior of the nucleus in all the fluorescent cells. The rabbit-derived signal targeting sequence may not have been able to direct the YFP solely to the ER in plant cells, or the presence of replicating TBSV in the cell may have disturbed the ER to such an extent that contents from the ER lumen were misdirected into the nucleus. Since GFP generally stayed within the nuclear envelope, while YFP escaped, (Fig. 4 C) it is more likely that the signal targeting sequence was not stringent enough in this system. This brings up interesting questions about the mechanisms of protein targeting in plants and animals. In animals the Golgi apparatus (GA) is represented by one or two large stacks of membranous sacks, generally situated close to the ER and generally stationary except during cell division (Cole and Lippincott-Schwartz, 1995). In plant cells, the structure of the Golgi apparatus is very different, with the stacks divided into hundreds of small, mobile vesicles that move in association with the ER (Boevink et al., 1998; Nebenfuehr et al., 1999). Yet, even with these rather dramatic differences, the GA targeting sequence from rat sialyl transferase seems to localize GFP to the plant Golgi unambiguously (Wee et al., 1998; Horsley et al., 1993). For the future, it will be important to determine what other systems are different in plants and animals, and if these differences impact protein targeting. In the meantime, it is important to consider the origin of targeting sequences when designing experiments.

Although the YFP ER construct displayed nuclear localization in addition to the expected cortical and smooth ER localization, it is still a useful visible marker for ER in the cell. The fact that GFP:p27 co-localized extensively with

YFP ER in co-inoculated cells supports the hypothesis that the RCNMV replicase accumulates at the ER in virus infected plants.

The ER is distorted when viruses are present

Transgenic plants expressing GFP-ER were inoculated with TBSV- based viral constructs and wt RCNMV to observe the effects of various viral proteins on the fluorescent ER. The only fluorescence in the system came from the GFP-ER, contained within the ER lumen. All of the constructs tested perturbed the ER to some degree, including the TBSV vector alone. This makes interpretation of the experiments using that vector problematic, as effects of the RCNMV proteins must be observed in a background of effects from the TBSV vector. It is clear that RCNMV p27 localizes to the ER. The fact that wt RCNMV caused perinuclear aggregates and small cytoplasmic aggregates in the GFP-ER plants indicates that some of the ER distortion observed in pHST2-GFP:p27 inoculated plants is due to the presence of p27. We cannot quantify how much of the distortion is due to RCNMV. The ER in RCNMV inoculated GFP-ER plants is similar in appearance to the fluorescence patterns in GFP:p27 and GFP:p88 inoculated cells. This is a confirmation that the ER localization observed in those experiments represents a biologically relevant part of the natural RCNMV replication cycle, and not an artifact of protein overexpression, an artifact of GFP expression, or a spurious localization.

In conclusion

Each of the methods of the expression of GFP:p27 has revealed new information about its localization. It is possible that the localization of p27 changes over the course of time, in response to undiscovered factors. Multifunctional proteins often have multiple localizations (Kong and Hanley-Bowdoin, 2002). It has been observed that TBSV p33 and p92 proteins accumulate in the membrane fractions isolated from protoplasts early in infection and accumulate in the cytoplasmic fraction later in infection, prior to collapse of the tissues (Scholthof et al., 1995b). It has also been shown that virus replication proteins can have multiple localizations correlated with time after infection. At early stages of infection the TMV 126/183k replicase co-localizes with ER (Mas and Beachy, 1999). During the middle stages of infection, the replicase moves from the ER to microtubules, and later traffics along them to the plasmodesmata (Mas and Beachy, 1999); (Gillespie et al., 2001).

In all cases, the fluorescence observed in GFP:p27 inoculated plants accumulated at the ER. In some cases, there appeared to be additional sites of localization such as MVB, Golgi apparatus, or unidentifiable diffuse fluorescence. Expression of GFP:p27 from the TBSV vector gave the highest percentage of fluorescent, phenotypically normal cells and was the most efficient system to work with. It is more challenging to interpret the results gained from this system however, as inoculation with TBSV vector alone changes the ER dynamics (Fig. 4 G). Fluorescent aggregates and tiny fluorescent bodies were observed in

transgenic plants expressing GFP-ER inoculated with PHST2-p27 and pHST2. The ER tubules also became thicker and had mobile inclusions. In spite of these distortions, the ER segregated normally into membrane fractions and fluorescent cells seemed to have normal streaming.

TBSV is a member of the family *Tombusviridae*, as is RCNMV. The two viruses have high sequence identity in the replicase proteins. While TBSV has also been shown to be associated with membrane fractions of virus-infected plants, no tombusvirus other than RCNMV has previously been shown to associate with the ER (Burgyan et al., 1996; Rubino and Russo, 1998). It is important to emphasize that while TBSV is related to RCNMV and appears to have a mild effect on ER structure, in this investigation it was used only as a vector and its relationship to RCNMV is incidental. The evidence that RCNMV replicase accumulates at the ER is persuasive, regardless of the perturbation of normal ER structure due to the vector.

GFP:p88 co-localizes with GFP:p27 in two expression systems. In addition to this, the fact that GFP:p27 localizes to the ER when expressed from three different promoters, in the presence of heterologous and homologous viral genomes, as well as in the absence of any viral proteins suggests that the two proteins co-localize to the cortical ER, the nuclear envelope, and tubular cytoplasmic ER domains. The RCNMV replicase components do not complement replication when expressed in *trans* from separate RNAs (Kim, 1993). It is therefore impossible to directly observe the individual labeled proteins in a functional replication complex. The fact that both proteins, when

expressed alone, accumulate in the ER and perturb the ER morphology suggests that the proteins function together, as part of a larger replication complex. Such a complex likely contains host proteins as well as those of RCNMV (Bastin and Hall, 1976; Lee et al., 2001; Schwartz et al., 2002).

Acknowledgements

Special thanks to Dr. A. Callaway for performing long PCR and creating RC169-p88. We thank Dr. J. Sheen for the sGFP, Dr. J. Carrington for pRTL2 vector, and Dr. H. Scholthof for the pHST2 vector. We thank Dr. D. A. Collings for assistance with microscopy, Dr. E. Johannes for advice on protoplasts and confocal microscopy, and Mara Massel for helpful discussion. We must also thank Dr. K. Nielsen for help with western blots, Dr. R. S. Boston for the anti-BiP, and Kirk Francis for help with protein quantification. This work was supported by a NSF/DOE/USDA training Grant # 546142-06284 to S.A.L. and K.A.T., USDA NRI competitive grant 98-02298 to S.A.L. and T.L.S., NSF competitive grants MCB-0077964 to S.A.L. and T.L.S, and NASA competitive grant NAGW-4984 to N. S. A.

Table 1. Primers used to produce cloning inserts for GFP:p27 and GFP:p88 expression vectors

FpRC169p88	CTAGGCGGCCCACTCAGCTTTCCGGTT
RpRC169p88	GAAATCCTCAAGGGATTTGAACCCGGCAACA
sGFP 3' ΔNM	GTACGCGTCCATGGCCTTGTACAGCTCGTCCATGC
sGFP 5' 6xHIS	GTCCATGGGATCGATGCATCATCATCATCATCATGTGAGCAAGGGC GAGGAGCTG
p27-5' Cla/Nco	CTATCGATGGCCATGGGTTTTATAAATCTTTCGC
p27-3' Xho/Mlu	GCACGCGTCTCGAGCTAAAAATCCTCAAGGGATTTG
sGFP 3' MKSX	GCATTCTAGATTAACTAGTCATGGTACCACGCGTCTTGT
P88-5' Mlu/Kpn	GATACGCGTGGTACCATGGGTTTTATAAATCTTTCGCTT
p27-3' Xba/Bam	CTAGGGATCCTCTAGACTAAAATCCTCAAGGGATTTGAAC
p88-3' Not/Spe	TAAACTATACTAGTGCGGCCGCTTATCGGGCTTTGATTA
ERYFP5' Sna/Xho	TAGCTATACGTACTCGAGATGCTGCTATCCGTGCCGTT
ERYFP3' Sca/Xba	CTAGAGCTCTCTAGATTACAGCTCGTCCTTCTTGTACAG

Figure 1. Genome maps of RCNMV and TBSV and various derivative p27- and p88-expressing constructs. (**A**) Schematic diagram of RCNMV RNA-1, RNA-2, R1sGFP, and R1G27. ORFs for p27, the –1 ribosomal frameshift (FS) product p88 and CP are labeled. R1sGFP replaces the CP with sGFP (shaded box) (Sit et al., 1998). The sGFP is expressed from subgenomic RNA-1. R1G27 produces p27 as a 3' translational fusion to GFP. GFP:p27 is produced from the subgenomic RNA-1. (**B**) Constructs prepared for microprojectile bombardment. A doubled CaMV 35S promoter, TEV leader sequence and NOS terminator are labeled (open arrows and hatched boxes). PRTL2-sGFP is based on pRT100 (Topfer et al., 1987) and expresses GFP to extremely high levels in the cytoplasm of bombarded tissues. pRTL2-GFP:p27 expresses p27 fused to the 3' end of GFP. pSX-GFP:p88 is also based on pRT100, but has three additional restriction sites beyond those in pRTL2. p88 is expressed as a 3' fusion to GFP. (**C**) Diagram of the TBSV genome, the TBSV expression vector pHST2, and derivatives produced for this study. In the pHST2 vector, the CP ORF was engineered to accept and express foreign genes (Scholthof and Scholthof, 1996). The dashed line shows the deleted portion of the CP gene. pHST2- sGFP produces GFP from the subgenomic RNA. PHST2-G27 produces p27 fused to the 3' terminus of GFP. pHST2-G27ΔAH produces GFP:27 as well, but the lack of TBSV p22 movement protein prevents it from trafficking out of the inoculated cell. pHST2-ER YFP produces YFP (darker shaded box) with an ER signal targeting sequence and cognate 'KDEL' retention signal. It has a functional TBSV p22 movement protein and can complement cell-to-cell movement of co-inoculated pHST2-G27ΔAH.

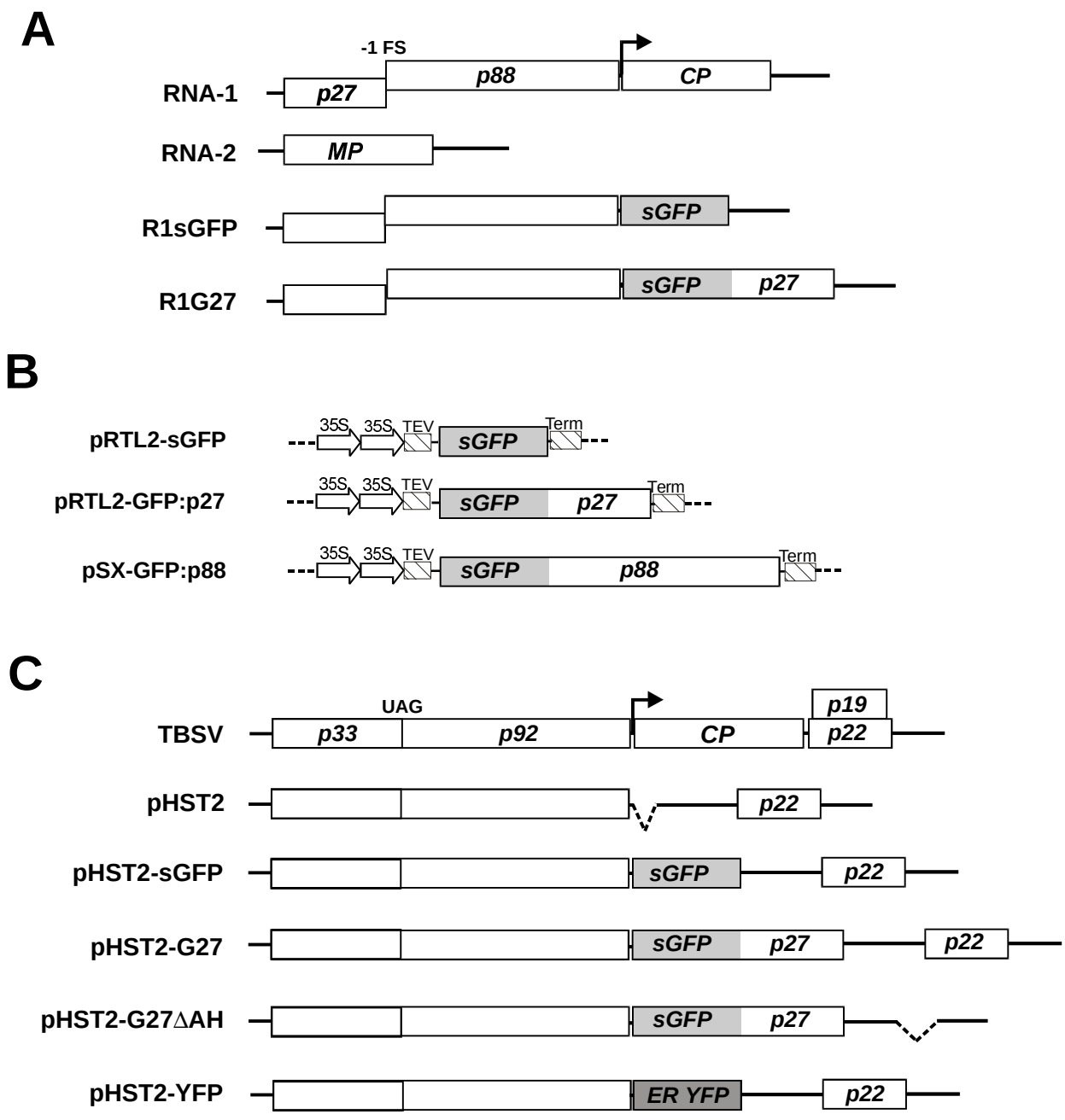
A
-1 FS
RNA-1
p27
p88
CP
RNA-2
MP
R1sGFP
sGFP
R1G27
sGFP
p27
B
pRTL2-sGFP
35S
35S
TEV
sGFP
Term
pRTL2-GFP:p27
35S
35S
TEV
sGFP
p27
Term
pSX-GFP:p88
35S
35S
TEV
sGFP
p88
Term
C
UAG
TBSV
p33
p92
CP
p19
p22
pHST2
p22
pHST2-sGFP
sGFP
p22
pHST2-G27
sGFP
p27
p22
pHST2-G27ΔAH
sGFP
p27
pHST2-YFP
ER YFP
p22

Figure 2. Confocal images of GFP:p27 and GFP:p88 accumulating in the ER of *N. benthamiana* epidermal cells. (A,C,E,G, I, J, K M, N, O, P) computer projections of multiple confocal sections of each cell, each section of approximately 1 μm focal depth. Each projection displays at least 10 sections. (B,D,F,H, L) 1 μm individual sections of the same cells. The boxes indicate which region of the cell is enlarged. Arrows indicate cortical ER. Arrowheads indicate the nuclear envelope. Small arrows indicate small motile bodies. Small arrowheads indicate fluorescence in nuclear strands or tubes. Doubled darts indicate spherical membranous structures. (**A** and **B**) *In vitro* transcripts of RCNMV RNA-1 expressing GFP:p27 from the subgenomic RNA were manually inoculated to *N. benthamiana* leaves and observed for fluorescence using laser scanning confocal microscopy. (**A**) typical pattern of fluorescence produced after inoculation with R1G27 (**B**) cortical section showing tubular cytoplasmic ER and polygonal cortical ER. (**C-H**) *N. benthamiana* epidermal cells expressing pRTL2-GFP:p27 after microprojectile bombardment. (**C** and **D**) prominent multivesicular bodies and ER tubules through the nucleus. (**E** and **F**) protein aggregates and very fine cortical ER, with tiny, highly fluorescent bodies. (**G** and **H**) bright motile bodies and stationary spheres. (**I, J**) unfused GFP with an even, cytoplasmic distribution. (**K-N**) *N. benthamiana* epidermal cells expressing pSX-p88 after microprojectile bombardment. (**K** and **L**) multivesicular bodies and reticular ER, as well as strands through the nucleus. (**M** and **N**) diffuse fluorescence pattern. (**O** and **P**) enlargements of areas within the small boxes in C and K to show detail. Scalebars equal 10 μm.

Go back to page
58 (69 of the PDF)

Go back to page
59 (70 of the PDF);page 67 (78 of the PDF)

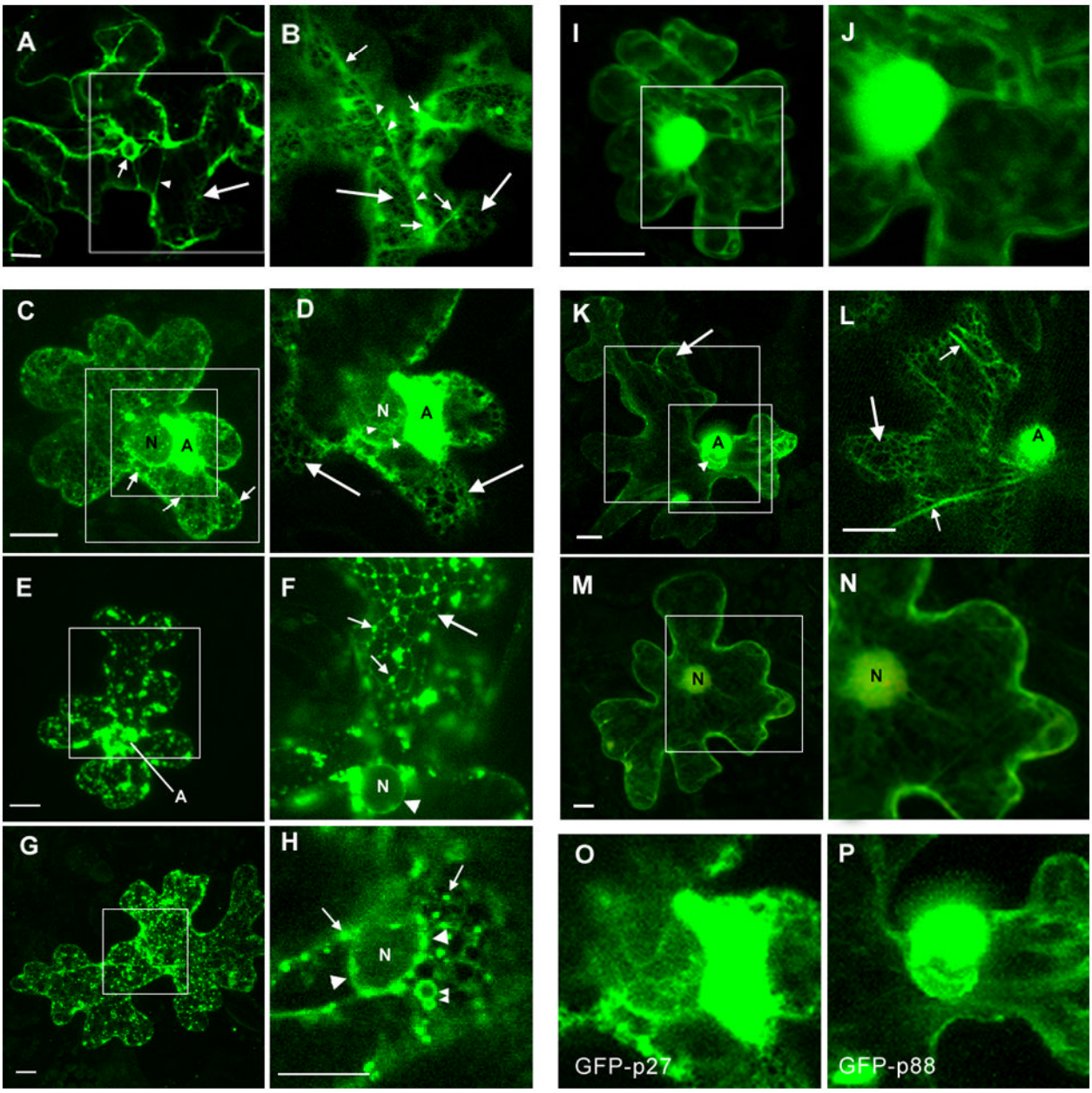

Figure 3. Confocal images of GFP:p27 and GFP:p88 in PEG-inoculated protoplasts. Protoplasts were prepared from *N. benthamiana* epidermal and mesophyll cells and inoculated with pRTL2-sGFP, pRTL2-GFPp27 or pSXp88. 24 hours after inoculation, the fluorescence was observed via confocal microscopy. **A-D**) Computer projections of multiple confocal sections. **A'-D'**) corresponding brightfield micrographs of the cells. (**E** and **F**) GFP:p27 + GFP:p88 single 1μm confocal section (**E'** and **F'**) GFP:p27 + GFP:p88 corresponding brightfield micrograph (**A**) pRTL2-sGFP characteristic diffuse fluorescence throughout the cytoplasm and nucleus. The large central vacuole does not contain GFP. (**B**) pRTL2-GFP:p27 protein aggregates and fine membranes stretched between them. (**C**) pSXp88 fluorescence appears to fill the volume of the cell. The dark circular patches represent where GFP:p88 is excluded from the chloroplasts. (**D**) pRTL2-GFP:p27 and pSxp88 fluorescence fills the entire volume of the cell, distorting the ER membranes. Fluorescent aggregates are within the nucleus. (**E** and **F**) pRTL2-GFP:p27 and pSxp88. Individual 1 μm sections demonstrate that the fluorescent aggregates occur in the area bounded by the nuclear membrane, and are not simply visible "through" the nucleus as an artifact of confocal imaging. Scalebar equals 10 μm.

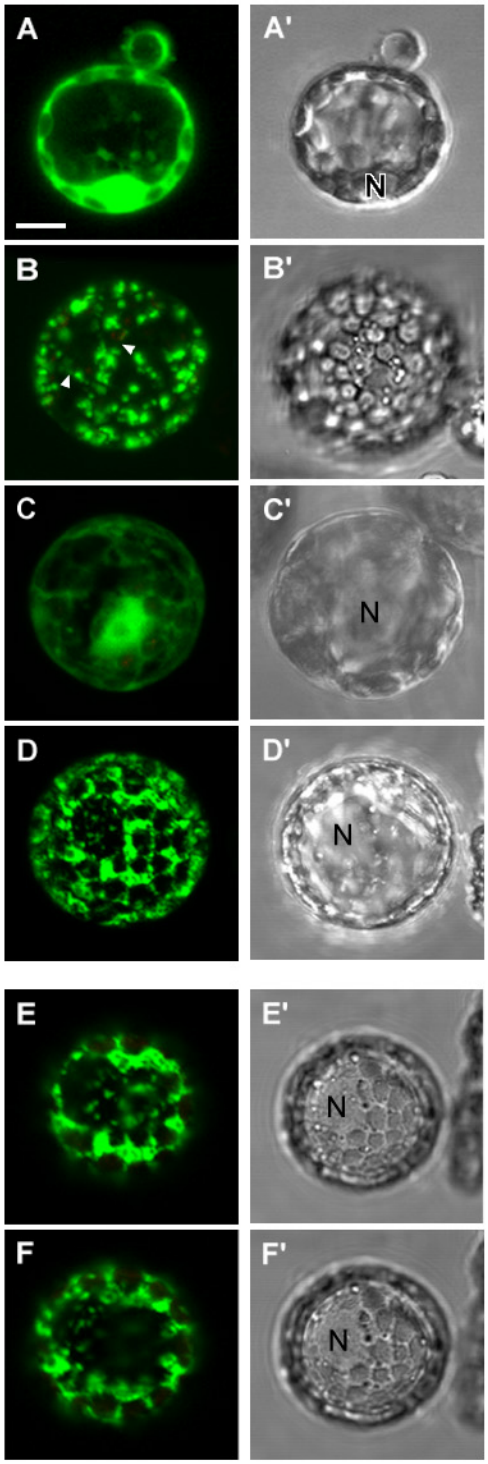
A
A'
N
B
B'
C
C'
N
D
D'
N
E
E'
N
F
F'
N

Figure 4. Confocal images of pHST2-GFP:p27, pHST2- ER YFP and pHST2-GFP:p27ΔAH. (A, C, G-K) computer projections of multiple confocal sections of each cell, each section approximately 1μm focal depth. Each projection displays at least 10 sections. (B, D, E, F) individual 1μm sections. The boxed area in A represents the area enlarged in D-F. *In vitro* transcripts of pHST2 constructs were manually inoculated to *N. benthamiana* leaves. Fluorescent cells were imaged using confocal microscopy. (**A**) A typical pattern of fluorescence produced after infection with pHST2-GFP:p27 (**B**) interior section of similar cell showing characteristic ring around the nucleus (large arrow), cortical ER and smooth ER tubules (arrowhead), as well as bright mobile spots (small arrows). (C) False color overlay of pHST2- ER YFP and pHST2-GFP:p27ΔAH. (**D**) pHST2-GFP:p27ΔAH in the cortical region, showing the reticular cortical ER and punctate spots. (**E**) pHST2-ER YFP in the same cell. (**F**) False color overlay of the two. GFP:p27 and ER YFP co-localize in the reticular network.
(**G-K**) Transgenic *N. benthamiana* plants expressing GFP-ER. The fluorescence shown is exclusively from the ER-localized GFP. Transgenic plants were manually inoculated with *in vitro* transcripts of pHST2 clones. (**G**) mock inoculation, represents unperturbed ER structure. (**H**) GFP-ER *N. benthamiana* inoculated with pHST2 vector. (**I**) GFP-ER *N. benthamiana* inoculated with pHST2- GFP:p27. (**J**) GFP-ER *N. benthamiana* inoculated with pHST2- ER YFP. The red circle indicates the nucleus. (**K**) GFP-ER *N. benthamiana* inoculated with wt RCNMV. The red circle indicates the nucleus (**L**) GFP-ER *N. benthamiana* after 4 hour incubation in 200 μg/mL brefeldin A, a fungal metabolite that disrupts ER structure (Boevink et al., 1998). The loss of fluorescence in the cortical region and large blebs of membrane are characteristic of stressed, disrupted ER.

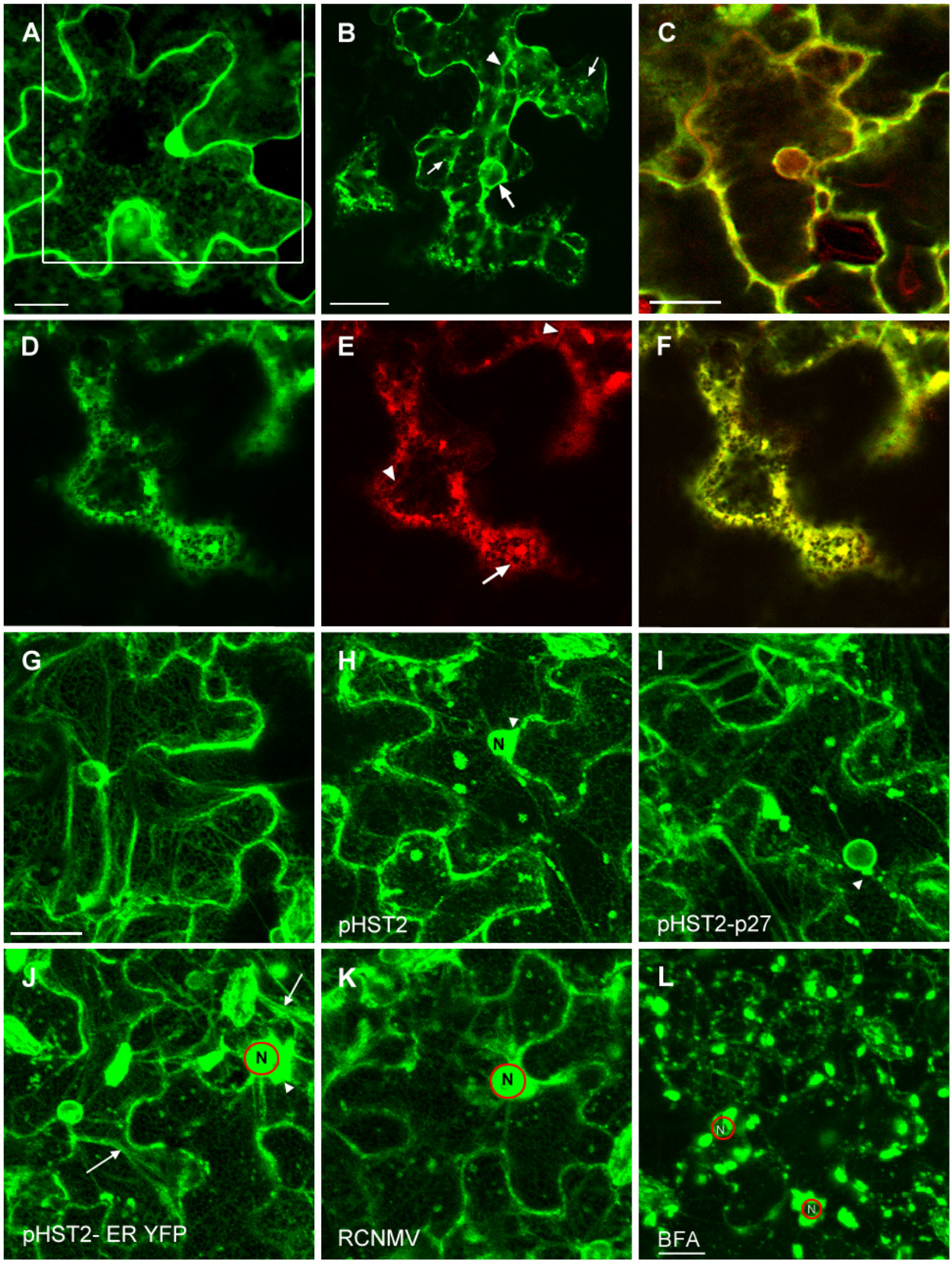
A
B
C
D
E
F
G
H
N
pHST2
I
pHST2-p27
J
N
pHST2- ER YFP
K
N
RCNMV
L
N
N
BFA

Figure 5. Immunoblot analysis of p27 and BiP proteins in fractions of RCNMV inoculated *N. benthamiana.* Mock- and RCNMV inoculated plant tissues were homogenized in buffer A, applied to a 40- 51% sucrose gradient, and centrifuged at 15,000 x g. Total (T), pellet (P), and supernatant (S) fractions were separated by SDS-PAGE and visualized with anti-p27 or anti-BiP. Cellular membranes remain in the supernatant. (**A**) RCNMV p27 is found predominantly in the membrane fraction of RCNMV inoculated tissue. A minor portion (less than 20%) remained in the pellet. No signal was detected in fractions from mock-inoculated tissue. (**B**) ER-resident binding protein (BiP) is found in the membrane fraction of mock- and RCNMV inoculated tissue. Trace amounts were visualized in the pellet fractions. The total amount of BiP present appears greater in RCNMV inoculated plants (compare Mock (T) with RCNMV (T) in B).

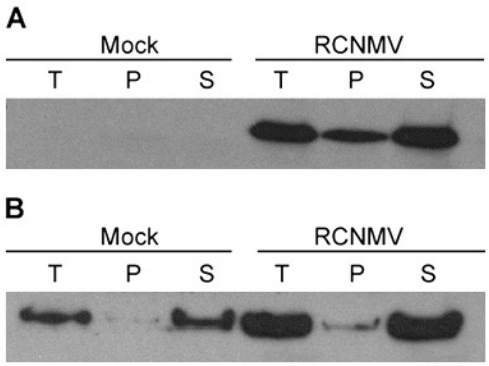
A
Mock
RCNMV
T
P
S
T
P
S
B
Mock
RCNMV
T
P
S
T
P
S

References

AHLQUIST, P., WU, S. X., KAESBERG, P., KAO, C. C., QUADT, R., DEJONG, W., and HERSHBERGER, R. (1994). Protein-protein interactions and glycerophospholipids in bromovirus and nodavirus RNA replication. *Arch Virol Suppl* **9,** 135-145.

ALLEN, N. S., and SCHUMM, J. H. (1990). Endoplasmic reticulum, calciosomes and their possible roles in signal transduction. *Protoplasma* **154,** 172-178.

ANGRES, B., and GREEN, G. (1999). Dual labeling using eCFP and eYFP in standard fluorescence microscopy. *Clontechniques*, April 1999, 28-29.

BASTIN, M., and HALL, T. C. (1976). Interaction of elongation factor 1 with aminoacylated brome mosaic virus and tRNAs. *J Virol* **20,** 117-122.

BATES, A. H., FARJAH, M., OSMAN, T. A. M., and BUCK, K. W. (1995). Isolation and characterization of an RNA-dependent RNA polymerase from *N. clevlandii* plants infected with Red cover necrotic mosaic dianthovirus. *J Gen Virol* **76,** 1483-1491.

BOEVINK, P., OPARKA, K., SANTA CRUZ, S., MARTIN, B., BETTERIDGE, A., and HAWES, C. (1998). Stacks on tracks: the plant Golgi apparatus traffics on an actin/ER network. *Plant Journal* **15,** 441-447.

BONG, D. T., STEINEM, C., JANSHOFF, A., JOHNSON, J. E., and REZA GHADIRI, M. (1999). A highly membrane -active peptide in flock house virus: implications for the mechanism of nodavirus infection. *Chem Biol* **6,** 473-481.

BOSTON, R., FONTES, E., SHANK, B., and WROBEL, R. (1991). Increased expression of the maize immunoglobulin binding protein homolog b-70 in three zein regulatory mutants. *Plant Cell* **3,** 483-496.

BUCK, K. W. (1996). Comparison of the replication of positive-stranded RNA viruses of plants and animals. *Adv Virus Res* **47,** 159-213.

BURGYAN, J., RUBINO, L., and RUSSO, M. (1996). The 5' terminal region of a tombusvirus determines the origin of multivesicular bodies. *J Gen Virol* **77,** 1967-1974.

CALLAWAY, A. S. (1998). PhD. A genetic approach to study host factors of Arabidopsis thaliana that influence susceptibility to Cauliflower mosaic virus. Cornell University, Ithaca, NY.

CARETTE, J. E., STUIVER, M., VAN LENT, J., WELLINK, J., and VAN KAMMEN, A. (2000). Cowpea mosaic virus infection induces a massive proliferation of endoplasmic reticulum but not Golgi membranes and is dependent on de novo membrane synthesis. *J Virol* **74,** 6556-6563.

CHIU, W. L., NIWA, Y., ZENG, W., HIRANO, T., KOBAYASHI, H., and SHEEN, J. (1996). Engineered GFP as a vital reporter in plants. *Curr Biol* **6,** 325.

COLE, N. B., and LIPPINCOTT-SCHWARTZ, J. (1995). Organization of organelles and membrane traffic by microtubules. *Curr Opin Cell Biol* **7,** 55-64.

COLLINGS, D. A., CARTER, C. N., RINK, J. C., SCOTT, A. C., WYATT, S., and ALLEN, N. S. (2000). Plant nuclei can contain extensive grooves and invaginations. *Plant Cell* **12,** 2425-2439.

DEN BOON, J. A., CHEN, J., and AHLQUIST, P. (2001). Identification of sequences in brome mosaic virus replicase protein 1a that mediate association with endoplasmic reticulum membranes. *J Virol* **75,** 12370-12381.

DUNOYER, P., RITZENTHALER, C., HEMMER, O., MICHLER, P., and FRITSCH, C. (2002). Intracellular localization of the *Peanut clump virus* replication complex in tobacco BY-2 protoplasts containing green fluorescent protein-labeled endoplasmic reticulum or Golgi apparatus. *J Virol* **76,** 865-874.

DOS REIS FIGUEIRA, A., GOLEM, S., GOREGAOKER, S. P., AND CULVER, J. S. (2002). A nuclear localization signal and a membrane association domain contribute to the cellular localization of the *Tobacco mosaic virus* 126-kDa replicase protein. Virology **301**, 81-89.

FLIEGEL, L. (1989). Molecular cloning of the high affinity calcium binding protein calreticulin of skeletal muscle sarcoplasmic reticulum. *J Biol Chem* **264,** 21522-21528.

FONTES, E., SHANK, B., WROBEL, R., MOOSE, S., OBRIAN, G., WURTZEL, E., and BOSTON, R. (1991). Characterization of an immunoglobulin binding protein homolog in the maize floury-2 endosperm mutant. *Plant Cell* **3,** 483-496.

FRICKER, M., HOLLINSHEAD, M., WHITE, N., and VAUX, D. (1997). Interphase nuclei of many mammalian cell types contain deep, dynamic, tubular membrane-bound invaginations of the nuclear envelope. *J Cell Biol* **136,** 531-544.

GEISMAN-COOKMEYER, D., and LOMMEL, S. A. (1993). Alanine scanning mutagenesis of a plant virus movement protein identifies three functional domains. *Plant Cell* **5,** 973-982.

GILLESPIE, T., TOTH, R. L., HAUPT, S., BOEVINK, P., ROBERTS, A. G., CHAPMAN, S., and OPARKA, K. (2001). *Plasmodesma 2001 Fourth International Conference, Capetown South Africa*.

GOMORD, V., DENMAT, L., FITCHETTE-LAINE, A., SATIAT-JEUNEMAITRE, B., HAWES, C., and FAYE, L. (1997). The C-terminal HDEL sequence is sufficient for retention of secretory proteins in the endoplasmic reticulum (ER) but promotes vacuolar targeting of proteins that escape the ER. *Plant J* **11,** 313-325.

HASELOFF, J., SIEMERING, K. R., PRASHER, D., and HODGE, S. (1997). Removal of a cryptic intron and subcellular localization of green fluorescent protein are required to mark transgenic *Arabidopsis* plants brightly. *Proc Natl Acad Sci U S A* **94,** 2122-2127.

HORSLEY, D., COLEMAN, J., EVANS, D., CROOKS, K., PEART, J., SATIAT-JEUNEMAITRE, B., and HAWES, C. (1993). A monoclonal antibody, JIM 84, recognizes the Golgi apparatus and plasma membrane in plant cells. *J Exp Bot* **44,** 223-229.

KIM, K.-H. (1993). Ph.D. Ribosomal frameshift regulation of viral polymerase: red clover necrotic mosaic virus as a model system. NC State University, Raleigh, NC.

KIM, K. H., and LOMMEL, S. A. (1994). Identification and analysis of the site of -1 ribosomal frameshifting in red clover necrotic mosaic virus. *Virology* **200,** 574-582.

KIM, K. H., and LOMMEL, S. A. (1998). Sequence element required for efficient -1 ribosomal frameshifting in red clover necrotic mosaic dianthovirus. *Virology* **250,** 50-59.

KNEBEL, W., QUADER, H., and SCHNEPF, E. (1990). Mobile and immobile endoplasmic reticulum in onion bulb epidermis cells: short- and long-term observations with a confocal laser scanning microscope. *Eur J Cell Biol* **52,** 328-340.

KONG, L., and HANLEY-BOWDOIN, L. (2002). A geminivirus replication protein interacts with a protein kinase and a motor protein that display different expression patterns during plant development. *Plant Cell* **14,** 1817-1832.

LAEMMLI, U. K. (1970). Cleavage of ultrastructural proteins during assembly of the head of bacteriophage T4. *Nature* **227,** 680-685.

LEE, W.-M., ISHIKAWA, M., and AHLQUIST, P. (2001). Mutation of Host delta-9 fatty acid desaturase inhibits brome mosaic virus RNA replication between template recognition and RNA synthesis. *J Virol* **75,** 2097-2106.

LUI, P., KONG, S. K., KWOK, T. T., and LEE, C. Y. (1998a). The nucleus of HeLa cells contains tubular structures for calcium signaling. *Biochem Biophys Res Commun* **247,** 88-93.

MAS, P., and BEACHY, R. N. (1999). Replication of tobacco mosaic virus on endoplasmic reticulum and role of the cytoskeleton in intercellular distribution of viral RNA. *J Cell Biol* **147,** 945-958.

MILLER, D., SCHWARTZ, M., and AHLQUIST, P. (2001). Flock house virus RNA replicates on outer mitochondrial membranes in Drosophila cells. *J Virol* **75,** 11664-11667.

NEBENFUEHR, A., GALLAGHER, L. A., DUNAHAY, T. G., FROHLICK, J. A., MAZURKIEWICZ, A. M., MEEHL, J. B., and STAEHELIN, L. A. (1999). Stop-and-Go movements of plant Golgi stacks are mediated by the acto-mysoin system. *Plant Phys* **121,** 1127-1141.

OPARKA, K., BOEVINK, P., and CRUZ, S. S. (1996). Studying the movement of plant viruses using green fluorescent protein. *Trends Plant Sci* **1,** 412-418.

OSMAN, T. A. M., and BUCK, K. W. (1987). Replication of red clover necrotic mosaic virus RNA in cowpea protoplasts: RNA-1 replicates independently of RNA-2. *J Gen Virol* **68,** 289-296.

PETTY, I. T. D., HUNTER, B. G., WEI, N., and JACKSON, A. O. (1989). Infectious barley stripe mosaic virus RNA transcribed *in vitro* from full length genomic cDNA clones. *Virology* **171,** 342-349.

PROD'HOMME, D., LE PANSE, S., DRUGEON, G., and JUPIN, I. (2001). Detection and subcellular localization of the turnip yellow mosaic virus 66K replication protein in infected cells. *Virology* **281,** 88-101.

REICHEL, C., and BEACHY, R. N. (1998). Tobacco mosaic virus infection induces severe morphological changes of the endoplasmic reticulum. *Proc Natl Acad Sci U S A* **95,** 11169-11174.

RESTREPO-HARTWIG, M., and AHLQUIST, P. (1999). Brome Mosaic Virus RNA replication proteins 1a and 2a colocalize and 1a independently localizes on the yeast endoplasmic reticulum. *J Virol* **73,** 10303-10309.

ROHOZINSKI, J., and HANCOCK, J. M. (1996). Do light induced pH changes within the chloroplast drive turnip yellow mosaic virus assembly? *J Gen Virol* **77,** 163-165.

RUBINO, L., DI FRANCO, A., and RUSSO, M. (2000). Expression of a plant virus non-structural protein in *S. cerevisiae* causes membrane proliferation and altered mitochondrial morphology. *J Gen Virol* **81**, 279-286.

RUBINO, L., and RUSSO, M. (1998). Membrane targeting sequences in tombusvirus infections. *Virology* **252,** 431-437.

RUBINO, L., WEBER-LOTFI, F., DIETRICH, A., STUSSI-GARAUD, C., and RUSSO, M. (2001). The open reading frame 1-encoded ('36K') protein of Carnation Italian ringspot virus localizes to mitochondria. *J Gen Virol* **82,** 29-34.

SANFORD, J. C., SMITH, F. D., and RUSSEL, J. A. (1993). Optimizing the biolistic process for different biological applications. *Meth Enz* **217,** 483-509.

SCHAAD, M. C., JENSEN, P. E., and CARRINGTON, J. C. (1997). Formation of plant RNA virus replication complexes on membranes: role of an endoplasmic reticulum-targeted viral protein. *EMBO J* **16,** 4049-4057.

SCHLEGEL, A., GIDDINGS, J., LANDINSKY, T. M., and KIKEGAARD, K. (1996). Cellular origin and ultrastructure of membranes induced during poliovirus infection. *J Virol* **70,** 6576-6588.

SCHOLTHOF, H. B., and SCHOLTHOF, K.-B. G. (1996). Plant virus gene vectors for transient expression of foreign proteins in plants. *Annu Rev Phytopath* **34,** 299-323.

SCHOLTHOF, K.-B. G., SCHOLTHOF, H. B., and JACKSON, A. O. (1995b). The tomato bushy stunt virus replicase proteins are coordinately expressed and membrane associated. *Virology* **208,** 365-369.

SCHWARTZ, M., CHEN, J., JANDA, M., SULLIVAN, M., DEN BOON, J. A., and AHLQUIST, P. (2002). A positive-strand RNA virus replication complex parallels form and function of retrovirus capsids. *Molecular Cell* **9,** 505-514.

SIT, T. L., VAEWHONGS, A. A., and LOMMEL, S. A. (1998). RNA-mediated trans-activation of transcription from a viral RNA. *Science* **281,** 829-832.

STAEHELIN, L. A. (1997). The plant ER: a dynamic organelle composed of a large number of discrete functional domains. *Plant Journal* **11,** 1151-1165.

TERASAKI, M., and REESE, T. S. (1992). Characterization of endoplasmic reticulum by co-localization of BiP and dicarbocyanine dyes. *J Cell Sci* **101,** 315-322.

TOPFER, R., VOLKER, M., GRONENBORN, B., SCHELL, J., and STEINBIIS, H.-H. (1987). A set of plant expression vectors for transcriptional and translational fusions. *Nucleic Acids Res* **15,** 25-31.

VAN DER HEIJDEN, M., CARETTE, J. E., REINHOUD, P., HAEGI, A., and BOL, J. F. (2001). Alfalfa Mosaic Virus replicase proteins P1 and P2 interact and colocalize at the vacuolar membrane. *J Virol* **75,** 1879-1887.

WEBER-LOTFI, F., DIETRICH, A., RUSSO, M., and RUBINO, L. (2002). Mitochondrial targeting and membrane anchoring of a viral replicase in plant and yeast cells. *J Virol* **76,** 10485-10496.

WEE, E. G.-T., SHERRIER, D. J., PRIME, T. A., and DUPREE, P. (1998). Targeting of active sialyltransferase to the plant Golgi apparatus. *Plant Cell* **10,** 1759-1768.

XIONG, Z., KIM, K. H., KENDALL, T. L., and LOMMEL, S. A. (1993). Synthesis of putative red clover necrotic mosaic virus RNA polymerase by ribosomal frameshifting *in vitro*. *Virology* **193,** 213-221.

XIONG, Z., and LOMMEL, S. A. (1989). The complete nucleotide sequence and genome organization of red clover necrotic mosaic virus RNA-1. *Virology* **171,** 543-554.

XIONG, Z., and LOMMEL, S. A. (1991). Red clover necrotic mosaic virus infectious transcripts synthesized *in vitro*. *Virology* **182,** 388-92.

Chapter 3

Removal of the Plant Cell Wall does not Perturb Endoplasmic Reticulum Channels and Grooves Through the Nucleus

KATHERINE A. TURNER[1], STEVEN A. LOMMEL[1, 3], and NINA S. ALLEN[2]

Departments of [1]Genetics, [2]Botany, and [3]Plant Pathology

NC State University, Raleigh North Carolina 27695-7616

Removal of the Plant Cell Wall does not Perturb Endoplasmic Reticulum Channels and Grooves Through the Nucleus

Abstract

The plant endoplasmic reticulum (ER) is directly involved in the detection of physical and chemical signals, their transmission through the release of secondary messengers, and their presentation to the nuclear machinery. The outer nuclear membrane is continuous with the ER and shares its proteins and functional properties, facilitating such signaling . The lumens of the ER and the nuclear envelope are continuous, and transmembrane proteins that directly interact with chromatin can be accessed via this shared compartment. The nuclear envelope often exhibits grooves, invaginations, and channels. These structures greatly increase the surface area of the membrane available for nucleo-cytoplasmic transport and often show affinity for nucleoli, further suggesting a role in transcriptional or translational regulation.

We investigated the effects of removing the cell wall on ER and nuclear membrane structure. Protoplasts were prepared from NT-1 suspension culture cells expressing GFP-ER and imaged using a laser scanning confocal microscope. Surprisingly, cells digested to remove the cell wall retained nuclear invaginations and normal cortical ER morphology 3 hours after protoplasting. We hypothesize that the nuclear invaginations and the ER in general are protected

from the disruptive effects of cell wall removal due to their critical role in providing access to chromosomal domains.

Introduction

Cells are composed of interacting systems of transport, communication, and development or growth. These systems often share components and depend on one another for feedback and regulation. One such system, the endoplasmic reticulum (ER), is involved in protein synthesis, intercellular communication, cell growth, and cell division (Buchanan, 2000; Staehelin, 1997; Gunning and Steer, 1996; Nebenfuehr, 2001). The ER is intimately associated with the cytoskeleton (Terasaki et al., 1986; Allen and Brown, 1988; Boevink et al., 1998; Fuhrmann et al., 1990) and with formation of the cell wall (Hepler, 1982; Staehelin, 1997). The ER may also interact with the cell wall via a cytoskeleton 'sheath' containing integrin-like proteins that mediate interactions between the cytoskeleton and the cell wall (Reuzeau et al., 1997).

Physical and chemical signals detected at the cell wall induce specific secondary messengers such as calcium and inositols that propagate the signals through intracellular compartments (primarily the ER) to the nuclei, where specific changes in gene expression allow the plant to respond to its environment (Davies et al., 1996; Edwards and Pickard, 1987). Facilitating such signaling, the outer nuclear membrane is continuous with the ER and shares its proteins and functional properties (Ellenberg et al., 1997). The lumens of the ER and the nuclear envelope (NE) are continuous, and in mammalian cells, transmembrane

proteins including lamin receptors and protein kinase C (Burn, 1988), which directly interact with chromatin, can be accessed via this shared compartment (Gunning and Steer, 1996). Nuclear lamins have not yet been identified in plants, but lamin-like proteins have been identified that perform similar functions though they have different sequences (Minguez and Diaz de la Espina, 1993). In this way the ER is directly involved in the detection of physical and chemical signals, their transmission through the release of secondary messengers, and their presentation to the nuclear machinery.

The nuclear envelope often exhibits grooves, invaginations, and channels (Broers et al., 1999; Collings et al., 2000; Ellenberg et al., 1997; Fricker et al., 1997). In certain cells, nuclear invaginations seem to originate during meiosis, and may be used to bring specific NE domains in contact with the condensing chromatin (Sheffield et al., 1979). These structures massively increase the surface area of the membrane available for nucleo-cytoplasmic transport (Singh et al., 1998) and often show affinity for nucleoli (Collings et al., 2000; Ellenberg et al., 1997; Fricker et al., 1997), further suggesting a role in transcriptional or translational regulation. Electron microscopy has shown the invaginations to be cytoplasmic channels bounded by double membranes that contain nuclear pores (Ellenberg et al., 1997). The lumen of the double membrane contains proteins commonly recognized as ER residents such as protein disulfide isomerase (Fassio and Sitia, 2002). Actin filaments can occupy the channels and grooves, sometimes passing completely through the nucleus (Collings et al., 2000).

Nuclear invaginations have been observed in *Nicotiana benthamiana*, tobacco suspension culture, onion (Collings et al., 2000) and *Lilium* (Singh et al., 1998) cells, as well as at least 10 different mammalian cell culture lines (Echevarria and Nathanson, 2002; Ellenberg et al., 1997; O'Neill et al., 2002; Thrower et al., 2001; Broers et al., 1999; Fricker et al., 1997) and even insect cells (Rasmussen, 1976). With so many types of cells exhibiting nuclear invaginations and evidence that the ER is involved in intercellular signaling, the question arises whether the interaction of the ER with the cell wall can have affects on the nucleus via the ER. With this in mind, we investigated the effects of removing the cell wall on ER and nuclear membrane structure in protoplasts prepared from NT-1 suspension culture cells expressing GFP-ER (Collings et al., 2000; Haseloff et al., 1997).

Materials and methods

Cell culture. *Nicotiana tobaccum* 1 (NT-1) cells stably transformed to express mGFP5 ER-targeted GFP (GFP-ER, courtesy of Dr. G. Allen; Collings et al., 2000; Haseloff et al., 1997) were maintained with shaking in MS-1 media (Gibco/Invitrogen, New York) at 27 °C. The cultures received 12 hours light per day. Cells were harvested by centrifugation at ~2000 rpm for 2 minutes in an IEC clinical tabletop centrifuge.

Protoplast preparation. Protoplasts were prepared from transformed NT-1 suspension cell culture (Collings et al., 2000) by incubation in digestion media

[0.1% pectolyase Y23 (Karlan Research Products, Santa Rosa, CA), 2.0% cellulase YC (Karlan), 0.7 M manitol (Fisher) pH 5.5] for one hour at room temp. Protoplasts were isolated from debris by centrifugation at 2400 rpm for 3 minutes through a 20-50% sucrose gradient and washed in fresh 0.7 M manitol prior to confocal microscopy.

Microscopy. Protoplasts were mounted in manitol on glass slides and protected by coverslips. Small dabs of vacuum grease at the corners of the coverslips kept the protoplasts from being crushed, and the coverslips were sealed with valap (1:1:1 vaseline, lanolin, paraffin). Confocal images were collected using a Leica DMIRBE inverted microscope (Leica, Wetzlar, Germany) equipped with a spectral scanning head using a 63X 1.2 N.A. water-immersion lens. The emission signal from GFP excited at 488 nm was collected via a photomultiplier tube from ca. 500-565 nm. DIC images were collected concurrently. Images were processed using Photoshop 4.0 software (Adobe Systems, Mountain View, CA).

Results

Tobacco NT-1 cells expressing GFP-ER (Collings et al., 2000) were digested to remove the cell wall. After washing to remove wall debris and enzymes, the cells were examined under epifluorescent light. Many of the cells appeared healthy, with trans-vacuolar cytoplasmic strands visible, particles traveling in the cytoplasmic strands, and intact vacuoles and plasma membranes. Some cells were clearly stressed, with no cytoplasmic movement, vesiculation of

the ER, and blebbing of the nucleus. Healthy cells were selected for further observation and imaged using the laser scanning confocal microscope. The cells were imaged 1-2 hours after protoplasting. Fluorescence from the GFP-ER was visible throughout the ER lumen, illuminating the cortical ER, cytoplasmic ER strands, and the nuclear membrane. A representative cell is presented in Figure 1. The protoplasts showed a normal distribution of ER in the cortical region (Figure 1A, arrows). The nuclei were large (ca. 20 μm), with rough surfaces and grooves visible (Figure 1A). Here nuclear grooves are defined as areas where the NE is folded inward to create a cleft or depression in the nuclear surface. Tubular invaginations of the nuclear envelope were visible in optical sections through the nuclei. Invaginations are cytoplasmic incursions into the intranuclear space, surrounded on three sides by the NE, while channels are invaginations that completely cross the nucleus, emerging on the opposite side. The membranous ER inclusions were most often long tubes, but a few vesicular inclusions were at the surface of the nucleus (Figure 1B, arrows, 1C, arrowhead, and 1I, arrowhead). Channels that passed completely through the nucleus were also observed (Figure 1G, arrowhead). A region lacking fluorescence in the center of each imagination indicated that they were hollow tubes with cytoplasm in the center (Figure 1C and 1D, arrows). One of the tubes caught in cross section also had a central region lacking fluorescence, consistent with its appearance as a tube composed of cytoplasm surrounded by double membranes (Figure 1E, arrowhead). The invaginations appeared to go directly through the nucleolus (compare Figure 1F and 1C). Due to the limited ability of transmitted

light to reveal three-dimensional structures, neither channels nor invaginations were visible in transmitted light micrographs (figure 1F). The transmitted light micrograph shown in Figure 1 H revealed some interior structure in the nucleus, but due to the reduced resolution inherent in vertical confocal scans it is not possible to determine if those structures correspond to nuclear envelope invaginations. It has been previously shown that untransformed NT-1 nuclei exhibit nuclear grooves and invaginations, demonstrating that the grooves were not induced by the transformation procedure (Collings et al., 2000).

Discussion

The nuclear membrane of NT-1 suspension culture cells exhibited channels and grooves on the cytoplasmic face, as well as extensive nuclear invaginations. Cells digested to remove the cell wall (producing protoplasts) retained normal cortical ER morphology as well as the nuclear ER tubules. The ER is a sensitive, dynamic organelle that quickly responds to changes in the intercellular environment (Staehelin, 1997), and physical manipulation of cells often results in changes to the architecture of the ER (Kiss et al., 1990; Ritzenthaler et al., 2002). We assumed that disruption of normal ER- and cytoskeleton-plasma membrane-cell wall connections would perturb the ER/cytoskeleton matrix to a perceptible degree.

In animal cells, actin and intermediate filaments promote cell-cell adhesion and communication. At the cell periphery, integrins interact with both the cytoskeleton and the extracellular matrix (Alberts et al., 1994). Plant cells

address adhesion and communication through the cell wall. Parallel systems to integrins and intermediate filaments in animal cells are being sought in plants. A spectrin-like polypeptide that could attach microtubules to the plasma membrane has been identified (Reuzeau et al., 1997) (Faraday and Spanswick, 1993) and microtubules have been shown to help cytoplasmic strands interface with the plasma membrane through an integral membrane protein (Lichtscheidl et al., 1990; Pont-Lezica et al., 1993). This interface is important for signal transduction from the cell wall to the cell interior (Edwards and Pickard, 1987; Schindler et al., 1989). The ER and the cell wall are part of a cellular communication and structural system, interconnected by the cytoskeleton and associated proteins (Collings and Allen, 2000a; Staehelin, 1997). Microtubules can play a critical role in the deposition and orientation of the plant cell wall under some conditions (reviewed in Baskin, 2001), and microfilaments are important in maintaining structure of the ER (Hepler et al., 1990). It seems clear that the animal extracelluar matrix and the plant cell wall are functionally related structures because they both provide structural support to the cell and provide anchorage for the internal scaffold proteins (reviewed in Baskin, 2001, and references therein). So how then can a dynamic and sensitive structure like the ER be at once interconnected with the cell wall and insulated from its disruption?

Perhaps clues lie in the form and function of the nuclear channels. The invaginations and channels observed in NT-1 protoplasts wrapped around and through the nucleolus. Singh (1998) found that the increased nuclear reticulum in *Lilium* cells ensured that no DNA was situated more than 0.5 μm from a

nuclear pore, greatly facilitating communication between the nucleus and the cytoplasm. The nuclear reticulum described by Singh (1998) was composed only of infoldings of the inner nuclear envelope membrane, in contrast to the present investigation, where tunnels composed of both NE bilayers cross the nucleus. Cytoskeletal proteins can access these tunnels (Collings et al., 2000) and capitalize on the proximity of the transcriptional machinery. The fact that the invaginations co-localize with DNA during chromatin condensation in animal cells suggests that they play a role in chromatin organization, perhaps through DNA interactions with the nucleoplasmic domains of lamin receptors (Collings et al., 2000; Ellenberg et al., 1997). The invaginations are stable in many cell types, persisting through nuclear migrations and reforming after mitosis (Collings, et al., 2000; Ellenberg et al., 1997; Fricker et al., 1997). It has been suggested that this stability is likely due to associations with the nuclear matrix (Yu et al., 1994), and depolymerization of actin does not affect the nuclear invaginations (Collings and Allen, 2000a). Recently, the *Arabidopsis* protein *ANGUSTIFOLIA* has been demonstrated to be both a regulator of the microtubule-based cytoskeleton and of transcription (Folkners et al., 2002; Kim et al., 2002; discussed in De Lanerolle and Cole, 2002). This discovery provides the direct evidence that a microtubule binding protein can affect gene expression. Plant elongation factor 1α (EF1α) also has a long-established role in translation but can bind both actin and microtubules and regulate actin filament assembly (Ransom et al., 1998). Perhaps cytoskeleton-associated proteins are regulating the form of the ER via its association with actin and microtubules to optimize gene expression. The

cytoskeleton is intimately associated with the ER and the nucleus (Allen and Brown, 1988; Davies et al., 1996; Staehelin, 1997), and may provide a stabilizing scaffold for the ER during cell shape changes. We hypothesize that ER nuclear invaginations and the ER in general are protected from the disruptive effects of cell wall removal due to their critical role in providing access to chromosomal domains. The reorganization of the cytoskeleton has previously been associated with wound response, (Davies et al., 1996; Grolig et al., 1990) and it could be speculated that upon removal of the cell wall, the cytoskeleton reorganizes to maintain the interior structure most efficient for cell recovery and growth.

We investigated the effects of cell wall removal on the ER and nuclear invaginations. The characteristic ER distribution and form appeared unchanged, as did that of the nuclear invaginations. It would be most interesting to know if specific genes were up- or downregulated in response to such a stimulus, and if the cytoskeleton, the ER, or both played a role in the transduction of the regulatory signals. With the discovery of a plant protein that is both a microtubule binding protein and transcriptional regulator, it is possible to envision myriad multifunctional proteins in signaling cascades that connect the cytoskeleton, the nucleus, and the endomembrane system. It will be interesting to see which of the many hypothesized interactions are active in plant cells.

Acknowledgements

We thank Dr. George Allen for the NT-1 GFP-ER cells and Tim Sit for helpful discussion. This work was supported by a NSF/DOE/USDA training Grant # 546142-06284 to S.A.L. and K.A.T., USDA NRI competitive grant 98-

02298 to S.A.L. and T.L.S., NSF competitive grants MCB-0077964 to S.A.L. and T.L.S and NASA competitive grant NAGW-4984 to N.S.A.

Figure 1. NT-1 protoplasts expressing GFP-ER. Confocal microscopy was used to generate ~0.5μm optical sections of a single cell. (**A-E**) Fluorescent ER in the protoplasts. The numbers indicate which section in the stack is presented. Arrows in A indicate cortical ER, in B indicate surface inclusions of the nuclear membrane, in C and D indicate hollow tubes. Arrowheads in C and I indicate surface inclusions of the nuclear membrane, while in E and G they indicate hollow tubes with cytoplasm centers. Inset in E shows hollow tube at higher magnification. (**F**) DIC image of the same section shown in C. N=nucleus, n= nucleolus (**G, H, I**) A vertical confocal scan (an XZ scan through the Y plane) of the same cell, showing a vertical channel through the nucleus. (**G, I**) Fluorescence from the ER. (**H**) DIC image of the same section shown in G. Scalebar = 10 μm.

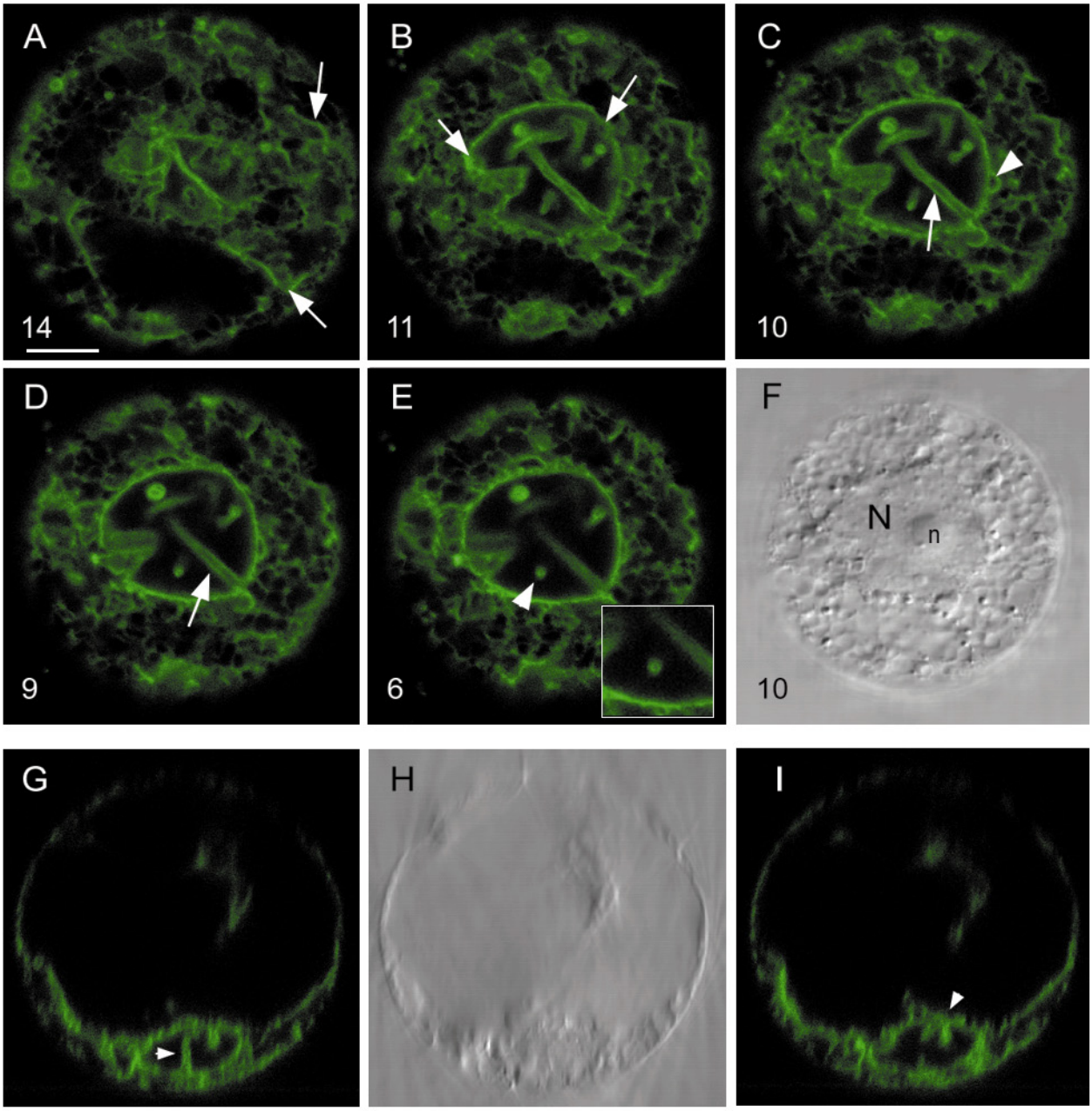
A
14
B
11
C
10
D
9
E
6
F
N
n
10
G
H
I

References

ALBERTS, B., BRAY, D., LEWIS, J., RAFF, M., ROBERTS, K., and WATSON, J. (1994). "Molecular biology of the cell." Garland Publishing, Inc., New York.

ALLEN, N. S., and BROWN, D. (1988). Dynamics of the endoplasmic reticulum in living onion epidermal cells in relation to microtubules, microfilaments and intracellular particle movement. *Cell Motil Cytoskel* **10,** 153-163.

BASKIN, T. (2001). On the alignment of cellulose microfibrils by cortical microtubules: a review and a model. *Protoplasma* **215,** 150-171.

BOEVINK, P., OPARKA, K., SANTA CRUZ, S., MARTIN, B., BETTERIDGE, A., and HAWES, C. (1998). Stacks on tracks: the plant Golgi apparatus traffics on an actin/ER network. *Plant Journal* **15,** 441-447.

BROERS, J., MACHIELS, B., VAN EYS, G., KUIJPERS, H., MANDERS, E., VAN DRIEL, R., and RAMAEKERS, F. (1999). Dynamics of the nuclear lamina as monitored by GFP-tagged A-type lamins. *J Cell Science* **112,** 3463-3475.

BUCHANAN, B., GRUISSEM, W., JONES, R., (2000). Chapter 1: Membrane structure and membranous organelles. First ed. *In* "Biochemistry and molecular biology of plants". pp. 10-83. Courier Companies, Inc.

BURN, P. (1988). Amphitropic proteins: a new class of membrane proteins. *Trends Biochem Sci* **13,** 79-83.

COLLINGS, D. A., and ALLEN, N. S. (2000a). Cortical actin interacts with the plasma membrane and microtubules. *In* "Actin: a dynamic framework for multiple cell functions" (C. J. Staiger, ed.) pp. 145-163. Kluwer Academic Publishers, The Netherlands.

COLLINGS, D. A., CARTER, C. N., RINK, J. C., SCOTT, A. C., WYATT, S., and ALLEN, N. S. (2000). Plant nuclei can contain extensive grooves and invaginations. *Plant Cell* **12,** 2425-2439.

DAVIES, E., FILLINGHAM, B., and ABE, S. (1996). The Plant Cytoskeleton. *In* "The Cytoskeleton", Vol. 3, pp. 405-449. JAI Press, Inc.

DE LANEROLLE, P., and COLE, A. (2002). Cytoskeletal proteins and gene regulation: Form, function and signal transduction in the nucleus. *Science's STKE***,** http://www.stke.org/cgi/content/full/sigtrans;2002/139/pe30.

ECHEVARRIA, W., and NATHANSON, M. (2002). Novel intranuclear structures are responsible for releasing calcium into the nucleus in a liver cell. *Gastroenterology* **122**, 134-145.

EDWARDS, K., and PICKARD, B. (1987). Detection and transduction of physical stimuli in plants. *In* "The Cell surface and signal transduction" (E. Wagner, H. Greppin, and B. Millet, Eds.), pp. 41-46. Springer-Verlag, Berlin.

ELLENBERG, J., SIGGIA, E., MORIERA, J. E., SMITH, C., PRESLEY, J., WORMAN, H., and LIPPINCOTT-SCHWARTZ, J. (1997). Nuclear membrane dynamics and reassembly in living cells: targeting of an inner nuclear membrane protein in interphase and mitosis. *J Cell Biol* **136,** 1193-1206.

FARADAY, C., and SPANSWICK, R. (1993). Evidence for a membrane skeleton in higher plants: A spectrin-like polypeptide co-isolates with rice root plasma membranes. *FEBS Lett* **318,** 313-316.

FASSIO, A., and SITIA, R. (2002). Formation, isomerisation and reduction of disulphide bonds during protein quality control in the endoplasmic reticulum. *Histochem Cell Biol* **117,** 151-157.

FOLKNERS, U., KIRIK, V., SCHOBINGER, U., FALK, S., KRISHNAKUMAR, S., POLLOCK, M., OPPENHEIMER, D., DAY, I., REDDY, A., JURGENS, G., and HULSKAMP, M. (2002). The cell morphogenesis gene *ANGUSTIFOLIA* encodes a CtBP/BARS-like protein and is involved in the control of the microtubule cytoskeleton. *EMBO J* **21,** 1280-1288.

FRICKER, M., HOLLINSHEAD, M., WHITE, N., and VAUX, D. (1997). Interphase nuclei of many mammalian cell types contain deep, dynamic, tubular membrane-bound invaginations of the nuclear envelope. *J Cell Biol* **136,** 531-544.

FUHRMANN, C., BEREITER-HAHN, J., and BRANDLE, K. (1990). Influence of the cytoskeleton, energy supply and protein synthesis on the structure of the endoplasmic reticulum. *Protoplasma* **158,** 53-65.

GROLIG, F., WEIGANG-KOHLER, K., and WAGNER, G. (1990). Different extent of F-actin bundling in walled cells and in protoplasts of *Mougeotia scalaris* P. *Protoplasma* **157,** 225-230.

GUNNING, B. E. S., and STEER, M. W. (1996). "Plant Cell Biology: Structure and Function." Jones and Bartlett, Boston.

HASELOFF, J., SIEMERING, K. R., PRASHER, D., and HODGE, S. (1997). Removal of a cryptic intron and subcellular localization of green fluorescent protein are required to mark transgenic *Arabidopsis* plants brightly. *Proc Natl Acad Sci U S A* **94,** 2122-2127.

HEPLER, P. K. (1982). Endoplasmic reticulum in the formation of the cell plate and plasmodesmata. *Protoplasma* **111,** 121-133.

HEPLER, P. K., PALEVITZ, B. A., LANCELLE, S. A., MCCAULEY, M. M., and LICHTSCHLEIDL, I. (1990). Cortical endoplasmic reticulum in plants. *J Cell Sci* **96,** 355-373.

KIM, G.-T., SHODA, K., TSUGE, T., CHO, K.-H., UCHIMIYA, H., YOKOYAMA, R., NISHITANI, K., and TSUKAYA, H. (2002). The *ANGUSTIFOLIA* gene of *Arabidopsis*, a plant CtBP gene, regulates leaf-cell expansion, the arrangement of cortical microtubules in leaf cells, and expression of a gene involved in cell-wall formation. *EMBO J* **21,** 1267-1269.

KISS, J. Z., H, G. T., STAEHELIN, L. A., and SACK, F. D. (1990). Comparison of the ultrastructure of conventionally fixed and high-pressure frozen/freeze substituted root tips of *Nicotiana* and *Arabidopsis*. *Protoplasma* **157,** 64-74.

LICHTSCHEIDL, I. K., LANCELLE, S. A., and HEPLER, P. K. (1990). Actin-endoplasmic reticulum complexes in Drosera: their structural relationship with the plasmalemma, nuclei and organelles. *Protoplasma* **155,** 116-126.

MINGUEZ, A., and DIAZ DE LA ESPINA, S. M. (1993). Immunological characterization of lamins in the nuclear matrix of onion cells. *J Cell Sci* **106,** 431-439.

NEBENFUEHR, A. (2001). Redistribution of Golgi stacks and other organelles during mitosis and cytokinesis in plant cells. *Plant Physiol* **124,** 135-151.

O'NEILL, A., HAGAR, R., ZIPFEL, W., NATHANSON, M., and EHRLICH, B. (2002). Regulation of type III InsP(3) receptor by InsP(3) and calcium. *Biochem Biophys Res Commun* **294,** 719-725.

PONT-LEZICA, R., MCNALLY, J., and PICKARD, B. (1993). Wall-to-membrane linkers in onion epidermis: some hypotheses. *Plant Cell Environ* **16,** 111-123.

RANSOM, W. D., LAO, P.-C., GAGE, D. A., and BOSS, W. F. (1998). Phosphoglycerylethanolamine posttranslational modification of plant eukaryotic elongation factor 1 alpha. *Plant Phys* **117,** 949-960.

RASMUSSEN, S. W. (1976). The meiotic prophase in *Bombyx mori* females analysed by three-dimensional reconstructions of synaptonemal complexes. *Chromosoma* **54,** 245-293.

REUZEAU, C., DOOLITLLE, K., MCNALLY, J., and PICKARD, B. (1997). Covisualization in living onion cells of putative integrin, putative spectrin, actin, putative intermediate filaments, and other proteins at the cell membrane and in an endomembrane sheath. *Protoplasma* **199,** 173-197.

RITZENTHALER, C., NEBENFUEHR, A., MOVAFEGHI, A., STUSSI-GARAUD, C., BEHNIA, L., PIMPL, P., STAEHELIN, L. A., and ROBINSON, D. G. (2002). Reevlauation of the effects of brefeldin A on plant cells using tobacco Bright Yellow 2 cells expressing Golgi-targeted green fluorescent protein and COPI antisera. *Plant Cell* **14,** 237-261.

SCHINDLER, M., MEINERS, S., and CHERESH, D. (1989). RDG-dependent linkage between plant cell wall and plasma membrane: consequences for growth. *J Cell Biol* **108,** 1955-1965.

SHEFFIELD, E., CAWOOD, A., BELL, P., and DICKINSON, H. (1979). The development of nuclear vacuoles during meiosis in plants. *Planta* **146,** 597-601.

SINGH, S., LAZZARO, M., and WALLES, B. (1998). The nuclear reticulum in placental cells of *Lilium regale* is a part of the endomembrane system. *Protoplasma* **203,** 144-152.

STAEHELIN, L. A. (1997). The plant ER: a dynamic organelle composed of a large number of discrete functional domains. *Plant Journal* **11,** 11511-11565.

TERASAKI, M., CHEN, L., and FUJIWARA, K. (1986). Microtubules and the endoplasmic reticulum are highly interdependent structures. *J Cell Biol* **103,** 1557-1568.

THROWER, E., HAGAR, R., and EHRLICH, B. (2001). Regulation of Ins(1,4,5)P(3) receptor isoforms by endogeneous modulators. *Trends Pharm Sci* **22,** 580-586.

YU, W., SHI-JIE, Y., MING-YI, L., and CHENG-HOU, L. (1994). Nuclear invaginations and nuclear vacuole formation in several plants. *Acta Bot Sin* **36,** 963-966.

Chapter 4

Expression of p27 and p88 in *E. coli*

Expression of p27 and p88 *in E. coli*

Introduction

A few experiments performed early in the Ph.D. program were not included in either of the manuscripts prepared for publication that were presented in Ch 2 and Ch 3 of this thesis. Those experiments are described here to provide a record of the aims, methods, and results for future investigators.

RCNMV p27 and p88 are the viral contribution to the replication complex. In other members of the *Tombusviridae*, the 5' ORF determines the origin of MVBs (Burgyan et al., 1996) and has been implicated in determining host range specificity (Rubino and Russo, 1998). p27 expressed in TBSV gives equivalent or better symptoms than intact virus (T. Sit, personal communication) and the 5' ORFs of *Tombusviridae* have been shown to be critical in host symptomatology (Burgyan et al., 2000).

Since the function of p27 is unknown, we wanted to test the ability of p27 to interact with the RCNMV MP and to bind viral RNA. To this end, p27, p88, and the post-readthrough portion p57 were expressed in *E. coli*. The expressed proteins were to be used to perform gel shift assays similar to those performed with expressed MP and RCNMV RNA (Fujiwara et al., 1993; Geisman-Cookmeyer and Lommel, 1993). It was also intended to investigate the physical

interaction between p27 and p88 using biochemical methods such as circular dichroism, which measures a change in absorption of polarized light due to changes in conformation of two proteins upon interaction.

Previously, p27 and p88 had been translated *in vitro* to study the polymerase frameshifting mechanism (Kim and Lommel, 1994) and antibodies had been produced to synthetic oligopeptides IRENKAVAGFKSLEDF representing the C terminus pf p27 and PTHYSRIHKDLIKAR representing the C terminus of p57 and p88 (Xiong et al., 1993). The antibodies were affinity-column purified and used to immunoprecipitate *in vitro* translation products of RNA-1. In another lab, fusion proteins of p27 and p57 with a maltose-binding protein were produced in *E. coli* and used to test antibodies raised against different peptides representing the p27 and p57 proteins (Bates et al., 1995). The proteins and antisera were unavailable, hence our attempts to express proteins and produce antibodies of our own.

Materials and methods

DNA manipulations. RCNMV p27 and p88 were cloned into pET 35b (ligation independent cloning- LIC) vector (Novagen) following the manufacturer's instructions (Novagen Xa/LIC vector kits manual, Novagen publication #TB184, 1/98). These vectors produce RCNMV proteins as fusions with the S Tag, a cellulose-binding domain used for purification. LIC-competent ends were created

on p27 and the post-readthrough portion of p88, designated p57, using primers p27 LIC S (5'ggtaatgagggtcgcatgggttttataaatctttcgcttttttg3'), p27 LIC AS (5'agaggagagttagagcccctaaaaatcctcaagggatttg3') and p57 LIC S (5'ggtattgagggtcgcatgaaaagtaagagagtcgtag 3'), p57 LIC AS (5'agaggagagttagagcctttatcgggctttgattagatc 3') respectively. To produce p88 with LIC ends, p27 LIC S and p57 LIC AS were used. The resultant plasmids were used to transform the expression strain BL21 DE3, pLys S (Novagen) using standard methods (Sambrook et al., 1989).

For expression in the baculovirus system, p27 was amplified using primers p27 3'Xba/Bam (see table 1, chapter 2) and pUC reverse sequencing primer (#1223, New England Biolabs) (5'gcggataacaatttcacacagga3'). p88 was amplified using primers p88 3' Nco/Spe (see table 1, chapter 2) and pUC reverse sequencing primer. The inserts were cloned into pIZ/V5-His (Invitrogen).

Protein analysis. 2 hours after induction of protein expression by isopropylthio-β-D-galactoside (IPTG) (Sigma), the cells were harvested by centrifugation and lysed by boiling in loading buffer (Laemmli, 1970). Samples were separated by SDS-polyacrylamide gel electrophoresis as described by Laemmli (1970), with the exception that 7.5% polyacrylamide gels were used. Proteins were transferred to PVDF membranes (Millipore, Bedford, MA) in transfer buffer (25mM Tris 40 mM glycine, 10%methanol) using a BioRad trans-blotter. Expressed p27 was detected by anti-p27 primary antibody (p27-663C) and horseradish peroxidase-conjugated secondary goat anti-rabbit antibodies as

previously described (Vaewhongs and Lommel, 1995), followed by visualization using the CDP-Star chemiluminescence kit (Novagen) as directed by the manufacturer. p88 was detected with anti-p88 (p88 Bam/Bgl II) primary antibody and alkaline phosphatase-conjugated secondary antibodies (Bio-Rad, Hercules, CA). The blot was developed in AP buffer (0.1M Tris-HCl, pH 9.5, 0.1M NaCl, 5mM $MgCl_2$) plus 0.1% NBT/BCIP (nitro blue tetrazolium/5-bromo-4chloro-3-indoyl phosphate; Fisher) for 10 minutes.

RNA structure modeling. The p27 nucleotide sequence was analyzed online using mFold software available from Dr. Michael Zucker at http://bioinfo.math.rpi.edu/~zuckerm/

Results and Discussion

In an effort to produce purified proteins with the intent of studying the physical properties of p27 and its interaction with p88, expression vectors producing RCNMV p27, p88, and p57 as fusions to the S Tag were produced and transformed into *E. coli*. After induction, the total bacterial proteins were analyzed by western blot (Figure 1 A). The bacteria harboring the p57 expression plasmids produced a protein of approximately 80 kDa after induction (Fig. 1B, arrowheads). No induced proteins were discernable in lanes representing the p27- and p88-transformed bacteria (Fig. 1 A). The anti-p88

antibody reacted non-specifically with many *E.coli* proteins, producing background bands present in all lanes. The amount of cell lysate loaded in each lane was very high, contributing to the background staining. A different antibody was chosen for further expression trials, and the proteins were visualized with expression-tag based chemiluminescence. After transfer of the cell lysates to PVDF membranes, the blots were incubated with S Tag- alkaline phosphatase conjugate, which detects the S Tag fused to expressed proteins.

This detection system also revealed strong induction of the p57- S Tag fusion (Figure 1C). Surprisingly, truncated protein products were also revealed in the lysates of p27- and p88-transformed bacteria (Figure 1C). The p57 S Tag fusion appeared to migrate at a rate comparable to that of an approximately 60 kDa protein, which is smaller than the anticipated fusion product. This rate is also faster than the apparent rate observed in the blot shown in fig. 1 A, which is comparable to an 80 kDa protein. The protein standards used in the two detection systems are produced by different manufacturers and are composed of different individual proteins. It is this variation that is the likely explanation for the difference in migration, rather than truncation of the fusion product. Further experiments are needed to resolve this confusion.

The p27 and p88 products detected by the S Tag alkaline phosphatase conjugate are very small, and most likely represent the S Tag (approximately 23 kDa) alone or the S Tag and a few amino acids of the p27 protein. A predicted structure model of the p27 (+) sense RNA revealed a large (250 nucleotides) and stable (energy = -195) stem loop beginning just after the AUG codon of p27 (Fig.

2). It is likely that this stem loop causes the ribosome to pause during translation of the fusion proteins, resulting in termination of translation. Since the N-terminus of p88 is identical to that of p27, this would explain why both constructs produced only truncated products *in vitro*.

It is possible that the presence of the native RCNMV 5' non-translated region of the RNA would prevent the RNA from forming the stem-loop structure that prevented efficient translation *in vitro*. To investigate this expression strategy, vectors were produced for expression of p27 and p88 in an insect cell culture system. In this system, expression of foreign genes is directed by a baculovirus, which allows the 5' non-translated region to be included in the construct. The results of expression trials using this system will be presented elsewhere.

Figure 1. Western Blot of cell lysates showing induction of RCNMV protein expression, and SDS-PAGE of expressed proteins. Lysates from induced (I) and uninduced (U) cell cultures are shown. The p57 and p88 10x I lanes show lysates of cultures induced with 10 x the amount of IPTG used to induce the other cultures. (**A**) Total proteins produced by BL21 DE3 pLys S cells transformed to express RCNMV p27, p57 or p88. A colorimetric alkaline phosphatase substrate and an antibody to the 5' half of p88 were used to detect the proteins. The antibody is reacting non-specifically with many *E.coli* proteins, producing background bands present in all lanes. (**B**) Magnification of boxed area in A. Darts show location of band representing p57-S Tag fusion protein induced by IPTG. (**C**) SDS-PAGE showing expressed RCNMV proteins detected by anti-p27 and visualized using chemiluminescence. The band representing the induced p57 protein (p57 I) is the correct size for the 57K RCNMV protein plus the 23K cellulose binding domain, while the bands representing the p27 and p88 induced proteins (p27 I and p88 I) are too small to be full-length proteins.

A

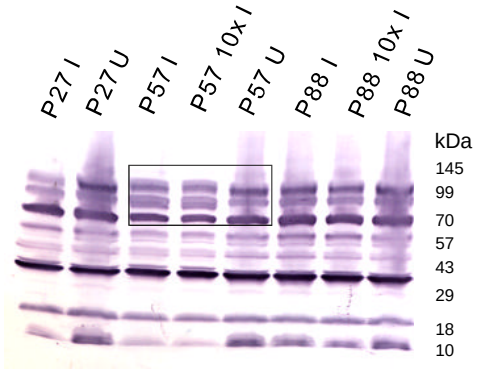
P27 I
P27 U
P57 I
P57 10x I
P57 U
P88 I
P88 10x I
P88 U
kDa
145
99
70
57
43
29
18
10

B

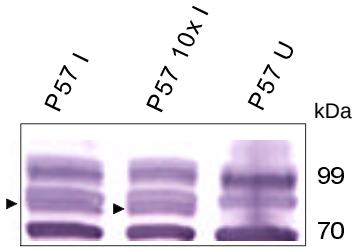
P57 I
P57 10x I
P57 U
kDa
99
70

C

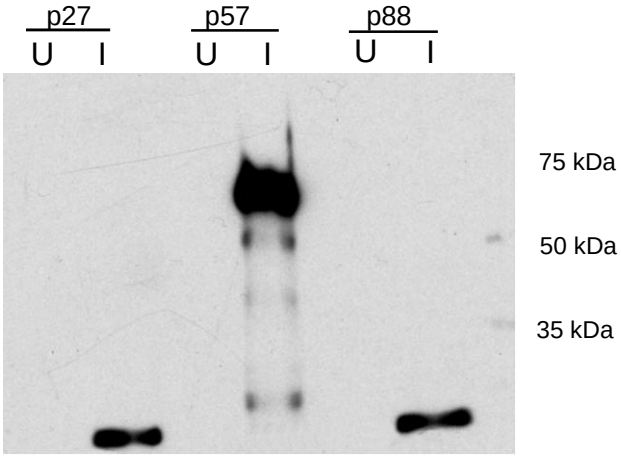
p27
p57
p88
U
I
U
I
U
I
75 kDa
50 kDa
35 kDa

Figure 2. Schematic diagram of the predicted structure of RCNMV RNA-1 , nucleotides 122-825 (the p27 ORF). The putative secondary structure was predicted by mFold software (Zuker, 2002). The arrows show the p27 5' end and indicate the number of nucleotides from the 5' end, progressing clockwise around the putative structure.

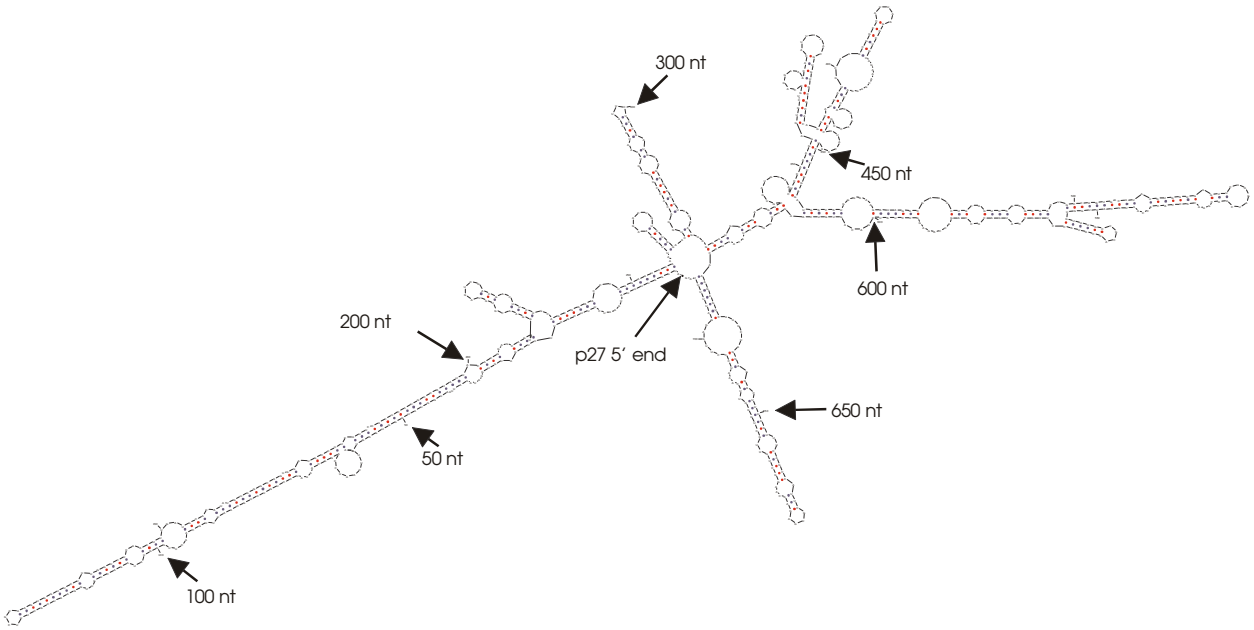

References

BATES, A. H., FARJAH, M., OSMAN, T. A. M., and BUCK, K. W. (1995). Isolation and characterization of an RNA-dependent RNA polymerase from *N. clevelandii* plants infected with *Red cover necrotic mosaic dianthovirus*. *J Gen Virol* **76,** 1483-1491.

BURGYAN, J., HORNYIK, C., SZITTYA, G., SILHAVY, D., and BISZTRAY, G. (2000). The ORF 1 products of tombusviruses play a critical role in lethal necrosis of virus-infected plants. *J Virol* **74,** 10873-10881.

BURGYAN, J., RUBINO, L., and RUSSO, M. (1996). The 5' terminal region of a tombusvirus determines the origin of multivesicular bodies. *J Gen Virol* **77,** 1967-1974.

FUJIWARA, T., GEISMAN-COOKMEYER, D., DING, B., LOMMEL, S. A., and LUCAS, W. J. (1993). Cell-to-cell trafficking of macromolecules through plasmodesmata potentiated by the Red clover necrotic mosaic virus protein. *Plant Cell* **5,** 1783-1794.

GEISMAN-COOKMEYER, D., and LOMMEL, S. A. (1993). Alanine scanning mutagenesis of a plant virus movement protein identifies three functional domains. *Plant Cell* **5,** 973-982.

KIM, K. H., and LOMMEL, S. A. (1994). Identification and analysis of the site of -1 ribosomal frameshifting in red clover necrotic mosaic virus. *Virology* **200,** 574-582.

LAEMMLI, U. K. (1970). Cleavage of ultrastructural proteins during assembly of the head of bacteriophage T4. *Nature* **227,** 680-685.

RUBINO, L., and RUSSO, M. (1998). Membrane targeting sequences in tombusvirus infections. *Virology* **252,** 431-37.

SAMBROOK, J., FRITSCH, E., and MANIATIS, T. (1989). "Molecular Cloning: A Laboratory Manual." 2nd ed. Cold Spring Harbor Laboratory, New York.

VAEWHONGS, A. A., and LOMMEL, S. A. (1995). Virion formation is required for the long-distance movement of Red clover necrotic mosaic virus in movement protein transgenic plants. *Virology* **212,** 607-613.

XIONG, Z., KIM, K. H., KENDALL, T. L., and LOMMEL, S. A. (1993). Synthesis of putative Red clover necrotic mosaic virus RNA polymerase by ribosomal frameshifting *in vitro*. *Virology* **193,** 213-221.

Chapter 5

Summary and Future Research

Summary and Future Research

The goal of this thesis project was to provide further evidence that RCNMV p27 and p88 interact *in vitro* and to investigate the subcellular *in vivo* location of that interaction. Many methods were employed to reach that goal, with varying degrees of success. Initially, we assumed that a biochemical approach would be most straightforward, hence the protein expression constructs described in Chapter 4. When the GFP-labeling experiments started to produce data early in the third year of the project, the protein expression studies became less important and were eventually discontinued.

The three expression strategies used to deliver GFP:p27 each provided unique and relevant information about the localization of p27 without providing a complete picture of the biology at work. GFP:p27 expressed from the subgenomic promoter of RCNMV best approximated the natural circumstances of infection, since most of the RCNMV genome including non-translated control regions was present in normal amounts. *In vitro* transcripts of this modified virus were only periodically infectious, and we were unable to determine what variables caused a productive infection one week but prevented it the next. The CaMV 35S constructs that expressed GFP:p27 and GFP:p88 consistently provided transiently transformed cells, but at such a low expression level that it was nearly impossible to identify the cells expressing p27 and p88. Attempts to improve the efficiency of the system were unsuccessful, leading us to believe

that an inherent property of RCNMV, or perhaps of p27 and p88, was preventing high expression of the GFP-labeled genes. The presence of replicating viruses is known to induce proliferation and pathology of intercellular membranes (Carette et al., 2000). It is likely that the presence of P27 and p88 in cells already damaged by bombardment and protoplasting induced a pathological condition that killed the cells. Only those cells that expressed GFP:p27 and GFP:p88 to very low levels survived. The last method employed, expressing GFP:p27 from a heterologous vector, was the most successful in providing high numbers of brightly fluorescent cells, but was most limited in that the vector alone induced changes in ER structure. The results obtained with this system had to be carefully analyzed to prevent vector effects from biasing our conclusions.

Even with these limitations, taken together, the data are convincing. GFP:p88 co-localizes with GFP:p27 in two expression systems. In addition to this, the fact that GFP:p27 localizes to the ER when expressed from three different promoters, in the presence of heterologous and homologous viral genomes, as well as in the absence of any viral proteins, suggests that the two proteins co-localize to the cortical ER, the nuclear envelope, and cytoplasmic ER domains. The fact that both proteins, when expressed alone, accumulate in the ER and perturb the ER morphology in similar ways suggests that the proteins function together, as part of the larger replication complex purified by Bates et al. (1995).

Inspection of protoplasts inoculated with GFP:p27 and GFP:p88 revealed that p27 and p88 associate with nuclear invaginations and channels. These

channels are membranes that are homologous to both the nuclear envelope and ER (Ellenberg et al., 1997; Fricker et al., 1997) with as-yet undiscovered functions. Viral replication complexes situated within these channels would be ideally placed to access the nuclear pores. It could be that p27 and p88 interact with chromatin to induce expression of host genes necessary for viral infection, or could interact with transmembrane proteins to indirectly affect signal transduction within the cell.

Future Research. Schwartz et al. (2002) proposed a model of BMV replication complexes that features the bipartite polymerase sequestered inside 'spherules' of ER. The ~ 60nm invaginations of the outer nuclear envelope provide a dedicated environment for production of viral RNA. It has been suggested (W.L.. Schneider, personal communication) that viruses that do not genetically protect themselves from gene-silencing based host defense mechanisms instead create physically protected domains for viral replication. This could explain the requirement for association with host membranes found in (+) strand RNA viruses. RCNMV does not encode a known suppressor of silencing protein. It would be very interesting to conduct EM studies of RCNMV infected tissues to investigate whether RCNMV produces similar spherules. Thin sections of the nuclear envelope treated to preserve membrane structure and enhance contrast should reveal the spherules, if they are present.

Experiments should also be performed to further investigate the nature of the fluorescent aggregates observed in GFP:p27- and GFP:p88-inoculated cells.

A labeling experiment following bromo-uridine incorporation into nascent RNA would determine if the aggregates represent active viral replication complexes producing viral RNA. Treatment of the cells with cerulinin, an inhibitor of *de novo* lipid synthesis, would indicate if p27 and p88 induce membrane proliferation or simply rearrangement. A control experiment with unrelated viruses such as AMV would verify that the concentration of cerulinin used was not inhibitory to viral replication in general, but was inhibitory to membrane synthesis-dependent replication (Carette et al., 2000). In addition, antibodies to p27 and p88 could be used with *in situ* hybridization to confirm the location of p27 and p88 within the fluorescent aggregates. At the same time, antibodies for the Golgi apparatus could be used to verify that the aggregates are not derived from Golgi stacks.

The nature of the membrane association could be investigated by treating isolated membrane fractions from RCNMV-inoculated cells with alkaline, urea, and high salt conditions. Transmembrane proteins are not disassociated from membranes under these conditions (den Boon et al., 2001). A detergent treatment will remove transmembrane proteins. Additionally, creating scanning mutations throughout the ORF and testing the mutants for loss of membrane association in isolated cell fractions could map the domains of p27/p88 required for the membrane association.

Experiments to confirm the association of p88 with ER, following the experiments performed with p27, would complete the current picture. A construct expressing GFP:p88 from the TBSV heterologous expression system and containing a deletion in the TBSV movement protein (similar to pHST2-G27ÄNE)

would produce labeled p88 in single cells. When co-inoculated with pHST2-YFP ER, the intact movement protein in the YFP clone would complement movement of the p88 clone, producing foci of-GFP:p88-expressing cells. Confocal microscopy would then be used to observe the localization of GFP:p88 and YFP ER in the cells.

References

BATES, A. H., FARJAH, M., OSMAN, T. A. M., and BUCK, K. W. (1995). Isolation and characterization of an RNA-dependent RNA polymerase from *N. clevelandii* plants infected with *Red cover necrotic mosaic dianthovirus*. *J Gen Virol* **76,** 1483-1491.

CARETTE, J. E., STUIVER, M., VAN LENT, J., WELLINK, J., and VAN KAMMEN, A. (2000). Cowpea mosaic virus infection induces a massive proliferation of endoplasmic reticulum but not Golgi membranes and is dependent on de novo membrane synthesis. *J Virol* **74,** 6556-6563.

DEN BOON, J. A., CHEN, J., and AHLQUIST, P. (2001). Identification of sequences in brome mosaic virus replicase protein 1a that mediate association with endoplasmic reticulum membranes. *J Virol* **75,** 12370-12381.

ELLENBERG, J., SIGGIA, E., MORIERA, J. E., SMITH, C., PRESLEY, J., WORMAN, H., and LIPPINCOTT-SCHWARTZ, J. (1997). Nuclear membrane dynamics and reassembly in living cells: targeting of an inner nuclear membrane protein in interphase and mitosis. *J Cell Biol* **136,** 1193-1206.

FRICKER, M., HOLLINSHEAD, M., WHITE, N., and VAUX, D. (1997). Interphase nuclei of many mammalian cell types contain deep, dynamic, tubular membrane-bound invaginations of the nuclear envelope. *J Cell Biol* **136,** 531-544.

APPENDIX

APPENDIX

Non-fluorescent GFP fusion clones

During the course of the investigations discussed in Chapter 2, many constructs were made that fused GFP to the C terminus of p27 and p88. None of these clones reproducibly gave fluorescence after manual inoculation or microprojectile bombardment. In addition, constructs were made that fused p27 and p88 to blue fluorescent protein (BFP). None of the BFP clones produced visible levels of fluorescence when inoculated via microprojectile bombardment.

R1 p27-GFP (Figure 1) was made with primers 5' p27 C/N previously described (see Chapter 2, table 1) and p27G 3' cla 2 (5'ttatcgataaatcctcaagggatttg3'). This construct codes for a leucine in place of a tryptophan at the final codon of the primer, because the final tg should have been a ttg. The amplified p27 product was digested and ligated to the 5'end of sGFP in R1sG3, producing p27-GFP. These clones did not produce fluorescence in multiple bombardment trials, and no further tests were performed. The DNA is stored at –80 C.

An RNA 1 vector expressing BFP (R1-BFP, Figure 1A) was made with primers p27 B/F (forward primer) (5'cccgggcgccgatatcgctagcatgcatcatcatcatcatcatagtaaagga 3') with a 6xHis tag (underlined) incorporated and primer p27 B/R (reverse) (5'gcctacgcgtgggccctttgtatagttcatccat 3'). In addition, 35S clones expressing

p27 and p88 fused to BFP were also produced (Figure 1B). These clones were designated pRB p27 and pRB p88 to signify derivation from p**R**TL2 and **B**FP. Primers Rp27-35S (5’ ccatggcaaatcctcaagggatttgaacc3’) and Rp88-35S2 (5’gggggaaccatggctcgggctttgattagatctttg3’) were used in conjunction with p27 5’ C/N. These clones produced only faint fluorescence in bombardment trials on onion epidermis, *N. benthamiana* and *N. clevelandii.* It was determined that excitation with 395 nm light was insufficient to produce strong blue fluorescence. The BFP chromophore is optimized for excitation with 360 nm light. While these clones were not useful for the current study, they could be useful in an experiment performed with a confocal microscope equipped with a 360 nm laser. The DNA is stored at –80 C.

35S clones expressing YFP (pRTL2-YFP) were produced with primers sGFP 3’ X/M and sGFP 5’ 6x HIS (see Chapter 2, table 1). These clones produced only faint fluorescence in bombardment trials on onion epidermis, *N. benthamiana* and *N. clevelandii.* They were not investigated further. The DNA is stored at –80 C.

Figure 1. Schematic diagram of RCNMV, CaMV, and TBSV based clones created for the current investigation but not used. (**A**) Clones expressing GFP and BFP from various positions in RCNMV RNA-1. (**B**) Clones utilizing the CaMV 35S promoter to drive expression of various fusions of GFP or BFP, and a control YFP vector that does not produce fusions.

A

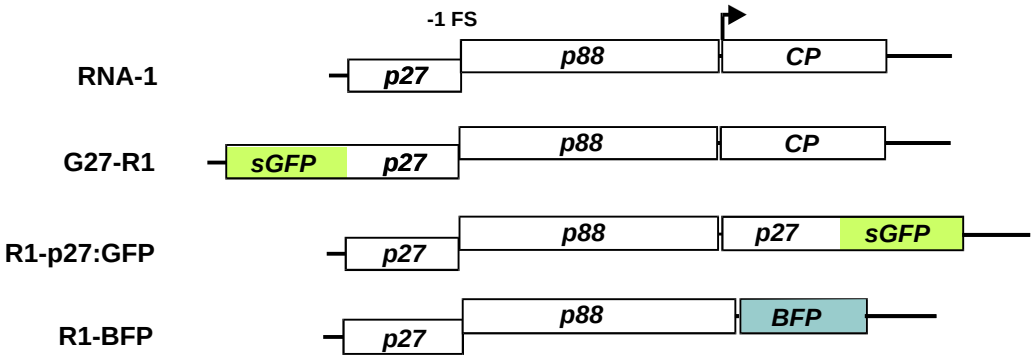
-1 FS
RNA-1
p27
p88
CP
G27-R1
sGFP
p27
p88
CP
R1-p27:GFP
p27
p88
p27
sGFP
R1-BFP
p27
p88
BFP

B

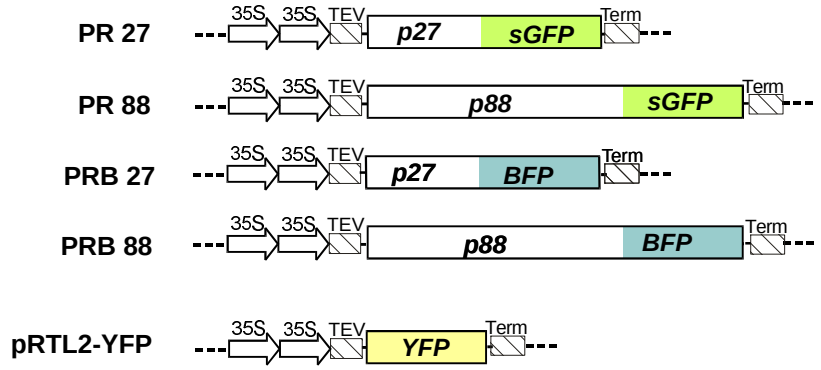
PR 27
35S
35S
TEV
p27
sGFP
Term
PR 88
35S
35S
TEV
p88
sGFP
Term
PRB 27
35S
35S
TEV
p27
BFP
Term
PRB 88
35S
35S
TEV
p88
BFP
Term
pRTL2-YFP
35S
35S
TEV
YFP
Term